DEVELOPMENT OF HIGHLY POLAR STRUCTURALLY-TUNED IONIC LIQUIDS WITH UNIQUE SELECTIVITY FOR GAS CHROMATOGRAPHY

by

MOHSEN TALEBI

Presented to the Faculty of the Graduate School of
The University of Texas at Arlington in Partial Fulfillment
of the Requirements
for the Degree of

DOCTOR OF PHILOSOPHY

THE UNIVERSITY OF TEXAS AT ARLINGTON
December 2018

Copyright © by Mohsen Talebi 2018

All Rights Reserved

This dissertation is dedicated to my wonderful mother, Afsaneh.

For her love, encouragement, and measureless support

Acknowledgements

There are people in everyone's lives who make success both possible and rewarding. I would like to express my special appreciation to my advisor, Dr. Daniel W. Armstrong for his guidance during graduate school. He has been both a teacher and a mentor during graduate school. I consider myself fortunate to have the opportunity to pursue my Ph.D. under his supervision.

I would also like to thank my graduate committee members: Professor Purnendu Dasgupta, Professor Saiful Chowdhury, and Professor Peter Kroll for their advice, guidance and times spent on my behalf during my graduate studies. I greatly appreciate the assistance of all faculty and staff in the Department of Chemistry and Biochemistry at the University of Texas at Arlington. Also, I would like to take this opportunity to express gratitude to our collaborators Len Sidisky (MilliporeSigma) and Ryo Takechi (Shimadzu) for their help over the course of my research. I thank Dr. Alain Berthod, Dr. Farooq Wahab, and Dr. John Lang for their helpful guidance throughout my Ph.D. I owe a great debt of gratitude to my colleague and friend, Dr. Rahul Patil, for his generous help and support during my research. I would like to thank Dr. Roy McDougald and Dr. Brian Edwards for training me on several instruments and helping with troubleshooting. Moreover, I acknowledge Dr. Jeff Crank, for mentoring me during my internship at 3M.

Finally, and most importantly, my heartfelt gratitude goes to my friends and family for their endless love, timely encouragement, and having faith in me throughout this journey. I deeply thank my parents, Asghar and Afsaneh, and my sister, Marjan, who always had confidence in me and offered me encouragement and support in all my endeavors. I am profoundly grateful to my best friends, Mehdi and Sajad, for keeping me motivated and supporting me during tough times. Finally, I would like to thank Yalda, for being an important part of my story.

November 19, 2018

Abstract

DEVELOPMENT OF HIGHLY POLAR STRUCTURALLY-TUNED IONIC LIQUIDS WITH UNIQUE SELECTIVITY FOR GAS CHROMATOGRAPHY

Mohsen Talebi, PhD

The University of Texas at Arlington, 2018

Supervising Professor: Daniel W. Armstrong

Ionic Liquids (ILs) are state-of-the-art fluids that have found broad application in separation science. Owing to their unique physicochemical properties such as low vapor pressure, high thermal stability, and high viscosity, they were successfully used as stationary phase in gas chromatography (GC). By properly engineering their molecular structure, ionic liquids with tailor-made properties can be designed. Therefore, a systematic structure-function relationship can be established to study the effect of structural modification on the properties of ionic liquids.

Herein, I describe the design and synthesis of several dicationic ionic liquids. The synthesized ILs were characterized in terms their physicochemical properties. The effect of different structural on their physicochemical properties variations was investigated. The selected ILs with highest thermal stabilities were utilized as GC stationary phase. Comparing the separation patterns of different compounds on these columns provided some insight about the effects of structural variations on the selectivities and polarities of dicationic ILs.

Due usually show higher melting points than conventional ILs. This increase in melting temperature narrows their utilization in some applications. To overcome this limitation, a systematic study was performed to fine-tune the properties of DILs by utilizing branched spacer linkage between two cationic head groups. A series of dicationic ionic liquids containing α-, β-, and γ-substituents on the alkane linkage chain were synthesized, and the effect of a substituent position on their physicochemical properties was evaluated. ILs with optimal properties they were coated on fused silica capillaries and evaluated for separation of fatty acid methyl esters (FAMEs). These novel stationary phases demonstrated excellent selectivity for separation of *cis* and *trans*, as well as omega-3 and omega-6 positional FAME isomers. The detailed analysis of cis and trans C18:1 isomers of a partially hydrogenated vegetable oil demonstrated the enhanced separation of FAMEs on the IL-based columns compared to the American Oil Chemists Society (AOCS) official method.

Further tuning of dicationic ILs properties was obtained using different accompanying anions. Combination of branched-chain dicationic moiety with fluorosulfonyl derivatized anions led to formation of highly polar ionic liquid stationary phases, with a McReynolds polarity passing 6000. These ILs showed unique selectivity for separation of FAMEs from biodiesel and bacterial sources.

Table of Contents

List of Illustrations

List of Tables

Chapter 1

INTRODUCTION

1.1 Fundamentals of ILs and strategies to govern their thermophysical properties

According to the commonly accepted definition, ILs are salts exclusively composed of ions, which have melting points below the temperature of 100 °C.[1] A large number of possible combinations of organic cations along with organic or inorganic anions provides broad opportunity for synthesis of ionic liquids with tuned physicochemical properties.[2] Figure 1-1 illustrates the structures of common cations and anions that are often used in the design of ILs. Task-specific ionic liquids can be designed depending on the desirable application by performing simple structural modifications.[3]

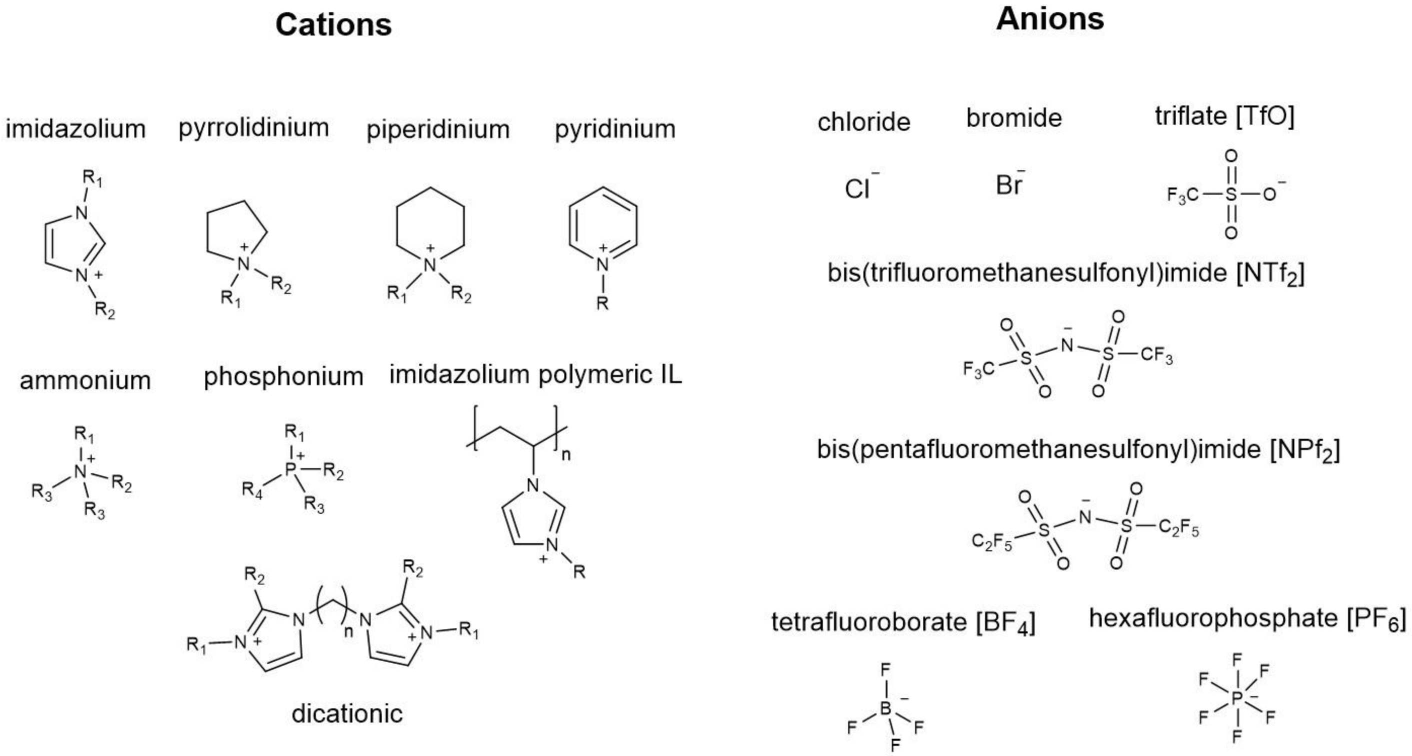

Figure 1-1 Chemical structures of selected cations and anions commonly used in synthesis of room temperature ionic liquids

1.1.1 Physicochemical properties of ionic liquids

The thermophysical properties of ionic liquids are principally dependent on the chemical composition of their associated ions. Thanks to their relatively low melting point and high thermal stability, ionic liquids exhibit a significantly greater liquidus range than that found for common molecular solvents.[1] The lower temperature limit is governed by the structure and interactions between ionic species. Low ion symmetry, weak intermolecular interactions, high conformational freedom, and efficient charge delocalization on both cationic and anionic moieties favor formation of ionic liquids with low solid-liquid transition temperatures.[4] Normally, ionic liquids containing halide anions show higher melting points. In such cases, the replacement of halides with weakly coordinated organic anions such as trifluoromethanesulfonate [TfO^-], or bis(trifluoromethanesulfonyl)imide [NTf_2^-] leads to decreased melting points.[5] This reduction is due to disruption of crystal packing and reduction of the crystal lattice energy.[1]

Since ionic liquids have little measurable vapor pressure, their upper liquid phase limit usually results from their thermal decomposition rather than vaporization.[1] Making small structural modifications on the ionic species can considerably influence thermal stabilities. Incorporation of functional groups or structural subunits usually lead to changes in IL thermal stabilities.[4] The stability of ionic liquids toward high temperature stress is often related to the nucleophilicity of associated anions. Generally, ILs that have weakly nucleophilic anions such as NTf_2^- are more stable to high temperature decomposition. Furthermore, there is a great difference in reactivity between cation types. For instance, tetraalkylphosphonium ILs are more temperature resistant than the tetraalkylammonium ILs and decompose by a more complex mechanism.[6-8]

Structural engineering of counterions may have further impact on an ionic liquid's physical properties. ILs viscosities and densities are highly dependent on the nature of incorporated ions. Highly symmetric or almost spherical ions, larger alkyl substituents on the cationic moiety, as well as stronger hydrogen bonding and/or π-π interactions results in higher viscosities of ionic liquids.[1,6,9,10] ILs with lower viscosity are predominantly desired for synthesis and extraction applications. On the contrary, higher viscosities may be favorable for other applications such as lubrication, supported separation membranes, and gas chromatography stationary phases.[1,10-13]

1.1.2 Dicationic ionic liquids

In comparison to monocationic ILs, multi-cation (dicationic or more) platforms provide more opportunities to control physicochemical properties. Dicationic ionic liquids (DILs) are comprised of two cationic and two anionic moieties, with a spacer chain separating the cationic terminal groups. By altering the length of spacer alkyl chain as well as cation/anion combination, ILs with a wide range of physicochemical properties can be produced.[7,9,14-17] In addition, tailor-made DILs comprised of aromatic or aliphatic hydrocarbon, polysiloxane, polyether, and fluoroalkyl linkers can be designed having unique properties.[16,18,19] DILs generally possess higher thermal stabilities than those of monocationic building blocks, because of greater charge and intermolecular interactions, higher molecular weight, higher density, smaller free volume and higher shear viscosity.[9,20] It is found that the melting points of dicationic ILs are often higher than that of monocationic ILs.[20] DILs melting point can be reduced by changing the spacer arm or introducing divergent cationic or anionic species.[9,21,22] Despite having lower melting points, unsymmetrical DILs were found to have comparable properties to symmetrical dicationic ionic liquids. Thanks to their high viscosities, DILs form consistent GC stationary phases, exceptionally resistant to disruption at high temperatures.[15] Further applications of DILs can be recognized as high temperature lubricants,[18] liquid thermal storage media,[23] heat transfer fluids in solar plants,[23-25] and high temperature solvents in organic synthesis.[26,27]

1.2 Separation characteristics of ionic liquid GC stationary phases

While ILs have been advantageously used in chemical synthesis and catalysis,[12,13] their use as novel functional materials for a huge number of different applications, including gas chromatography stationary phases, has also been playing an important role in their wide dissemination.[28] Ionic liquids encompass an exceptional combination of intrinsic properties such as broad liquid range, high viscosity, and good wetting characteristics.[15] Ionic liquids have been shown to have good wettability with respect to fused silica capillaries.[4] Their high stability upon water or oxygen exposure make ILs even more broadly useful.[29-36] Yet, their most important feature is perhaps their tunability, which makes them undeniably unique and incomparable to other GC stationary phases.[15]

1.2.1 Selectivity of IL-based GC columns

In 1999, Armstrong and coworkers reported the “dual nature” of IL stationary phases, suggesting that they separated both polar and nonpolar compounds through wide range of interaction mechanisms.[28] Separation of analytes occur due to their different volatilities and/or specific interactions with the stationary phase.[4] However, predicting retention mechanism of IL stationary phases appears to be complicated. In general, ILs retain relatively polar to polar compounds by gas-liquid partitioning, whereas low-polarity to non-polar compounds are chiefly retained by interfacial adsorption.[4,37,38] Unlike traditional stationary phases, ILs are capable of undergoing multiple solvation interactions, including dispersive, hydrogen-bonding, π-π, dipolar and ionic interactions.[5,17,39-41] In addition, chemical modification of the IL structures through functionalization of the cation or altering the anionic moiety can cause substantial change in selectivity or separation capacity for analytes of interest.[38] The anion contributes to the unique selectivity of ionic liquid stationary phases.[22] While, dipolarity and hydrogen-bond basicity of the ionic liquids are mainly governed by the nature of anionic group, the cation influences the dispersive and π-π interactions.

1.2.1 Polarity of IL-based GC columns

Ionic liquid stationary phases also exhibit remarkably higher polarities than most conventional polymer-based stationary phases.[3] The Rohrschneider-McReynolds system is a commonly accepted method to estimate the polarity of GC stationary phases.[42] Retention indices for five judiciously selected probe molecules – benzene, 2-pentanone, 1-butanol, 1-nitropropane and pyridine are determined to estimate the position of a phase on the polarity scale. Accordingly, ILs polarities represent an individual or a combination of interactions and allows evaluation of their retention behavior towards different solutes.[38] Highly polar stationary phases are useful in separation of polarizable compounds containing double bonds. Another use is in GC×GC applications due to their orthogonal selectivity to non-polar columns resulting in unique elution patterns.

1.3 Gas chromatographic analysis of fatty acids on ionic liquid stationary phases

1.3.1 GC analysis of fatty acid methyl esters (FAMEs)

Fatty acids (FAs) are building blocks of fats and oils and one of the most important classes of lipids being essential for living cells. They can be found in animals, plants, and microorganisms in different forms. Their chemical structure consists of a carboxylic acid group bonded to a hydrocarbon chain. Many types of fatty acids exist, including saturated, monounsaturated, and polyunsaturated fats, typically having 0-6 double bonds. The system *a:b n-c* is normally used to abbreviate the molecular formula of common unbranched fatty acids, where *a* and *b* represent the number of carbon atoms and double bonds in the fatty acid, respectively, and c denotes the position of the first double bond relative to the terminal methyl group. For example, C18:1n6 represents the ω-6 isomer of octadecenoic acid.[43]

Prior to analysis, fatty acids are being converted to their methyl esters (FAMEs) through a transesterification reaction to reduce the polarity of carboxyl functional group. This leads to decreasing strong intermolecular interactions (i.e. hydrogen bonding interactions) between fatty acid molecules and lowers their boiling points. The resulting methyl esters offer great stability and provide quick and quantitative samples for gas chromatographic analysis.[44]

GC along with flame ionization detection (FID) or mass spectrometry (MS) is generally used for FAME characterizations.[45,46] Although mass spectrometry (MS) is a powerful tool for peak identification, it is somewhat difficult to adequately identify FA isomers with similar molecular mass using MS alone. Also, FID is a nonselective detector, not capable of identifying unknown peaks in the complex samples. Thus, high chromatographic resolution is still required to reliably interpret MS data.[47]

The natural occurrence of saturated and unsaturated fatty acids with many isomers, means that a large variety of selected compounds have to be analyzed in biological and food samples. In addition, possible *cis/trans* geometrical configuration of double bonds adds additional complexity to the separation and analysis of these samples. Considering the slight difference between the *cis* and *trans* FAME isomers of the same carbon length and degree of unsaturation, very efficient capillary GC columns composed of highly selective stationary phases are required to achieve adequate separation.[45-48] Accordingly, the official American Oil Chemists' society (AOCS Method Ce 1h-05) suggests the use of a 100 m poly(bis-cyanopropyl siloxane) column operating isothermally at 180 °C.[49] Additionally, a prior fractionation of fatty acids by silver-ion chromatography is required to achieve better identification of *cis* and *trans* isomers.[45,50-54]

1.3.2 Selectivity of ionic liquid columns toward FAMEs

Over the last few years, development of more efficient ionic liquid GC columns has provided a fantastic opportunity for detailed characterization of fatty acids (FA). Highly polar ionic liquids, i.e. SLB-IL100 and SLB-IL111, are particularly adept in detailed analysis of fatty acids.[43,55] Generally, the following behaviors can be observed when separating FAMEs on highly polar ionic liquid columns: (a) shorter analysis times than traditional GC stationary phases, (b) increased retention with greater degrees of unsaturation, (c) elution of trans FAME isomers before cis isomers, (d) longer retention of unsaturated FAMEs with the double bond located closer to the fatty chain end (e.g. ω-3 fatty acids tend to retain longer than ω-6 isomers).[43,55,56]

Furthermore, the retention patterns on ionic liquid columns are greatly dependent on chromatographic conditions. Retention crossover was observed upon slight changes in column temperature for isothermal and gradient analysis of fatty acids on the IL columns.[57] Therefore, the peak identification should be verified when working with ionic liquid columns at different temperatures, especially if a nonselective detector (e.g. FID) is utilized.[48,57]

Equivalent chain length (ECL) is the most established method to assess selectivity of columns based on retention of unsaturated FAMEs. It corresponds to the theoretical fractional saturated chain length that would result in the same retention that observed for the unsaturated FAME.[48,58,59] The ECL value can be calculated using the two saturated FAMEs that bracket the peak of the unsaturated FAME.[55] A significant increase in the ECL values with increasing column polarity can be expected for ionic liquid columns, specifically in case of polyunsaturated FAMEs.[47,48,55] Moreover, determination of ECL values is particularly important for evaluation of overlap patterns on different stationary phases. For instance, the FAMEs elution order is identical for the IL59, IL60, and IL61 columns.[47] Several overlaps between nutritionally important fatty acids occur on these columns, limiting their application for clinical and nutritional studies of the fatty acids components.[48] On the other hand, the highly polar SLB-IL111 with the greatest ECL values among commercially available columns, offers exceptional selectivity for the separation of unsaturated FAMEs.

1.3.3 Application of ionic liquid columns for the separation of cis and trans isomers

Determining the fatty acid composition of a food product may be challenging since foods contain a complex mixture of saturated (SFA), monounsaturated (MUFA), and polyunsaturated (PUFA) fatty acids with a variety of hydrocarbon chain length. Furthermore, the presence of *trans* fatty acids in processed foods, containing partially hydrogenated oils, interferes with natural metabolic processes. This necessitates the determination of the levels of each type of fatty acid by food manufacturers, as each has different known or suspected health effects.[45-47,60-62]

The SLB-IL111 column with length of 100 m or 200 m is usually used for detailed analysis of fatty acids in food samples.[45,46,63,64] The exceptionally polar characteristic of SLB-IL111 column allows separation of key cis/trans FAME isomers that are not resolved on other columns. It also provides a complementary elution profile of FAMEs typically separated on the biscyanopropyl siloxane columns.[46] Excellent performance of theSLB-IL111 was shown in separation of cis/trans conjugated linoleic acid (CLA) isomers, where c9, t11-CLA and t7, c9-CLA, the most abundant CLA isomers in ruminant fats, were completely resolved from each other.[46] Octadecenoic acid (C18:1) is the foremost constituent of dietary fats and oils, with distributions of 26 cis and trans isomers having various double bond positions in the range of Δ4-16. Oleic acid (C18:1 cis-Δ9), the most naturally abundant isomer, is quantifiable with the SLB-IL111 column separation and not with any other commercial column due to coelution with other C18:1 isomers.[62] The major trans C18:1 fatty acid in ruminant-derived foods, especially milk fat, is trans vaccenic acid (tVA, t11-C18:1). Studies have shown that t11-C18:1 is beneficial for human body and it is a precursor for conjugated linoleic acids (CLA). Trans-10 is another notable trans C18:1 isomer, which unlike trans-11, is not known to provide any useful health benefits in humans.[65-68] While using the official AOCS method results in coelution of trans 9-11 C18:1 isomers, most of the trans FAME geometrical isomers including t10-C18:1 and t11-C18:1 can be separated using the SLB-IL111 column.[45,60]

The 200 m SLB-IL111 column was further used for determination of total, trans, saturated, and cis unsaturated fats in 32 representative fast food samples.[60] The content of trans fat ranged from 0.1-3.1 g per serving, as determined according to AOCS official method Ce 1j-07. The improved separation of trans C18:1 positional isomers and enhanced resolution of trans C18:2 and C18:3 FAME isomers are two major advantages of the SLB-IL111 column, relative to the biscyanopropyl siloxane stationary phases.

In addition, analysis of fatty acids in marine oil omega-3 supplements on a 200 m SLB-IL111 column permitted quantification of rarely reported fatty acids such as C21:5n3 and the n-4 and n-1 PUFA. The presence of predominant mono-trans isomers of eicosapentaenoic acid (EPA; C20:5n3) and docosahexaenoic acid (DHA; C22:6n3) was confirmed in these samples.[69] The SLB-IL100 was tested for analysis of cis positional isomers of eicosenoic (C20:1) and docosenoic (C22:1) fatty acids of fish origin. The high polarity of SLB-IL100 allowed separation of several isomers including C20:1n11 from C20:1n13, unresolvable on conventional polar polymer phase columns.[70]

1.3.4 Separation of branched-chain fatty acids using ionic liquid columns

The SLB-IL111 is also proficient to discriminate odd and branched-chain fatty acids (OBCFAs) from other milk FAs eluting in the same chromatographic region.[71] These fatty acids are the chief lipids in bacterial membrane and considered as biomarkers of ruminant fat intake.[72] By definition, the branching on the *iso*-methyl branched fatty acids is positioned on the penultimate carbon (ω-1), while the methyl substituent in *anteiso*-branched fatty acids is located on the *ante*-penultimate carbon atom (ω-2). The elution behavior of *iso* fatty acids on the SLB-IL111 is very similar to the conventional polymer stationary phases. The *iso* FA with n C-atoms elutes at a carbon number (CN) of (n-1+0.5). Accordingly, *iso*-C13:0 elutes right in the middle of C12:0 and C13:0 fatty acids (or CN=12.5). On the other hand, the *aiso (anteiso)* FA containing n C-atoms retains slightly longer than *iso* isomer, at CN of (n-1+0.7). Furthermore, unlike *cis* and *trans* FA isomers, the relative retention times are not affected for *iso* and *aiso* isomers by changing the isothermal program on ionic liquid columns.[71]

The *Rhodobacter sphaeroides* is a rod shaped, gram negative, purple non-sulfur bacterium utilized as a model microorganism for anoxygenic photosynthesis and carbon fixation.[73-78] The use of a 100 m SLB-IL111 column allowed effective separation of geometrical isomers of monounsaturated C16:1 and C18:1 fatty acids extracted from *R. sphaeroides* 2.4.1.[73] An unprecedented separation of oleic acid (C18:1 cis-Δ^9) from the most predominant cis-vaccenic acid (C18:1 cis-Δ^{11}) isomer was achieved using the highly polar ionic liquid column. In addition, the unusual occurrence of 11-methyl-trans-Δ^{12}-octadecanoic acid was demonstrated in the lepidic matrix of *R. sphaeroides*.

The fatty acids composition in marine oils and products are very complex with a wide variety of chain length and unsaturation.[48] The SLB-IL111 column has been successfully used for separation of extracted fats from marine products. Using this ionic liquid column along with time of flight (TOF) mass spectrometry, the separation and accurate identification of 125 fatty acids in menhaden oil, including two novel branched fats having trans configuration, namely 7-methyl-6-heaxadecenoic and 7-methyl-6-octadecenoic fatty acids was achieved.[63]

1.3.5 Characterization of biodiesel profile using ionic liquid columns

Biodiesel is an alternatively derived fuel, obtained from different biological sources of fatty acids. Animal fats, vegetable oils, recyclable cooking oils, and plant and waste products are usually processed for extraction of fatty acid methyl esters.[79] A petroleum-based diesel is often blended with a biomass-based diesel before consumer use. Due to overlap between the petroleum-based biodiesel compounds of saturated and aromatic hydrocarbons, the FAME profile is difficult to see in blended biodiesel using traditional GC stationary phases.[80-85] The importance of fatty acid ester analysis in biofuel and fuel samples is twofold. First, to monitor cross-contamination in tankers and storage facilities used for multiple fuel types.[81] This is specifically important in case of fuels that are used in aviation and other specialized fuels employed by defense forces where small amounts of FAME contamination contributes to poor thermal and storage stability of the fuel.[86] Second, to investigate the influence of FAME chemical structure on exhaust emissions.[85] Studies have shown that the hydrocarbon chain length and degree of unsaturation can affect the carbon monoxide (CO) levels and nitrogen oxide (NO_x) emissions from combustion of fatty esters.[87-89] According to the UNI EN 14331 procedure, a hydrocarbon LC pre-separation step is required prior to gas chromatographic determination of FAME profile.[90] This procedure can be time and labor intensive. Therefore, a simple, rapid and less expensive approach to effectively separate the FAMEs from the petroleum-based portion appears to be necessary. Fast analysis of biodiesel can be achieved on SLB-IL100 and SLB-IL-111 micro-bore columns.[43,80,85] The key feature of these stationary phases, namely extremely high polarity, allows excellent separation of the FAME components from the less-retained hydrocarbons. Fast GC analysis of the soybean B20 biodiesel blend on the micro-bore SLB-IL100 (12 × 0.1 mm × 0.08 µm d_f) column resulted in separation of compounds before 2.5 min. Particularly, the methyl palmitate (C16:0) eluted after C26, the last significant n-alkane in the sample.[80] Biodiesel samples obtained through the transesterification reaction of different vegetable oils were analyzed utilizing a customized narrow-bore SLB-IL111 (14 × 0.1 mm × 0.08 µm d_f) column.[85] This fast method could be used to quantify the FAME content in basic and acidic transesterified vegetable oils, and to control the quality of biodiesel using routine analyses.

1.4 Research objective and organization

This dissertation focuses on the development of extremely polar dicationic ionic liquids and examining their exceptional selectivities as gas chromatography stationary phases. The research in Chapters 2 and 3 represent the effect of 3 potential structural modifications on the thermophysical properties of dicationic ionic liquids as well as their separation characteristics. It is shown that varying cationic terminal groups and different side chains attached to them as well as altering alkyl spacer chains with different lengths can hugely impact the chromatographic properties of ionic liquid stationary phases. Chapters 4 and 5 of the dissertation focus on the development of branched-chain dicationic ionic liquids and their wide application for gas chromatographic separation. The decreased melting point of branched-chain DILs facilitates their applicability in coating capillary columns. The impact of different types of alkyl substituents on the physicochemical properties of these novel materials is documented in Chapter 4. The research presented in Chapter 5 examines the selectivity of branched-chain DILs toward separation of FAMEs.

Finally, Chapter 6 concentrates on the thermophysical and chromatographic properties of branched-chain DILs paired with various anions. The effect of different sulfo-fluorinated anions on the selectivity and polarity of ionic liquid columns is extensively discussed in this chapter.

Chapter 2

SYNTHESIS OF THERMALLY STABLE GEMINAL DICATIONIC IONIC LIQUIDS AND RELATED IONIC COMPOUNDS: AN EXAMINATION OF PHYSICOCHEMICAL PROPERTIES BY STRUCTURAL MODIFICATION

Abstract

Geminal dicationic ionic liquids (ILs) often display higher thermal stabilities, viscosities, and densities compared to traditional monocationic ILs. Also, dicationic ILs have advantages in terms of tuning of their physicochemical properties by different structural modifications. They can be considered as a combination of three structural moieties: (1) cationic head groups, (2) an alkane linker chain, and (3) the associated anions. Two types of each imidazolium, pyrrolidinium, and phosphonium cations were joined by different alkane linkages (C_6, C_9, and C_{12}) to develop 18 different dications. These dications were paired with two different anions (NTf_2^- and $PFOS^-$) to synthesize 36 different dicationic ILs. The effect of variations in the structural moieties of these related ILs on their physicochemical properties, including melting points, densities, viscosities, solubilities, and thermal stabilities, were evaluated. ILs synthesized in this study displayed TGA thermal stabilities in the range 330–467 °C. Also, nine ILs with high TGA stability and low melting points were tested with inverse gas chromatography, and some of them displayed stabilities up to 400 °C.

2.1 Introduction

Ionic liquids (ILs) are salts with melting points generally less than 100 °C.[13] The unique physical and chemical properties of ILs make them a versatile class of materials for numerous applications.[5,13,41,91-107] Most of their properties can be tuned to meet the needs of specific applications by employing different combinations of cations and anions or by suitable structural modification of those entities.[108] Some of the properties that make them suitable for high temperature applications (like gas chromatography stationary phases, solvents for high temperature reactions, high temperature lubricants, liquid thermal storage media, and heat transfer fluids in solar thermal plants) include high thermal stability, high density, wide liquid temperature range, tunable viscosity, high chemical stability, nonvolatility, and nonflammability. Very few studies have examined the structural effects of dicationic ILs on their physiochemical properties. In order to design ILs for specific applications, one must understand their structure–property relationship. Within ionic liquids, monocationic ILs often display lower thermal stabilities and viscosities compared to geminal dicationic and some polycationic ILs.[17,94,109] Even at high temperatures, dicationic ILs show higher viscosities, and this property makes them attractive as lubricants and stationary phases. The higher molecular weights, charge, and greater intermolecular interactions of dicationic ILs can provide even lower volatility and also alter their stability.[8,16,17] Geminal dicationic ILs were often found to have higher melting points than monocationic ILs with the same anion and sometimes are solids at room temperature.[17,94] Recently, many different dicationic ILs were synthesized, and the effect of anion type, symmetry of the dications, substituents, and the nature of the linkage chain on thermal stability and melting point was studied.[17,108] These studies indicated some advantages of dicationic ILs over monocationic ILs with respect to tailoring of physicochemical properties. In addition, structurally they provide a modular approach to fine-tune desired properties.

Anderson et al. showed that some imidazolium and pyrrolidinium based dicationic ILs have good thermal stabilities.[17] The high thermal stability of phosphonium dicationic ILs was demonstrated by Breitbach et al.[94] In the case of imidazolium ILs, substitution of the acidic C(2) hydrogen with a methyl group leads to an increase in thermal stability.[110] In addition it is known that the nature and length of the linkage chain or “tether” coupling two cationic moieties affect stability, melting point, and the viscosity of dicationic ILs.[17]

According to the limited literature studies on this subject, ILs with short alkane linkage chains (C_3) tend to have higher melting points, and ILs with longer alkane linkage up to C_9–C_{16} tend to have comparatively lower melting points. Viscosity tends to increase with chain length as expected. The thermal stability and density can be highly variable though.[17]

In order to investigate the role of anions on the physicochemical properties of ILs, especially thermal stabilities and viscosities, eight different anions were paired with a tributyltetradecylphosphonium cation. On the basis of the higher thermal stability of bis(trifluoromethane)sulfonimide (NTf_2^-) and perfluorooctanesulfonate ($PFOS^-$) anions, they were paired with imidazolium, pyrrolidinium, and phosphonium based dications. This resulted in the synthesis of 36 different ILs. The effects of each structural modification, i.e., variations in the alkane linker, nature of dication, and nature of the counteranion on the physical properties, were evaluated.

By varying these structural features, we were able to synthesize ILs with high thermal stability. There have been extensive reports of ILs with NTf_2^- anions. However, IL literature involving the $PFOS^-$ counteranion is limited. The use of the $PFOS^-$ anion for the synthesis of thermally stable ionic liquids is demonstrated in this study. The current study presents and discusses the synthesis and structure–property relationships of geminal dicationic ionic liquids.

2.2 Experimental

2.2.1 Materials

1-Benzyl-2-methylimidazole (90%), 1,2-dimethylimidazole (98%), N-methylpyrrolidine (97%), 1-butylpyrrolidine (98%), tripropylphosphine (97%), triphenylphosphine (99%), 1,6-dibromohexane (96%), 1,9-dibromononane (97%), 1,12-dibromododecane (98%), bis(trifluoromethane)sulfonimide lithium salt (99.95%), heptadecafluorooctanesulfonic acid potassium salt (98%), bis(pentafluoromethane)sulfonimide lithium salt (98%), iron(III) chloride (97%), bis(2-ethylhexyl) sulfosuccinate sodium salt (96%), 1-octanesulfonic acid sodium salt (98%), potassium dodecafluoro-closo-dodecaborate (97%), and N,N-dimethylformamide (99.8%) were purchased from Sigma-Aldrich (St. Louis, MO). 1-Hexyl-3-methylimidazolium tris(pentafluoroethyl)trifluorophosphate was obtained from Millipore Corp. (Bedford, MA). It was converted to tris(pentafluoroethyl)trifluorophosphate hydride through ion-exchange resin prior to use. Tributyltetradecylphosphonium chloride was purchased from Cytec (Woodland Park, NJ). Acetonitrile, methanol, dichloromethane, and heptane were purchased from Fisher Scientific (Fair Lawn, NJ). Salt treated fused silica capillary tubing (0.25 mm i.d.) and C9-(m2im)2-NTf2 IL coated column (30 m × 0.25 mm i.d.) were provided by Supelco (Bellefonte, PA). Deionized water was from Synergy 185 water purification system (Millipore, Billeria, MA).

2.2.2 Analysis methods

The monocationic ionic liquids and dicationic ionic liquids were characterized by electrospray ionization mass spectrometry (ESI-MS) for molecular weight. ESI-MS spectra were acquired by using a Finnigan LXQ (Thermo Fisher Scientific, San Jose, CA). ^{1}H NMR, ^{13}C NMR and ^{31}P NMR experiments were performed on 500 MHz JEOL Eclipse Plus 500 instrument for spectral analysis. Thermogravimetric analysis were performed using Shimadzu TGA-51 Thermogravimetric Analyzer (Kyoto, Kyoto Prefecture, Japan) for the stability testing. Samples (~10 mg) were placed in the platinum pans, and heated at 10 °C min^{-1} from room temperature to 600 °C in a nitrogen atmosphere (flow – 30mL min^{-1}). The decomposition temperature were determined at 1%, 5% and 15% weight loss. 5% weight loss of the sample which corresponds to 95% w value was considered as measure of thermal stability. The GC thermal stability measurements were made using Agilent 6890N Gas Chromatograph equipped with flame ionization detector (FID). The studies were performed ramping the column oven temperature from 100 to 450 °C at 1 °C min^{-1} and using helium as carrier gas at flow rate of 1 mL min^{-1}. The injector and FID temperatures were set at 250 °C and 400 °C respectively. The DSC measurements were carried out on a Shimadzu DSC-60 (Kyoto, Kyoto Prefecture, Japan) differential scanning calorimeter (DSC). The samples (~ 10 mg) were sealed in aluminum pans, and then heated at rate of 10 °C min^{-1} up to 500 °C. Melting points were determined using a *Mel-Temp* apparatus (Laboratory Devices, *Cambridge*, *MA*). Density was measured using 10 mL Kimble specific gravity pycnometer at 22 °C. Heptane was used as an immiscible solvent for these measurements. Kinematic viscosity was determined using a Cannon-Manning semi-micro viscometer at 30 °C and 50 °C. All compounds synthesized in this study were tested for solubility with polar (water) and non-polar (heptane) solvent. This study was performed by placing a small amount (60-100 mg) of the compound in the solvent (15 mL) and through observation of whether the solute was miscible or immiscible in the solvent.

2.2.3 Synthesis

2.2.3.1 Synthesis of monocationic ILs

Compounds **IL1, IL2, IL3, IL4, IL5, IL6, IL7,** and **IL8** were made through metathesis reactions of 1 molar equivalents of tributyltetradecylphosphonium chloride salt with 1 molar equivalents of bis(trifluoromethane)sulfonimide lithium ($LiNTf_2$), bis(pentafluoromethane)sulfonimide lithium ($LiNPf_2$), heptadecafluorooctanesulfonic acid potassium salt (KPFOS), Iron (III) chloride($FeCl_3$), tris(pentafluoroethyl)trifluorophosphate hydride (FAP), bis(2-ethylhexyl) sulfosuccinate sodium (NaAOT), 1-octanesulfonic acid sodium salt (NaOS), and potassium dodecafluoro-closo-dodecaborate ($KB_{12}F_{12}$), respectively. The reactions for all ILs were performed in water at room-temperature for 12 h with the exception of heptadecafluorooctanesulfonic acid potassium salt (KPFOS), which was performed at elevated temperature (110 °C) with oil-bath. Dichloromethane was added to the resulting solution to dissolve the target product. The aqueous layer was then removed and the organic layer washed three times with water to remove any starting material. Dichloromethane was then removed by rotary evaporation followed by vacuum drying over phosphorous pentoxide at 40 °C for 24 h. The procedure resulted in the pure monocationic ionic liquid.

2.2.3.2 Synthesis of dicationic ILs

Synthesis of dicationic ionic liquids involved two steps. First step involved a nucleophilic substitution reaction of imidazoles / pyrrolidones / phosphines with corresponding terminal dibromoalkanes to obtain bromide salt of dication. Second step was metathesis dibromodicationic salt with $LiNTf_2$ and KPFOS. In metathesis step bromide ions were exchanged by NTf_2^- or $PFOS^-$ anions to obtain final product ILs and LiBr and KBr as side products.

To synthesis different imidazolium based Ionic Liquids three procedures were employed.

Procedure 1:

Step 1) **IL9, IL21 and IL 33** were made by refluxing 2 molar equivalents of 1-butyl-2-methylimidazole with 1 molar equivalent of 1, 6-dibromohexane, 1, 9-dibromononane and 1, 12-dibromododecane respectively in acetonitrile at 80 °C for 72 h.(Scheme 1) Rotary evaporation of solvent yielded the crude dibromodicationic salt. The salt was then dissolved in water and transferred to a separatory funnel and washed with dichloromethane (3×50 ml) to remove excess starting material. The aqueous layer containing dibromodications was then dried by rotary evaporation of water. Further, vacuum drying over phosphorous pentoxide at 40 °C for 24h resulted in the pure dibromodicationic salts. The products were then verified by mass spectrometry analysis.

Step 2) For the synthesis of final products, the dibromodications synthesized in the first step were dissolved in water and reacted with 2 molar equivalents of ($LiNTf_2$)(Scheme 2). The solution was stirred for 24 h at room temperature. The metathesis process resulted in exchange of bromide anions with NTf_2^- anions. Following that, dichloromethane (40 mL) was added to the solution to extract NTf_2^- salt of the ionic liquid that has phase separated from the water. The lithium bromide and excess NTf_2^- were removed from the dichloromethane phase with successive extraction with water (3x40mL). Removal of dichloromethane through rotary evaporation followed by vacuum drying over P_2O_5 at 40 °C for 24 h resulted in the pure dicationic 1-butyl-2-methylimidazolium ILs with NTf_2^- counter anion.

Procedure 2:

For the synthesis of **IL15, IL27** and **IL 39** with PFOS$^-$ anion; dibromodications and heptadecafluorooctanesulfonic acid potassium salt (KPFOS) were dissolved in a mixture of methanol and water (1:1) and stirred for 12 h.(Scheme 2) The solvents were evaporated using rotary evaporation method and similar protocol as mentioned in Step 2 of procedure 1 was followed for the rest of the reaction workup.

Procedure 3:

For the synthesis of **IL10, IL22, IL34, IL15, IL28** and **IL40** similar protocol as procedure 1 and 2 was followed except 2 moles of 1, 2-dimethylimidazole used instead of 1-butyl-2-methylimidazole.

Similarly, pyrrolidinium DILs were synthesized using the following procedures.

Procedure 4:

For the synthesis of **IL11, IL23, IL35, IL17, IL29** and **IL41** similar protocol as procedure 1 and 2 was followed except 2 moles of 1-butylpyrrolidine was used instead of 1-butyl-2-methylimidazole.

Procedure 5:

For the synthesis of **IL12, IL24, IL36, IL18, IL30** and **IL42** similar protocol as procedure 1 and 2 was followed except 2 moles of N-methylpyrrolidine was used instead of 1-butyl-2-methylimidazole.

Finally, the phosphonium DILs were synthesized using the following protocols.

Procedure 6:

Step 1) **IL13, IL25, IL37, IL19, IL31** and **IL43** were made by refluxing 2 molar equivalents of tripropylphosphine with 1 molar equivalent of 1,6-dibromohexane, 1,9-dibromononane and 1,12-dibromododecane respectively in acetonitrile at 80 °C for 72 h.(Scheme 1) The reaction was performed under inert argon condition to prevent oxidation of tripropylphosphine. Rotary evaporation of solvent yielded the crude dibromodicationic salt. Similar protocol as mentioned in Procedure 1 and 2 was followed for the rest of the reaction workup.

Procedure 7:

Step 1) Compounds **IL14, IL26** and **IL38** were synthesized by refluxing 2 molar equivalents of triphenylphosphine with 1 molar equivalent of 1,6-dibromohexane, 1,9-dibromononane and 1,12-dibromododecane respectively in N,N-Dimethylformamide at 95 °C for 72 h.(Scheme 1) Rotary evaporation of solvent yielded the crude dibromodicationic salt. The salt was then washed with five aliquots of ethyl acetate (3×50 mL) to remove unreacted starting material. The rotary evaporation of solvent and further vacuum drying over phosphorous pentoxide resulted in the pure dibromodicationic salts. Obtained products then verified by mass spectrometry analysis.

Step 2) For the synthesis of final products, the dibromodications synthesized in the first step were dissolved in methanol and water (1:1) and reacted with 2 molar equivalents of ($LiNTf_2$). The solution was stirred for 24 h at room temperature.(Scheme 2) This metathesis process resulted in final IL with bromide anions exchanged with NTf_2^- anions. The solvents were evaporated using rotary evaporation method. The crude NTf_2^- salt was dissolved in dichloromethane. The lithium bromide and excess NTf_2^- were removed from the dichloromethane phase with successive extractions with water (3x40 mL). Removal of dichloromethane through rotary evaporation followed by vacuum drying over P_2O_5 at 40 °C for 24 h resulted in the pure dicationic triphenylphosphonium ILs with NTf_2^- counter anion.

Procedure 8:

To synthesize compounds **IL20, IL32** and **IL44**; dibromodications and heptadecafluorooctanesulfonic acid potassium salt (KPFOS) were dissolved in a mixture of methanol and water (1:1) and stirred for 24 h. The solvents were evaporated using rotary evaporation method and similar protocol as mentioned in Step 2 of Procedure 7 was followed for the rest of the reaction workup.

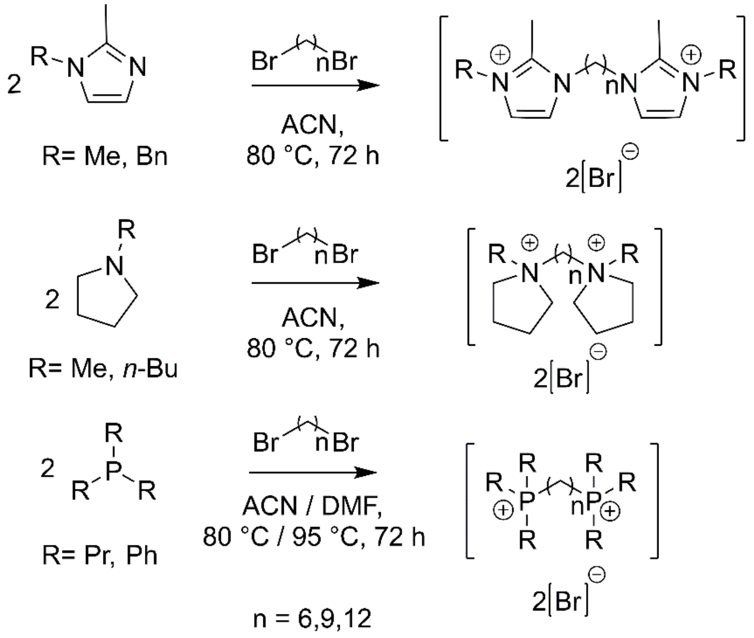

Figure 2-1 Synthesis of bromide of dicationions

2.2.4 Preparation of IL columns

All IL columns were prepared by using the static coating method at 40–60 °C with a 0.20% (w/v) coating solution of IL in dichloromethane or methanol. Methanol was used as a coating solvent for PFOS anionic IL to improve the solubility of these IL. ILs were coated on inner walls of salt treated fused silica capillary with dimensions 3 m × 0.25 mm i.d. After the coating process, columns were conditioned at 250 °C for 12 h. The efficiency of column was tested using naphthalene at 100 °C. The columns showed efficiency ranging from 2000 to 2500 plates m^{-1}.

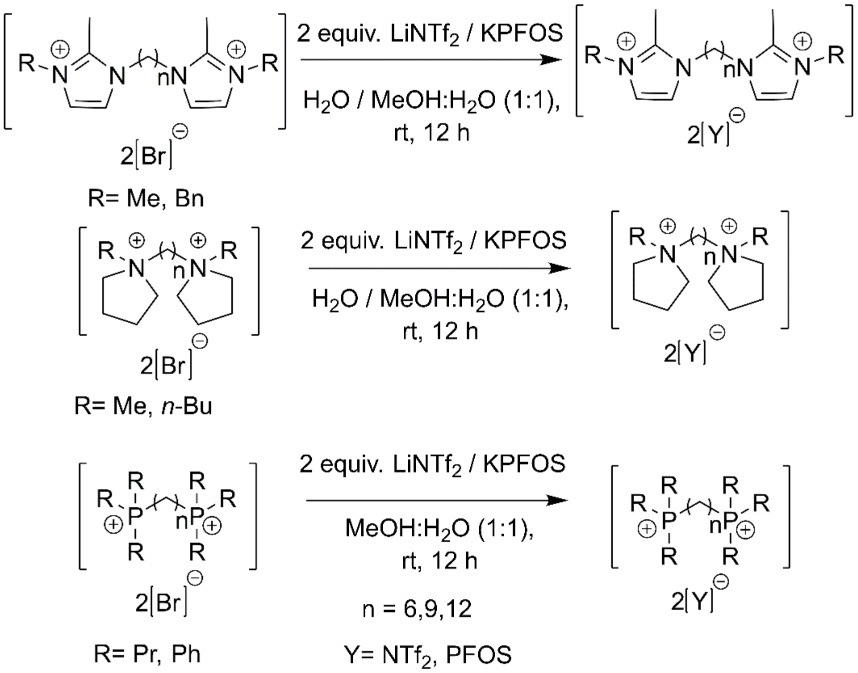

Figure 2-2 Metathesis of bromide salts to synthesize dicationic ILs

2.3 Results and discussions

Eight different anions were screened using thermogravimetric analysis (TGA) after pairing them with the same cation of known high thermal stability. The cation used was tributyltetradecylphosphonium (TBTD-P). This cation was selected because phosphonium ILs have high thermal stabilities while the anions evaluated were bis[(trifluoromethyl)sulfonyl] imide (NTf_2^-), bis[(pentafluoroethyl)sulfonyl] imide (NPf_2^-), perfluorooctanesulfonate($PFOS^-$), iron tetrachloride ($FeCl_4^-$), tris(pentafluoroethyl)trifluorophosphate ($FAP^–$), dioctyl sulfosuccinate ($docusate^–$), 1-octanesulfonate ($1\text{-oct-sulf}^–$), and dodecafluoro-closo-dodecaborate ($B_{12}F_{12}^–$). The structures of these monocationic ILs are shown in Figure 2-3. The physicochemical data obtained from the analysis of these monocationic ILs is compiled in Table 2-1. All monocationic ILs were liquids at room temperature. IL1, IL2, IL3, and IL4 appeared to be stable under the TGA experimental conditions to temperatures ≥400 °C. Thermal stabilities (via TGA) of IL5, IL6, IL7, and IL8 were lower than 350 °C. On the basis of this study, the $NTf_2^–$, $NPf_2^–$, and $PFOS^–$ anions provided the best thermal stability (Table 2-1). The structural similarity of $NPf_2^–$ and $NTf_2^–$ anions led us to select $NTf_2^–$ for our study due to its lower cost. $NTf_2^–$ and $PFOS^–$ were chosen as counteranions for the synthesis of "high stability ILs".

Table 2-1 Physicochemical properties of monocationic ILs

	ionic liquid	MW (g/mol)	Physical state at rt^e	thermal stability^a (°C)			density^b (g/cm^3)	viscosity^c (cP)		miscibility with heptane^d	miscibility with water^d
				99%w	95%w	85%w		30°C	50°C		
IL1	tribut-tetradec-P-NTf_2	679.8	liquid	330	405	454	1.10	202	73	M	I
IL2	tribut-tetradec-P-NPf_2	779.9	liquid	379	418	440	1.13	311	91	M	I
IL3	tribut-tetradec-P-PFOS	898.8	liquid	380	426	455	1.22	1672	350	M	I
IL4	tribut-tetradec-P-$FeCl_4$	597.4	liquid	311	401	450	0.98	1364	397	I	I
IL5	tribut-tetradec-P-FAP	844.7	liquid	241	303	336	1.23	327	130	I	I
IL6	tribut-tetradec-P-AOT	821.3	liquid	288	330	355	0.94	1393	387	M	I
IL7	tribut-tetradec-P-OS	593.0	liquid	93	194	369	0.89	125	53	M	I
IL8	tribut-tetradec-P-$B_{12}F_{12}$	757.4	liquid	194	298	432	0.90	-	-	I	I

[a] Thermal gravimetric analysis (TGA) analysis conditions: temperature program= 10 °C/min from room temperature (22 °C) to 600 °C, atmosphere= nitrogen, 99% w= temperature of 1% mass decrease of sample, 95% w= temperature of 5% mass decrease of sample, 85% w= temperature of 15% mass decrease of sample.

[b] Measured using pycnometer.

[c] Measured using capillary viscometer.

[d] I= immiscible, M= miscible.

[e] physical state at room temperature.

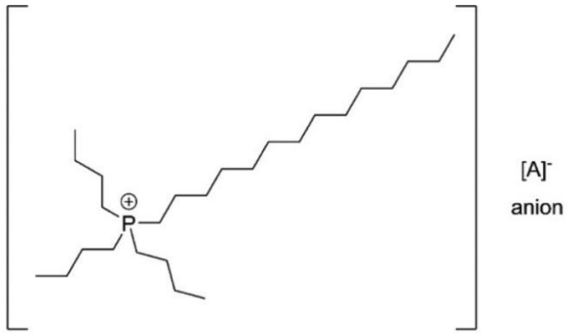

tributyltetradecyl phosphonium (TBTD-P) cation

cation	anion (A)	ionic liquid abbreviation	ionic liquid
tributyltetradecyl phosphonium (TBTD-P)	bis(trifluoromethane)sulfonimide (NTf_2)	TBTD-P-NTf_2	**IL1**
	bis(pentafluoromethane)sulfonimide (NPf_2)	TBTD-P-NPf_2	**IL2**
	perfluorooctanesulfonate (PFOS)	TBTD-P-PFOS	**IL3**
	iron tetrachloride ($FeCl_4$)	TBTD-P-$FeCl_4$	**IL4**
	tris(pentafluoroethyl)trifluorophosphate (FAP)	TBTD-P-FAP	**IL5**
	bis(2-ethylhexyl) sulfosuccinate (AOT)	TBTD-P-AOT	**IL6**
	1-octanesulfonate (OS)	TBTD-P-OS	**IL7**
	dodecafluoro-closo-dodecaborate ($B_{12}F_{12}$)	TBTD-P-$B_{12}F_{12}$	**IL8**

structures of anions:

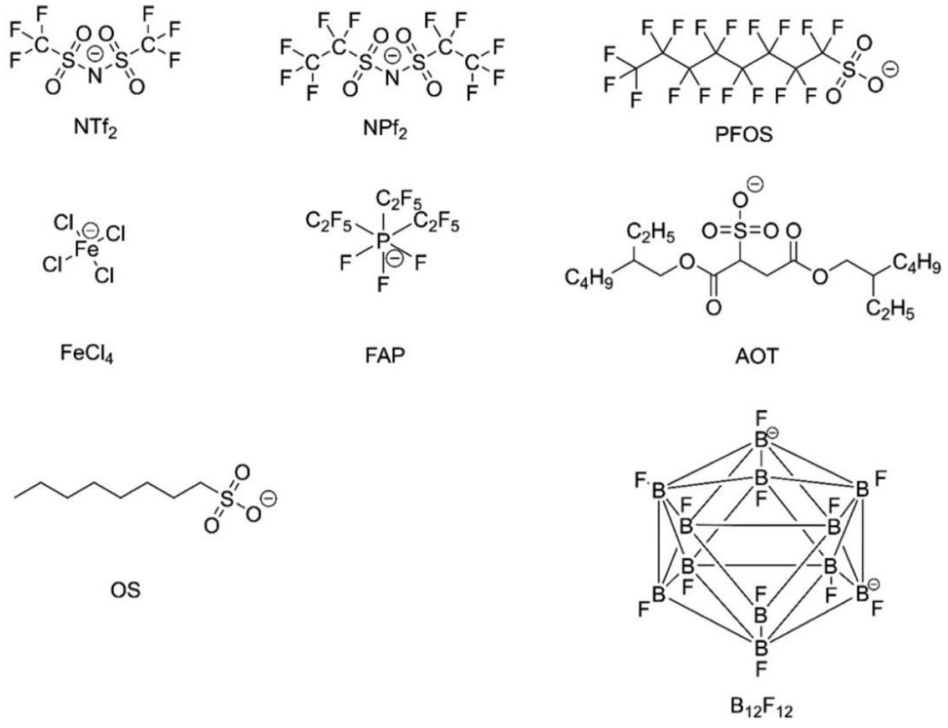

Figure 2-3 Structure and abbreviations of conventional ILs synthesized in this study

Monocationic ILs with $PFOS^-$ (IL3), $FeCl_4^-$ (IL4), and AOT (IL6) anions displayed higher viscosities compared to other monocationic ILs. The observed densities for monocationic ILs were in the range 0.89–1.23 g/cm^3, and the highest densities were observed for ILs with FAP (IL5) and $PFOS^-$ (IL3) anions. All the synthesized monocationic ILs were insoluble in water, but the ILs with NTf_2^-, NPf_2^-, $PFOS^-$, AOT^-, and OS^- anions were soluble in heptane.

Three general classes of dications were chosen for examination: (1) imidazolium, (2) pyrrolidinium, and (3) phosphonium. These dications were chosen on the basis of previous research which indicated that they had good thermal stabilities.[17,94] The presence of methyl or benzyl substituents at the C(3) position of the imidazolium ring was shown to enhance stability and/or decrease volatility.[17] Replacement of the acidic C(2) hydrogen with a methyl group appeared to confer additional stability to imidazolium ILs due to inhibition of reaction leading to the formation of carbenes.[110] So, the dications chosen had methyl groups at the C(2) position, and the C(3) position had either a benzyl or methyl substituent (see Figure 2-4). High stability dicationic ILs with N-substituted methyl and butyl groups on the pyrrolidinium ring were synthesized previously and shown to have good thermal stability and/or low volatility.[17] The same dications were selected for this study. However, the effect of short and long alkyl chains on pyrrolidinium stability was studied. Likewise, tripropyl and triphenyl substituted phosphonium dicationic salts were evaluated. The two cationic moieties were linked with 6 carbon (C_6), 9 carbon (C_9), and 12 carbon (C_{12}) alkane chains. Thus, 18 different symmetrical dications were evaluated. These dications were paired with the selected NTf_2^- and $PFOS^-$ anions. The dication and anion combinations resulted in 36 different dicationic ionic liquids. The structures of these ionic liquids are shown in Figure 2-4. The physicochemical data of all these ionic liquids is combined in Table 2-2 (C_6), Table 2-3 (C_9), and Table 2-4 (C_{12}).

Table 2-2 *Physicochemical Properties of C_6 alkane linkage chain ILs*

	ionic liquid	MW (g/mol)	melting point (°C)	thermal stability[a] (°C)			density[b] (g/cm^3)	viscosity[c] (cP)		miscibility with heptane[d]	miscibility with water[d]
				99%w	95%w	85%w		30°C	50°C		
IL9	$C_6(bmim)_2$-NTf_2	989.0	85-86	263	412	434	-	-	-	I	I
IL10	$C_6(m_2im)_2$-NTf_2	836.8	82-84	377	437	454	-	-	-	I	I
IL11	$C_6(bpy)_2$-NTf_2	899.0	99-101	351	403	421	-	-	-	I	I
IL12	$C_6(mpy)_2$-NTf_2	814.8	64-66	404	433	454	-	-	-	I	I
IL13	$C_6(pr_3p)_2$-NTf_2	965.0	95-96	396	408	422	-	-	-	I	I
IL14	$C_6(ph_3p)_2$-NTf_2	1169.1	146-148	367	405	443	-	-	-	I	I
IL15	$C_6(bmim)_2$-PFOS	1444.9	100-102	376	405	429	-	-	-	I	I
IL16	$C_6(m_2im)_2$-PFOS	1274.7	101-103	387	425	453	-	-	-	I	I
IL17	$C_6(bpy)_2$-PFOS	1336.9	155-157	369	391	407	-	-	-	I	I
IL18	$C_6(mpy)_2$-PFOS	1252.8	138-140	347	382	397	-	-	-	I	I
IL19	$C_6(pr_3p)_2$-PFOS	1403.0	121-123	368	401	417	-	-	-	I	I
IL20	$C_6(ph_3p)_2$-PFOS	1605.0	62-64	311	395	424	-	-	-	I	I

[a] *Thermal gravimetric analysis (TGA) analysis conditions: temperature program= 10 °C/min from room temperature (22 °C) to 600 °C, 99% w= temperature of 1% mass decrease of sample, 95% w= temperature of 5% mass decrease of sample, 85% w= temperature of 15% mass decrease of sample.*

[b] *Measured using pycnometer.*

[c] *Measured using capillary viscometer.*

[d] *I= immiscible, M= miscible.*

Table 2-3 *Physicochemical Properties of C_9 alkane linkage chain ILs*

	ionic liquid	MW (g/mol)	melting point (°C)	thermal stability[a] (°C)			density[b] (g/cm^3)	viscosity[c] (cP)		miscibility with heptane[d]	miscibility with water[d]
				99%w	95%w	85%w		30°C	50°C		
IL21	$C_9(bmim)_2$-NTf_2	1031.0	>-76, <-22[e]	166	437	453	1.42	3132	568	I	I
IL22	$C_9(m_2im)_2$-NTf_2	878.8	>-76, <-22[e]	185	467	485	1.47	690	198	I	I
IL23	$C_9(bpy)_2$-NTf_2	941.0	87-89	344	426	449	-	-	-	I	I
IL24	$C_9(mpy)_2$-NTf_2	856.8	>-22, <4[e]	310	447	461	1.46	1040	290	I	I
IL25	$C_9(pr_3p)_2$-NTf_2	1007.0	89-91	366	464	480	-	-	-	I	I
IL26	$C_9(ph_3p)_2$-NTf_2	1211.1	82-84	378	424	457	-	-	-	I	I
IL27	$C_9(bmim)_2$-PFOS	1468.9	147-148	409	416	451	-	-	-	I	I
IL28	$C_9(m_2im)_2$-PFOS	1316.7	133-135	428	450	473	-	-	-	I	I
IL29	$C_9(bpy)_2$-PFOS	1378.9	214-216	317	353	391	-	-	-	I	I
IL30	$C_9(mpy)_2$-PFOS	1294.8	157-159	332	373	421	-	-	-	I	I
IL31	$C_9(pr_3p)_2$-PFOS	1445.0	78-80	368	412	423	-	-	-	I	I
IL32	$C_9(ph_3p)_2$-PFOS	1649.0	56-58	301	407	420	-	-	-	I	I

[a] *Thermal gravimetric analysis (TGA) analysis conditions: temperature program= 10 °C/min from room temperature (22 °C) to 600 °C, 99% w= temperature of 1% mass decrease of sample, 95% w= temperature of 5% mass decrease of sample, 85% w= temperature of 15% mass decrease of sample.*

[b] *Measured using pycnometer.*

[c] *Measured using capillary viscometer.*

[d] *I= immiscible, M= miscible.*

[e] *Liquid at room temperature, melting point is in the given range.*

2.3.1 Melting point

The melting point of an ionic liquid depends on the crystal lattice energy between the cation and anion.[1] The crystal lattice energy depends on interionic forces, molecular symmetry, and conformational degrees of freedom of the molecule.[111] ILs with PFOS$^-$ anions have higher melting point than ILs with NTf_2^- anions. The NTf_2^- anion has more charge delocalization than the PFOS$^-$ anion. More charge delocalization generally leads to a decrease in melting point.[112] Also, the PFOS$^-$ anion has a higher molar mass than

NTf_2^- which can also raise the melting point. The only exceptions to this trend were the ph_3p-dicationic ILs in which the NTf_2^- ILs have higher melting point than $PFOS^-$ ILs.

Table 2-4 *Physicochemical Properties of C_{12} alkane linkage chain ILs*

	ionic liquid	MW (g/mol)	melting point (°C)	thermal stability[a] (°C)			density[b] (g/cm^3)	viscosity[c] (cP)		miscibility with heptane[d]	miscibility with water[d]
				99% w	95% w	85% w		30°C	50°C		
IL33	$C_{12}(bmim)_2$-NTf_2	1085.0	>-76, <-22[e]	182	394	419	1.36	2970	612.5	I	I
IL34	$C_{12}(m_2im)_2$-NTf_2	932.8	55-56	418	442	455	-	-	-	I	I
IL35	$C_{12}(bpy)_2$-NTf_2	995.0	53-54	352	398	425	-	-	-	I	I
IL36	$C_{12}(mpy)_2$-NTf_2	910.8	>-76, <-22[e]	400	422	434	1.38	930	282.5	I	I
IL37	$C_{12}(pr_3p)_2$-NTf_2	1061.0	40-45	234	392	422	-	-	-	I	I
IL38	$C_{12}(ph_3p)_2$-NTf_2	1265.1	118-119	352	385	403	-	-	-	I	I
IL39	$C_{12}(bmim)_2$- PFOS	1540.9	99-101	354	385	410	-	-	-	I	I
IL40	$C_{12}(m_2im)_2$-PFOS	1370.7	98-100	387	412	429	-	-	-	I	I
IL41	$C_{12}(bpy)_2$-PFOS	1432.9	165-167	243	329	369	-	-	-	I	I
IL42	$C_{12}(mpy)_2$-PFOS	1348.8	136-137	343	369	383	-	-	-	I	I
IL43	$C_{12}(pr_3p)_2$-PFOS	1499.0	86-87	232	387	419	-	-	-	I	I
IL44	$C_{12}(ph_3p)_2$-PFOS	1701.0	71-73	346	381	401	-	-	-	I	I

[a] *Thermal gravimetric analysis (TGA) analysis conditions: temperature program= 10 °C/min from room temperature (22 °C) to 600 °C, 99% w= temperature of 1% mass decrease of sample, 95% w= temperature of 5% mass decrease of sample, 85% w= temperature of 15% mass decrease of sample.*

[b] *Measured using pycnometer.*

[c] *Measured using capillary viscometer.*

[d] *I= immiscible, M= miscible.*

[e] *Liquid at room temperature, melting point is in the given range.*

In general, the melting points of dicationic ILs with NTf_2^- anions are dependent on the length of the alkyl linkage chain. ILs with C_6 linkage chains have higher melting points than analogous ILs with C_9 and C_{12} linkage chains. Also, C_9 ILs with NTf_2^- anions have higher melting points than C_{12} ILs with the same cationic groups. As the length of spacer alkane chain length increases, melting points decrease due to the added conformational degrees of freedom.[111] Some exceptions were observed to this trend. The $m_2$im and ph_3ph dicationic ILs with C_{12} linkages had slightly higher melting points than the analogous dicationic ILs with C_9 linkers. In the case of pyrrolidinium based ILs, the butyl substituted ILs (bpy) have higher melting points than those of the methyl substituted ILs.[17]

The melting points of $PFOS^-$ ILs were found to exhibit a different behavior. The imidazolium and pyrrolidinium based ILs with C_9 linkages had higher melting points, and the C_6 and C_{12} linked ILs had lower, but comparable, melting points. Conversely, the phosphonium based ILs with C_9 linkers had lower melting points than those with C_6 and C_{12} linkage chains. All the synthesized ILs were symmetrical, and most of them were solids at room temperature. The ILs which were liquid at room temperature were $C_9(bmim)_2$-NTf_2, $C_{12}(bmim)_2$-NTf_2, $C_9(m_2im)_2$-NTf_2, $C_9(mpy)_2$-NTf_2, and $C_{12}(mpy)_2$-NTf_2. ILs with the $PFOS^-$ anion were all solids at room temperature.

Some analogous solid ILs with high thermal stabilities were combined to lower the melting points of the resulting IL mixture (Table 2-5). The ILs with the same cation and anion but different alkane linkage chains (C_9 and C_{12}) were mixed in different weight percentages. Thus, 13 different mixtures of ILs (IL45 to IL57) were synthesized from four groups of analogous ILs which are $(bpy)_2$-NTf_2, $(pr_3p)_2$-NTf_2, $(bmim)_2$-PFOS, and $(pr_3p)_2$-PFOS. A significant decrease in melting points was achieved with the mixtures. The mixtures with lowest melting points from every group were selected and used for coating on GC columns.

2.3.2 Viscosity

The viscosities were determined at 30 and 50 °C for the five ILs that were liquids at room temperature. Imidazolium ILs containing benzyl groups have considerably higher viscosities than pyrrolidinium and dimethyl imidazolium ILs. The presence of benzyl group adds extra intermolecular π–π interactions which may be a factor leading to higher viscosity. Methylpyrrolidine ILs had higher viscosities than dimethylimidazolium ILs of the same connecting chain lengths.

Table 2-5 *Melting points of mixtures of ILs*

	ionic liquid A (IL-A) (C_9 linkage chain)	weight percentage of IL-A	ionic liquid B (IL-B) (C_{12} linkage chain)	weight percentage of IL-B	final ionic liquid[a] (IL-A + IL-B)	melting point (°C)
IL45 mix	$C_9(bpy)_2$-NTf_2	30	$C_{12}(bpy)_2$-NTf_2	70	$C_{mix}(bpy)_2$-NTf_2	43-55
IL46 mix	$C_9(bpy)_2$-NTf_2	50	$C_{12}(bpy)_2$-NTf_2	50	-	49-65
IL47 mix	$C_9(bpy)_2$-NTf_2	70	$C_{12}(bpy)_2$-NTf_2	30	-	69-73
IL48 mix	$C_9(pr_3p)_2$-NTf_2	30	$C_{12}(pr_3p)_2$-NTf_2	70	-	58-62
IL49 mix	$C_9(pr_3p)_2$-NTf_2	40	$C_{12}(pr_3p)_2$-NTf_2	60	$C_{mix}(pr_3p)_2$-NTf_2	55-62
IL50 mix	$C_9(pr_3p)_2$-NTf_2	50	$C_{12}(pr_3p)_2$-NTf_2	50	-	58-69
IL51 mix	$C_9(pr_3p)_2$-NTf_2	70	$C_{12}(pr_3p)_2$-NTf_2	30	-	73-79
IL52 mix	$C_9(bmim)_2$-PFOS	30	$C_{12}(bmim)_2$- PFOS	70	-	69-78
IL53 mix	$C_9(bmim)_2$-PFOS	50	$C_{12}(bmim)_2$- PFOS	50	-	65-76
IL54 mix	$C_9(bmim)_2$-PFOS	70	$C_{12}(bmim)_2$- PFOS	30	$C_{mix}(bmim)_2$-PFOS	59-70
IL55 mix	$C_9(pr_3p)_2$-PFOS	30	$C_{12}(pr_3p)_2$-PFOS	70	-	72-85
IL56 mix	$C_9(pr_3p)_2$-PFOS	50	$C_{12}(pr_3p)_2$-PFOS	50	-	70-81
IL57 mix	$C_9(pr_3p)_2$-PFOS	70	$C_{12}(pr_3p)_2$-PFOS	30	-	63-74

[a] *Naming was done only to mixtures with low melting points and were selected for GC-FID study*

2.3.3 Density

Similar to viscosity, density measurements were done for the ILs that were liquids at room temperature. Densities for dicationic ILs were found to be higher than those for monocationic ILs. ILs with C_9 alkane linkages have somewhat higher densities than ILs with C_{12} linkages. The decrease in density with increase in alkane linkage for dicationic ILs has been reported previously.[17]

2.3.4 Solubility

All the dicationic ILs synthesized in this study were insoluble in both water and heptane. All the monocationic ILs were insoluble in water, but some of these ILs, with NTf_2^-, NPf_2^-, $PFOS^-$, AOT^-, and OS^- anions, were soluble in heptane.

2.3.5 Thermal stability

Thermal stability of ILs was determined using thermogravimetric analysis (TGA). The thermal stability of dicationic ILs were compared in Figure 2-5 at the 5% weight loss level. Geminal dicationic ILs can be considered as a combination of three main structural moieties: (1) a cation head group, (2) an alkane linker chain, and (3) the anions. The effect of each component on the physical and chemical properties was studied by single variable modifications.

Base structure

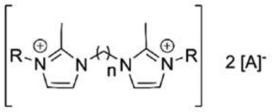

Imidazolium

substituent (R)	anion (A)	linker chain length (n)	ionic liquid abbreviation	ionic liquid
benzyl	NTf_2	6	C_6(bmim)$_2$-NTf$_2$	**IL9**
		9	C_9(bmim)$_2$-NTf$_2$	**IL21**
		12	C_{12}(bmim)$_2$-NTf$_2$	**IL33**
	PFOS	6	C_6(bmim)$_2$-PFOS	**IL15**
		9	C_9(bmim)$_2$-PFOS	**IL27**
		12	C_{12}(bmim)$_2$-PFOS	**IL39**
methyl	NTf_2	6	C_6(m$_2$im)$_2$-NTf$_2$	**IL10**
		9	C_9(m$_2$im)$_2$-NTf$_2$	**IL22**
		12	C_{12}(m$_2$im)$_2$-NTf$_2$	**IL34**
	PFOS	6	C_6(m$_2$im)$_2$-PFOS	**IL16**
		9	C_9(m$_2$im)$_2$-PFOS	**IL28**
		12	C_{12}(m$_2$im)$_2$-PFOS	**IL40**

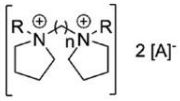

Pyrrolidinium

substituent (R)	anion (A)	linker chain length (n)	ionic liquid abbreviation	ionic liquid
n-butyl	NTf_2	6	C_6(bpy)$_2$-NTf$_2$	**IL11**
		9	C_9(bpy)$_2$-NTf$_2$	**IL23**
		12	C_{12}(bpy)$_2$-NTf$_2$	**IL35**
	PFOS	6	C_6(bpy)$_2$-PFOS	**IL17**
		9	C_9(bpy)$_2$-PFOS	**IL29**
		12	C_{12}(bpy)$_2$-PFOS	**IL41**
methyl	NTf_2	6	C_6(mpy)$_2$-NTf$_2$	**IL12**
		9	C_9(mpy)$_2$-NTf$_2$	**IL24**
		12	C_{12}(mpy)$_2$-NTf$_2$	**IL36**
	PFOS	6	C_6(mpy)$_2$-PFOS	**IL18**
		9	C_9(mpy)$_2$-PFOS	**IL30**
		12	C_{12}(mpy)$_2$-PFOS	**IL42**

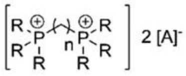

Phosphonium

substituent (R)	anion (A)	linker chain length (n)	ionic liquid abbreviation	ionic liquid
propyl	NTf_2	6	C_6(pr$_3$p)$_2$-NTf$_2$	**IL13**
		9	C_9(pr$_3$p $_2$-NTf$_2$	**IL25**
		12	C_{12}(pr$_3$p)$_2$-NTf$_2$	**IL37**
	PFOS	6	C_6(pr$_3$p)$_2$-PFOS	**IL19**
		9	C_9(pr$_3$p)$_2$-PFOS	**IL31**
		12	C_{12}(pr$_3$p)$_2$-PFOS	**IL43**
phenyl	NTf_2	6	C_6(ph$_3$p)$_2$-NTf$_2$	**IL14**
		9	C_9(ph$_3$p)$_2$-NTf$_2$	**IL26**
		12	C_{12}(ph$_3$p)$_2$-NTf$_2$	**IL38**
	PFOS	6	C_6(ph$_3$p)$_2$-PFOS	**IL20**
		9	C_9(ph$_3$p)$_2$-PFOS	**IL32**
		12	C_{12}(ph$_3$p)$_2$-PFOS	**IL44**

Figure 2-4 Structure and abbreviations of dicationic ILs synthesized in this study

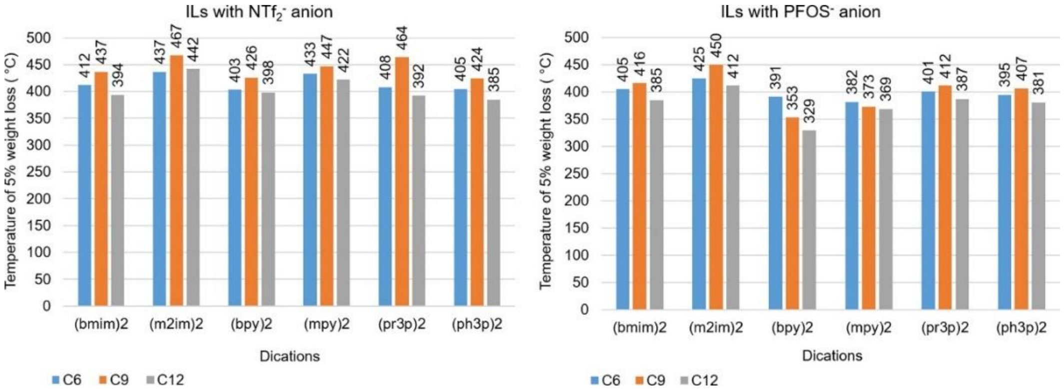

Figure 2-5 Thermal stability comparison of ILs synthesized in this study

2.3.5.1 Effect of the anion

NTf$_2^-$ based ILs were observed to have somewhat greater thermal stability compared to analogous ILs with PFOS$^-$ counteranions. This may be attributed to the higher nucleophilicity of the PFOS$^-$ anion as compared to the NTf$_2^-$ anion, as NTf$_2^-$ shows greater negative charge delocalization. The decrease in IL thermal stability with increasing nucleophilicity of the anion was previously reported by Bonhote et al.[113]

2.3.5.2 Effect of linker chain length

The thermal stabilities of dicationic ILs with C$_9$ linkage chains were observed to be higher than those of the analogous C$_6$ and C$_{12}$ ILs. In addition, it can be seen that the densities and viscosities of the C$_9$ ILs are generally greater than those of their C$_6$ and C$_{12}$ analogues. Higher densities, meaning smaller free volumes between molecules and higher shear viscosities, may favor reversibility of breakdown reactions or recombination of fragments. The reversibility leading to recombination of fragments, also known as the "cage effect", can lead to higher thermal stabilities.[8,20] ILs with C$_6$ linkage chains have higher thermal stabilities than those analogous dications with C$_{12}$ linkage chains. Therefore, an increase in the alkane linkage from C$_6$ to C$_9$ leads to an increase in thermal stability while further increases in chain length lead to a decrease in thermal stability ($C_{12} < C_6 < C_9$).

In the case of ILs with the $PFOS^-$ anion, imidazolium and phosphonium based ILs with the C_9 linker chains were found to be more stable than C_6 and C_{12} linked ILs, thereby following a similar trend to the NTf_2^- ILs. Conversely, pyrrolidinium based dicationic ILs with C_6 linkages showed higher thermal stability than the analogous C_9 and C_{12} ILs. $C_6(bpy)_2$-PFOS is more stable than $C_9(bpy)_2$-PFOS and $C_{12}(bpy)_2$-PFOS, and $C_6(mpy)_2$-PFOS is more stable than $C_9(mpy)_2$-PFOS and $C_{12}(mpy)_2$-PFOS.

2.3.5.3 Effect of cationic head group

In case of imidazolium based ILs, the C(3) methylated (m_2im) dicationic ILs are more stable than the corresponding (bmim) dicationic ILs. The presence of methyl groups at the C(3) positions of the imidazole ring conferred more stability than did benzyl groups at the same position. The TGA experiments indicated that the ILs containing the dimethylimidazolium dications usually showed slightly higher thermal stabilities. In the case of the pyrrolidinium based ILs, those substituted with methyl groups (mpy) were more stable than those substituted with butyl groups (bpy). Increasing the length of the alkyl chain substituent on the pyrrolidinium nitrogen leads to a decrease in the IL thermal stability. The stability of linear, aliphatic carbocations and carbon radicals increases with increasing chain length. This stability means that longer chains can be better leaving groups during heating processes, and this infers a more facile disconnection of the C–N bond. Overall, this effect tends to decrease the thermal stability of analogous compounds with longer alkyl chains.[114]

For phosphonium based ILs, the thermal stability of the tripropylphosphonium ILs (pr_3p) was higher than that of the analogous triphenylphosphonium ILs (ph_3p). Obviously,

ph_3p dications are bulkier than pr_3p due to the presence of three phenyl rings on a single phosphorus atom (cone angle of ph_3p > cone angle of pr_3p).[115] Breaking of the ph_3p C–P bond may be accentuated at higher temperatures to lower the steric strain, which, in turn, would lead to lower thermal stabilities. $C_9(m_2im)_2$-NTf_2 (467 °C) and $C_9(pr_3ph)_2$-NTf_2 (464 °C) showed the best TGA stability (at the 95% weight loss level) of all the synthesized ILs. Other ILs which displayed high TGA stability were $C_9(m_2im)_2$-PFOS (450 °C), $C_9(mpy)_2$-NTf_2 (447 °C), and $C_{12}(m_2im)_2$-NTf_2 (442 °C). TGA is not the only way to measure thermal stability/volatility. Indeed, depending on the analysis program used, its results can sometimes differ from those of other tests (see the following section).

2.3.6 Thermal stability with inverse-GC

Nine different dicationic ILs with TGA thermal stabilities higher than 400 °C and having low melting points were selected and coated on GC capillary columns. Some ILs having high thermal stability but melting points around 60 °C were mixed with an analogous IL with a different alkane linkage but the same cations and anions. This was done to lower the melting point of mixture. Low melting ILs can act as good GC stationary phases. For example, $C_9(pr_3p)_2$-NTf_2, $C_{12}(pr_3p)_2$-NTf_2, $C_9(bpy)_2$-NTf_2, $C_{12}(bpy)_2$-NTf_2, $C_9(bmim)_2$-PFOS, and $C_{12}(bmim)_2$-PFOS ILs have high thermal stabilities (>400 °C) but also high melting points. In order to lower melting points, analogous ILs with C_9 and C_{12} alkane linkage were mixed together in different ratios. The mixtures with the lowest melting points were chosen to coat the inner surface of capillary GC columns.

Inverse gas chromatography with FID can be a more sensitive method than TGA when examining the thermal stability of ILs.[17] In a reverse GC experiment, the IL coated columns were heated from room temperature (22 °C) to 450 °C at a temperature ramp of 1 °C/min, which is much slower than the temperature ramp used in TGA (10 °C/min). FID is a very sensitive detector and allows sensitive detection of even trace volatile/decomposed products from ILs. Consequently, stability testing with GC-FID can sometimes give a more accurate indication of the stability of ILs depending on the experimental conditions. The data collected with GC-FID is shown in Figure 2-6. The highest thermal stabilities were observed for $C_{mix}(pr_3ph)_2$-NTf_2 and $C_{12}(m_2im)_2$-NTf_2 (first bleeding at 400 °C), followed by $C_9(mpy)_2$-NTf_2 (bleeding at 390 °C) and $C_{12}(m_2im)_2$-NTf_2 (bleeding at 380 °C). $(bmim)_2$-NTf_2 with C_9 and C_{12} linkages were stable up to 300 °C (lower than observed with TGA). $C_{12}(mpy)_2$-NTf_2 and $C_{mix}(bpy)_2$-NTf_2 started bleeding at 320 °C. $C_{mix}(bmim)_2$-PFOS IL was the least stable and started bleeding at 260 °C.

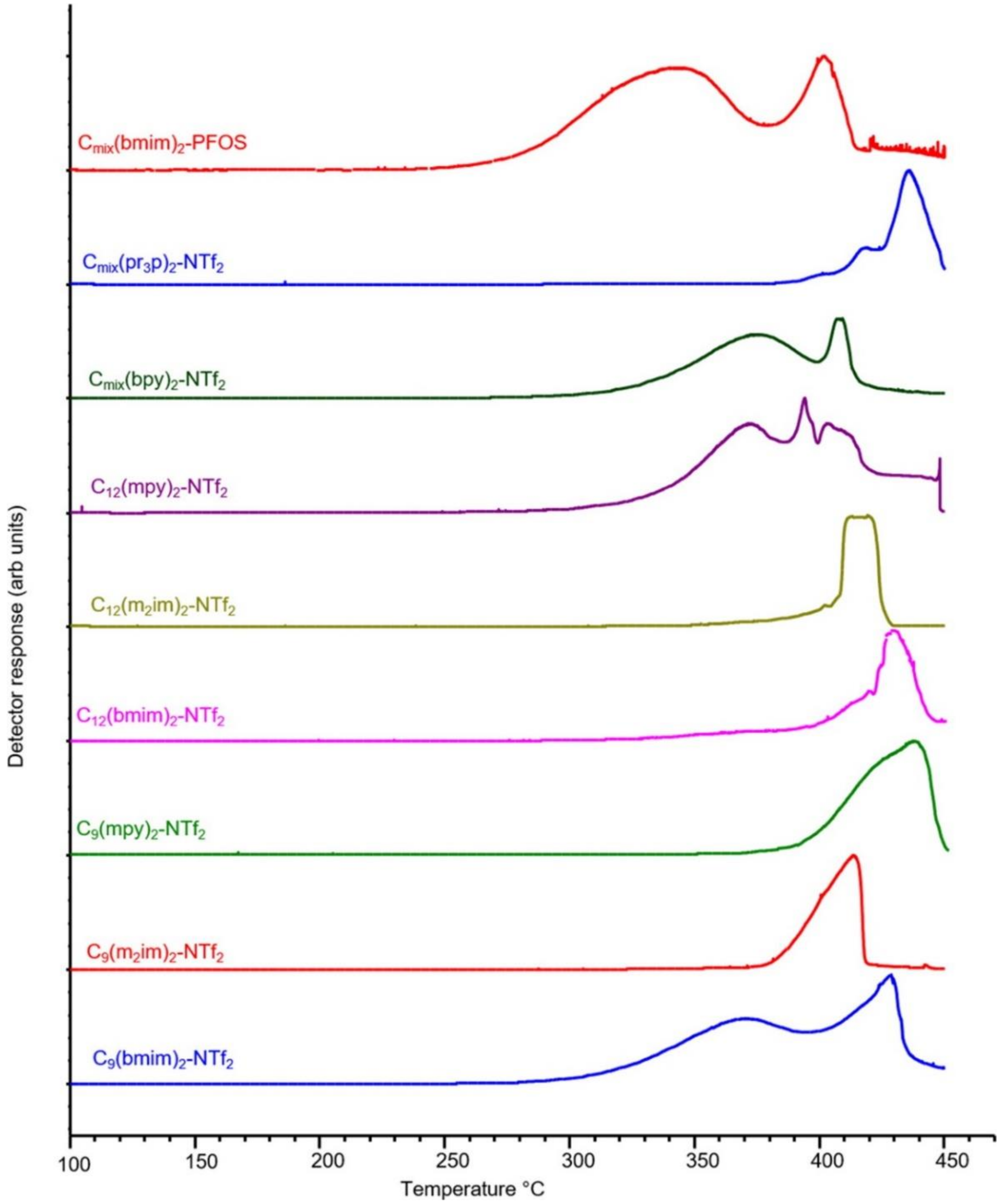

Figure 2-6 Thermal stability diagram with GC-FID for nine dicationic ILs. Plot shows the bleeding temperature of ILs as GC stationary phases. The study was done with oven temperature ramp of 1 °C/min with helium as carrier gas and flow 1 mL/min

2.3.6 Performance Testing of ILs as GC Stationary Phases

One of the synthesized ILs, C9-(m2im)2-NTf2, which showed GC-FID stability up to 350 °C, was further evaluated for performance as the GC stationary phase. The selected IL was coated on a 30 m capillary column (internal diameter of 0.25 mm), and the column was used for the separation of polycyclic aromatic hydrocarbons (PAHs). PAHs are ubiquitous environmental pollutants derived mainly from incomplete combustion of organic materials.[116] "Benzo-fluoranthenes" are PAHs with three structural isomers: benzo[b]-fluoranthene, benzo[j]-fluoranthene, and benzo[k]-fluoranthene. The separation and detection of these structural isomers is difficult due to high degree of overlap in the boiling points of these compounds.[117] Typically, the separation of PAHs is performed on methyl and phenyl substituted polysiloxanes stationary phases.[118] The traditional polysiloxane based stationary phases are not efficient for the separation of these structural isomers, and they typically coelute. However, the thermally stable C9-(m2im)2-NTf2 IL based column effectively separated the structural isomers at temperature of 280 °C. The separation is shown in Figure 2-7.

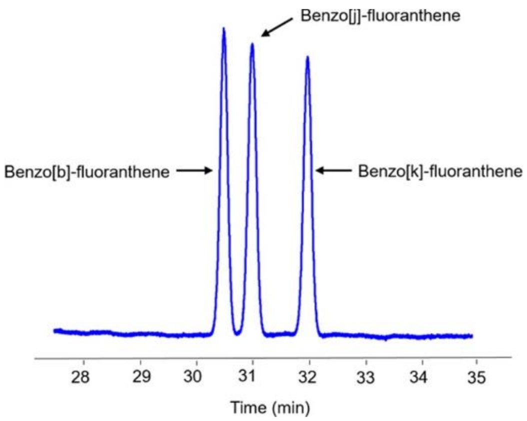

Figure 2-7 Separation of structural isomers of benzofluoranthene by GC on C_9-$(m_2im)_2$-NTf_2 IL column (30 m × 0.25 mm i.d.). GC separation conditions: 150–250 °C at 20 °C/min, hold 2 min, 20 °C/min to 280 °C, 1 mL/min He; FID

2.4 Conclusions

In this study, we have demonstrated the effect of different structural modifications including alkane linkage chain, substituents, and type, of dications and anions on the physicochemical properties of ILs. The new series of synthesized dicationic ILs with different structural moieties displayed excellent TGA thermal stabilities up to 460 °C. A correlation between the physicochemical properties of analogous ILs and their unique structural features was observed. In general, ILs with C_9 linkage chains had higher stability than C_6 and C_{12} linkage chain ILs. They also had higher viscosities and densities. Within the three different classes of dications, comparison of stabilities of analogous ILs led to following observations: imidazolium group, $m_2im > bmim$; pyrrolidinium group, mpy > bpy; and phosphonium group, $pr_3p > ph_3p$. Also, some ILs tested with GC-FID showed stability up to 400 °C ($C_{mix}(pr_3p)_2$-NTf_2 and $C_{12}(m_2im)_2$-NTf_2). The thermal stability of ILs with NTf_2^- anions was higher than those with $PFOS^-$ anions. Also, NTf_2^- anions tended to lower the melting points of ILs. Dicationic ILs with $PFOS^-$ anions were all solids at room temperature and had higher melting points compared to NTf_2^- based ILs. The melting points of ILs found to decrease with length of alkane linkage chain due to added conformational degrees of freedom. N-Butyl substituted pyrrolidinium dicationic ILs have higher melting points than N-methyl substituted pyrrolidinium ILs. The densities of dicationic ILs were higher than monocationic ILs, and dicationic ILs with C_9 alkane linkages had higher densities than analogous ILs with C_{12} linkers. Benzyl substituted imidazolium ILs displayed the highest viscosities of all the dicationic ILs studied.

Performance testing of C_9-$(m_2im)_2$-NTf_2 IL as GC stationary phase at high temperatures provided an exceptional separation of the benzo-fluoranthene isomers.

Chapter 3

EXAMINATION OF SELECTIVITIES OF THERMALLY STABLE GEMINAL DICATIONIC IONIC LIQUIDS BY STRUCTURAL MODIFICATION

Abstract

Dicationic ionic liquid (IL) are widely used as gas chromatography (GC) stationary phases as they show higher thermal stabilities, variety of polarities and unique selectivities towards certain compounds. An important aspect contributing to them is that they show multiple solvation interactions compared to traditional GC stationary phases. Dicationic ILs are considered as combination of three structural moieties: 1) cationic head groups, 2) a linkage chain, and 3) the counter anions. Modifications in these structural moieties can alter the chromatographic properties of IL stationary phases. In this study a series of nine thermally stable ionic liquid stationary phases were synthesized by the combination of five different cations, two different linkage chains, and two different anions. Different test mixtures composed of a variety of compounds having different functional groups and polarities were analyzed on these columns. A comparison of the separation patterns of these different compounds on nine different IL columns provided some insights about the effects of structural modifications on the selectivities and polarities of dicationic ionic liquids.

3.1 Introduction

Ionic Liquids (ILs) are salts with melting points generally less than 100 °C.[13] ILs generally consist of nitrogen or phosphorus containing organic cations and an inorganic or organic anion.[119] ILs are of interest to researchers due to their many fascinating properties such as high thermal stabilities, low volatilities (negligible vapor pressure), non-flammability, tunable viscosities, high densities, wide liquid temperature range, adjustable miscibility, conductivity, high chemical stability and so on.[17,120] These unique physical and chemical properties are the reasons for their usefulness in many different areas of chemistry such as solvents for organic synthesis reactions,[26,121-124] gas chromatographic stationary phases,[11,94,120] high temperature lubricants,[18,125] solvents for liquid-liquid extractions,[126-129] matrices for MALDI-MS,[130-134] and electrochemical studies.[135-140]

The best performance of ILs as gas chromatography (GC) stationary phases is obtained when they are liquids at room temperature.[120] The specific properties of RTILs such as low volatility, high thermal stability, excellent selectivities for certain compounds and good wetting abilities have made them suitable and popular as GC stationary phases.[28,39,141] Generally, traditional stationary phases show one dominant type of chemical interaction, while IL phases show multiple solvation interactions and this is the origin of their unique selectivity toward a variety of molecules with many different functional groups.[39] As ILs provide different selectivities, IL stationary phases have been used in different applications. They are popular in the separation of fatty acid methyl esters (FAMEs), flavors, fragrances, aromatic hydrocarbons and environmental pollutants.[45-47,56,142-146] Most of the ILs are air and moisture stable, they have been used in the analysis of water content in pharmaceuticals, petroleum products, and foods.[29-33] ILs with higher thermal stabilities and a variety of polarities have opened new exciting possibilities in the field of multidimensional gas chromatography.[144,147-149] Currently more research is being done towards the improvement of the thermal stabilities of ILs and producing even greater variations in their selectivities.

Geminal dicationic ILs often display higher thermal stabilities compared to traditional monocationic ILs.[7,17] Also, dicationic ionic liquids have advantages in terms of tuning their physicochemical properties by structural modifications. The geminal dicationic ILs are considered as a combination of three structural moieties: 1) cationic head groups, (2) a linkage chain and (3) the counter anions. Modifications in these structural moieties can alter their physicochemical properties such as thermal stabilities, viscosities, densities, and melting points.[7,17] Also, such structural modifications can modify the chromatographic properties of IL stationary phases. Since the selectivities of dicationic ILs vary with their structure, a systematic study showing the effects of modification of each structural moiety on the polarities and selectivities of dicationic ILs is needed.

We recently synthesized a series of thirty-six thermally stable geminal dicationic ionic liquids.[7] The thermogravimetric analysis (TGA) stabilities of these ILs were in the range of 330 – 467 °C. Nine ILs with high TGA stability and low melting points were tested for stability with inverse gas chromatography – flame ionization detector (GC-FID) and they displayed short term stability up to 400 °C. The current study focuses on the further evaluation of these nine thermally stable ILs as GC stationary phases. The selected dicationic ILs are combinations of five different cations, two different alkane linker chains and two different anions. Different test mixtures composed of a variety of compounds with different polarities and functional groups were injected on these IL columns. A comparison of separation patterns of different compounds on the IL columns provided insights into the effects of structural modifications on the polarities and selectivities of dicationic ILs.

3.2 Experimental

2.2.1 Materials:

1-Benzyl-2-methylimidazole (90%), 1,2-dimethylimidazole (98%), N-methylpyrrolidine (97%), 1-butylpyrrolidine (98%), tripropylphosphine (97%), 1,9-dibromononane (97%), 1,12-dibromododecane (98%), bis(trifluoromethane)sulfonimide lithium salt (99.95%), and heptadecafluorooctanesulfonic acid potassium salt (98%) were purchased from Sigma-Aldrich (St. Louis, MO). The detailed procedures for synthesis of ILs are reported in the literature.[150] The structures of synthesized IL stationary phases are given in Figure 3-1. The ILs were coated on fused silica capillary columns with dimensions 30m x 0.25 mm i.d. and film thickness of 0.20 µm. All the IL coated columns were provided by Supelco (Bellefonte, PA). The commercial SLB IL111 column and all test mixes used to characterize the stationary phases were provided by MilliporeSigma (Bellefonte, PA).

FAME test mix is a mixture of 11 compounds; methyl myristate (C14:0), methyl palmitate (C16:0), methyl stearate (C18:0), methyl oleate (C18:1n9), methyl linoleate (C18:2n6), methyl linolenate (C18:3n3), methyl arachidate (C20:0), cis-11-Eicosenoic acid methyl ester (C20:1), methyl behenate (C22:0), erucic acid methyl ester (C22:1), and methyl tetracosanoate (C24:0) at different concentrations in dichloromethane. Grob test mix is a mixture of 12 compounds; dicyclohexylamine, methyl decanoate, methyl undecanoate, methyl laurate, decane, undecane, 1-nonanal, 1-octanol, 2-ethylhexanoic acid, 2,3-butanediol, 2,6-dimethylaniline, and 2,6-dimethylphenol at different concentrations in dichloromethane. Polar Plus test mix is a mixture of 13 compounds; 2-octanone, 1-octanol, 2,6-dimethylaniline, 2,6-dimethylphenol, pentadecane, hexadecane, heptadecane, octadecane, icosane, heneicosane, docosane, tetracosane, and pentacosane at concentrations of 500 ppm each in dichloromethane. PAM-HC test mix is a mixture of 15 compounds; naphthalene, acenaphthylene, acenaphthene, fluorene, phenanthrene, anthracene, fluoranthene, pyrene, triacontane, dotriacontane, tetratriacontane, hexatriacontane, octatriacontane, tetracontane, and tetratetracontane at concentrations of 100 ppm each in dichloromethane. Custom-PAM test mix is a mixture of 9 compounds; naphthalene, phenanthrene, anthracene, benzo(a)anthracene, chrysene, triphenylene, benzo(b)fluoranthene, benzo(k)fluoranthene, and benzo(j)fluoranthene (MW- 252) S) at concentrations of 100 ppm each in dichloromethane. Ionic Liquid test mix is a mixture of 14 compounds; toluene, camphene, tridecane, 2,6-di-t-butyl-4-methylene-2,5 cyclohexadiene-1-one, naphthalene, 2,6-dimethylaniline, dimethylsulfoxide, methyl linolenate, methyl arachidate, cis-11-Eicosenoic acid methyl ester, coumarin, dioctyladipate, tetracosane, and tetracontane at different concentrations in dichloromethane.

The identification of different compounds of the test mixtures was done by analyzing individual standards of each compound.

2.2.2 Instrumentation

The gas chromatographic analyses were made using Agilent 6890N gas chromatograph equipped with flame ionization detector. Helium was used as a carrier gas. Efficiencies of all the IL columns were determined by using naphthalene at 110 °C and were ~4000 plates m^{-1}.

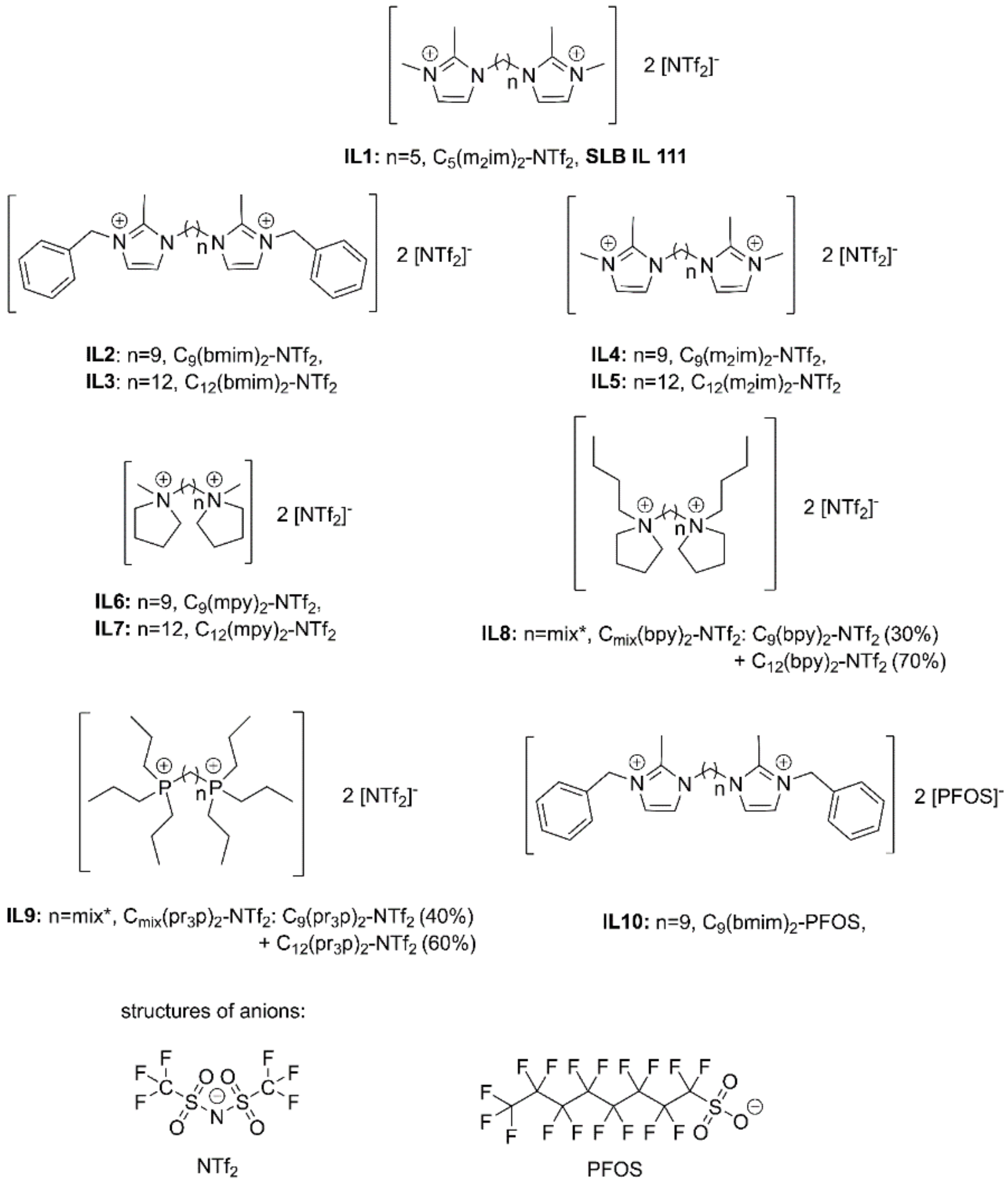

*The ionic liquids with the same cation and anion but different alkane linkage chains (C_9 and C_{12}) were mixed in the given weight percentages

Figure 3-1 Structures and abbreviations of dicationic ILs studied in this analysis

3.3 Results and Discussion

Nine different geminal dicationic ILs which are combination of different cationic groups, alkane linkage chains and anions were chosen for analysis (see Figure 3-1). The three general classes of dications were; (1) Imidazolium: benzylmethylimidazolium and dimethylimidazolium, (2) pyrrolidinium: methylpyrrolidinium and butyl pyrrolidinium, and (3) phosphonium: tripropylphosphonium. The two cationic moieties were linked together by two different alkane linkage chains; 9 carbon (C_9) and 12 carbon (C_{12}). The resulting dications were paired with NTf_2^- and $PFOS^-$ anions. **IL8 and IL9** are mixtures of analogous ILs with same cation and anion but different alkane linkage chains (C_9 and C_{12}) with a specific weight percentages (**IL8**: mixture of $C_9(bpy)_2$-NTf_2 (30%) and $C_{12}(bpy)_2$-NTf_2 (70%); **IL9**: mixture of $C_9(pr_3p)_2$-NTf_2 (40%) and $C_{12}(pr_3p)_2$-NTf_2 (60%)) (see Figure 3-1). This was necessary in order to decrease the melting points of the resulting mixtures to a level that was amenable for gas-liquid chromatography. The individual ILs had good thermal stabilities but high melting points.[7]

The chromatographic properties and selectivities of the IL coated capillary columns were investigated by using different compound test mixtures. The FAME test mix was injected on all the nine new IL columns along with the commercial SLB-IL111 which is currently the most polar commercially available column. The thermal stability evaluation of ILs using inverse GC-FID showed that only four ILs; $C_9(m_2im)_2$-NTf_2, $C_{12}(m_2im)_2$-NTf_2, $C_9(mpy)_2$-NTf_2, and $C_{mix}(pr_3p)$-NTf_2 were stable at temperatures greater than 350 °C.[7] The other high temperature test mixes Grob, Polar Plus, PAM-HC, Custom-PAM, and Ionic Liquid mix were analyzed only on these four IL columns.

3.3.1 FAME Test Mix

The FAME test mix is based on rapeseed oil which has a mixture of eleven fatty acid methyl esters (see Experimental). The isothermal chromatographic profiles obtained from the analysis of the FAME test mix is shown in Figure 3-2. This test mix was used to compare the polarities of the newly synthesized ILs. Also, the elution patterns of eleven FAMEs were helpful in understanding the effects of cations, alkane linkage chains, and anions on the selectivities of ILs. The most important compounds in the test mix are methyl linolenate (C18:3n3) (6), methyl arachidate (C20:0) (7), and cis-11-eicosenoic acid methyl ester (C20:1) (8). Compounds C18:3 (6), C20:1 (8), and C20:0 (7) contain three, one, and zero double bonds respectively. So, the C18:3 FAME is more polarizable compared to C20:1 and C20:0. In general, the relative retention of compound 6 increases while compound 7 decreases with increases in the polarity of the stationary phase.

3.3.1.1 Effect of linker chain length

The synthesized ILs contain three pairs (**IL2** and **IL3**, **IL4** and **IL5**, and **IL6** and **IL7**) of analogous ILs with two different linker chain lengths (C_9 and C_{12}). Comparison of bmim-dicationic ILs with NTf_2^- anion (**IL2** and **IL3**) showed that C18:3n3 (6) was retained longer on the C_9 linkage chain IL(**IL2**) than the C_{12} linkage chain IL (**IL3**). C18:3n3 (6) was retained longer compared to both compounds C20:0 (7) and (C20:1) (8) on $C_9(m_2im)_2$-NTf_2 (**IL4**) while C18:3n6 (6) showed shorter retention than both C20:0 (7) and (C20:1) (8) on $C_{12}(m_2im)_2$-NTf_2 (**IL5**). In case of mpy-dicationic ILs with NTf_2^- anions (**IL6** and **IL7**), C18:3n3 (6) was more retained on the C_9 linkage chain IL (**IL6**) as compared to the C_{12} linkage chain IL (**IL7**). The C_9 linked ILs (**IL2** and **IL4**) showed different selectivities to compounds C18:3n6 (6) and C20:0 (7) (reversal of elution order) compared to analogous C_{12} linked ILs (**IL3** and **IL5**). The compounds C18:3n3 (6) and (C20:1) (8) also showed different selectivities (reversal of elution order) on C_9 and C_{12}

linked (mpy) ILs, **IL6** and **IL7**. Methyl tetracosanoate (C24:0) (11) is the most nonpolar compound in the FAME test mix. The relative retention of (C24:0) (11) was longer on C_{12} linkage chain ILs than the analogous ILs with C_9 linkages. The selectivity (k_{11}/k_{10}) for **IL4** was 1.33 while for **IL5** it was 1.58; the C_{12} linked IL showed higher selectivity to C24:0 compared to analogous C_9 IL. Hence, from the above results it can be concluded that the C_9 linked ILs are more polar than their C_{12} analogues. The C9 linked ILs (**IL2** and **IL4**) showed The FAME test mix also was analyzed on the commercially available SLB-IL111 (**IL1**) column which is the most polar known IL stationary phase. SLB IL111 can be abbreviated as $C_5(m_2im)_2$-NTf_2 based on its structure. This shorter linkage chain (C_5) IL column showed the least retention of the FAMEs as compared to the IL columns used in this study. From the elution patterns of FAMEs on all these ILs it can be concluded that the polarity of stationary phase increases with decrease in length of alkane linkage chain.

3.3.1.2 Effect of the anion

To understand the effect of anions on the polarities of ILs, we compared the relative retention of FAMEs on **IL2** and **IL10** which are analogous ILs with different anions (NTf_2^- and $PFOS^-$). C18:3n3 (6) was retained longer than C20:0 (7) on $C_9(bmim)_2$-NTf_2 (**IL2**) while the order of elution was reversed on $C_9(bmim)_2$-PFOS (**IL10**). The selectivities (k_{10}/k_9 and k_8/k_7) for unsaturated and saturated analogues of same chain length FAMEs were also higher for **IL2** (k_{10}/k_9 = 1.15 and k_8/k_7 = 1.16) compared to **IL3** (k_{10}/k_9 = 1.03 and k_8/k_7 = 1.02). This shows that the ILs with NTf_2^- anion are more polar as compared to the analogous ILs with $PFOS^-$ anions and also they have different selectivities.

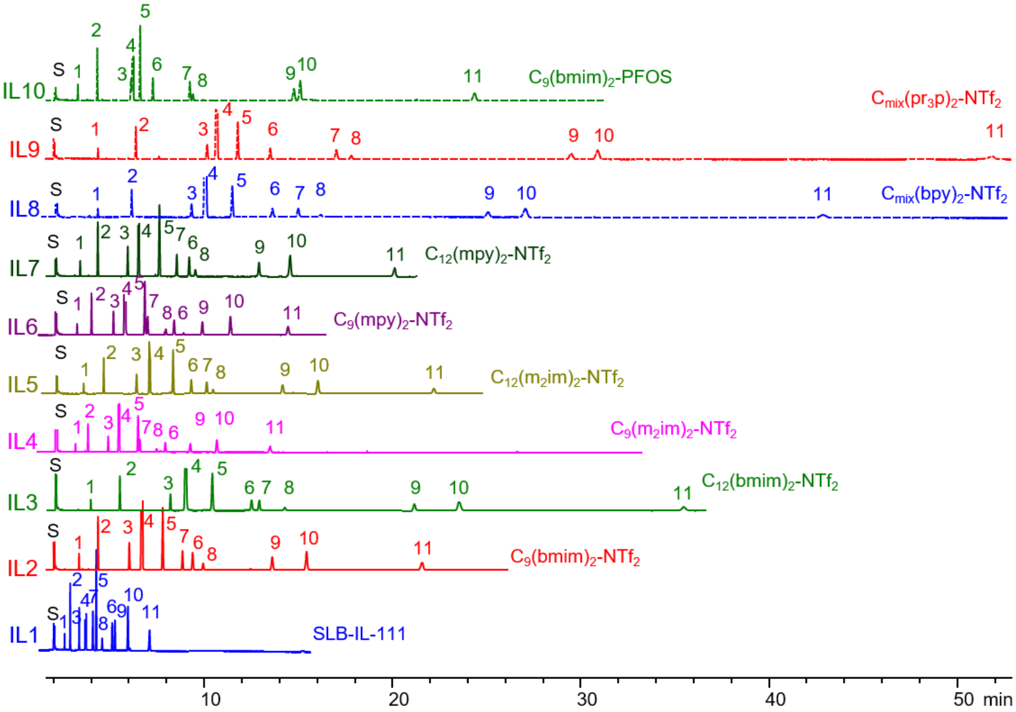

Figure 3-2 Separation of FAME test mix. 1) methyl myristate (C14:0) 2) methyl palmitate (C16:0) 3) methyl stearate (C18:0) 4) methyl oleate (C18:1n9) 5) methyl linoleate (C18:2n6) 6) methyl linolenate (C18:3n3) 7) methyl arachidate (C20:0) 8) cis-11-Eicosenoic acid methyl ester (C20:1) 9) methyl behenate (C22:0) 10) erucic acid methyl ester (C22:1) 11) methyl tetracosanoate (C24:0) S: dichloromethane. GC separation conditions: 180 °C isothermal; 1 mL min^{-1} He; FID

3.3.1.3 Effect of the cation

The synthesized groups of the ILs contain two types of each imidazolium and pyrrolidinium dications and one type of phosphonium dication. The relative retention of C18:3n3 (6) was longer compared to C20:0 (7) and (C20:1) (8) on $C_9(m_2im)_2$-NTf_2 (**IL4**) IL, while C18:3n3 (6) eluted before (C20:1) (8) on the $C_9(bmim)_2$-NTf_2 (**IL2**) IL. Substitution of benzyl group instead of methyl group on the imidazolium ring leads to a decrease in the polarity of the IL. The elution order of compounds C18:3n3 (6), C20:0 (7), and (C20:1) (8) on the $C_{mix}(bpy)_2$-NTf_2 (**IL8**) column was 6 < 7 < 8 while C18:3n3 (6) was retained longer than C20:0 (7) on both $C_9(mpy)_2$-NTf_2 (**IL6**) and $C_{12}(mpy)_2$-NTf_2 (**IL7**). Replacement of a methyl group by a butyl group on the pyrrolidinium nitrogen may significantly decrease the polarity of an IL. This was also supported by the longer retention of the C24:0 (11) FAME on the bpy-dicationic column compared to the mpy-dicationic columns. The relative polarities of mpy and $m_2$im dications were compared by observing the relative elution of C18:3n3 (6) and C20:0 (7) on $C_{12}(m_2im)_2$-NTf_2 (**IL5**) and $C_{12}(mpy)_2$-NTf_2 (**IL7**) ILs. C18:3n3 (6) eluted later than C20:0 (7) on $C_{12}(mpy)_2$-NTf_2 (**IL7**) while the order was reversed on $C_{12}(m_2im)_2$-NTf_2 (**IL5**). This shows that pyrrolidinium dicationic ILs are more polar as compared to the imidazolium dicationic ILs. The IL $C_{mix}(pr_3p)_2$-NTf_2 (**IL9**) displayed longest retention of C24:0 (11) compared to the tested IL stationary phases. Also, the phosphonium IL (**IL9**) showed longer retention of compounds C20:0 (7), C20:1 (8), C22:0 (9), and C22:1 (10) as compared to imidazolium (**IL2**, **IL3**, **IL4**, and **IL5**) and pyrrolidinium (**IL6**, **IL7**, and **IL8**) ILs. This makes the phosphonium IL less polar than both the imidazolium and pyrrolidinium ILs. The overall comparison showed that $C_9(mpy)_2$-NTf_2 (**IL6**) is the most polar while $C_{mix}(pr_3p)_2$-NTf_2 (**IL9**) is the least polar of all the ILs analyzed in this study.

3.3.1.4 Equivalent chain length (ECL) values

The ECL values can be used for the quantitative comparison of selectivities and retention indices of FAMEs on different IL columns.[48,57] The ECL values for unsaturated fatty acid methyl esters were calculated at 180 °C and they are reported in Table 1. The FAMEs with higher degree of unsaturation showed higher ECL values on all the IL columns. The ECL values increased with increase in the length of the unsaturated FAMEs. The ECL values for unsaturated FAMEs were also observed to be increasing with the increase in the polarity of IL stationary phases; consistent with the polarity trends discussed in the previous section. The ECL values for all the FAMEs were higher on SLB-IL111 (IL1) column compared to all other IL columns (IL2 to IL10). The $C_9(m_2im)_2$-NTf_2 (IL4) and $C_9(mpy)_2$-NTf_2 (IL6) showed comparable ECL values and their ECL values were higher than all the other newly synthesized IL columns (IL2, IL3, IL5, and IL7 to IL10) analyzed in this study.

Table 3-1 ECL values of unsaturated fatty acid methyl esters on IL columns at 180 °C

		ECL Values									
FAME No.	FAME Abbreviation	IL1	IL2	IL3	IL4	IL5	IL6	IL7	IL8	IL9	IL10
4	C18:1n9	19.02	18.56	18.43	18.78	18.46	18.76	18.55	18.32	18.19	18.10
5	C18:2n6	20.34	19.34	19.06	19.90	19.15	19.86	19.37	18.88	18.58	18.38
6	C18:3n3	21.76	20.27	19.86	21.09	19.64	21.06	20.36	19.59	19.11	18.84
8	C20:1	20.91	20.54	20.41	20.76	20.19	20.74	20.53	20.30	20.17	20.07
10	C22:1	22.85	22.55	22.41	22.75	22.55	22.75	22.54	22.29	22.17	22.09

3.3.2 Grob Test Mix

Grob test mix is a mixture of twelve different components at varied concentrations in dichloromethane as a solvent (all compounds are at concentrations less than 500 ppm). The test mix contains saturated alkanes, FAMEs, acid/base pairs, alcohols, and an aldehyde (see Experimental). The Grob test mix is used to evaluate the capillary column chromatographically and each compound gives a specific information about the column.[151,152] The test mix is useful to evaluate the separation efficiency, adsorptive activity, hydrogen bonding interactions, and inertness (acid/base characteristic) of the column. Figure 3-3 shows the analysis of the Grob test mix on four highest stability IL columns.

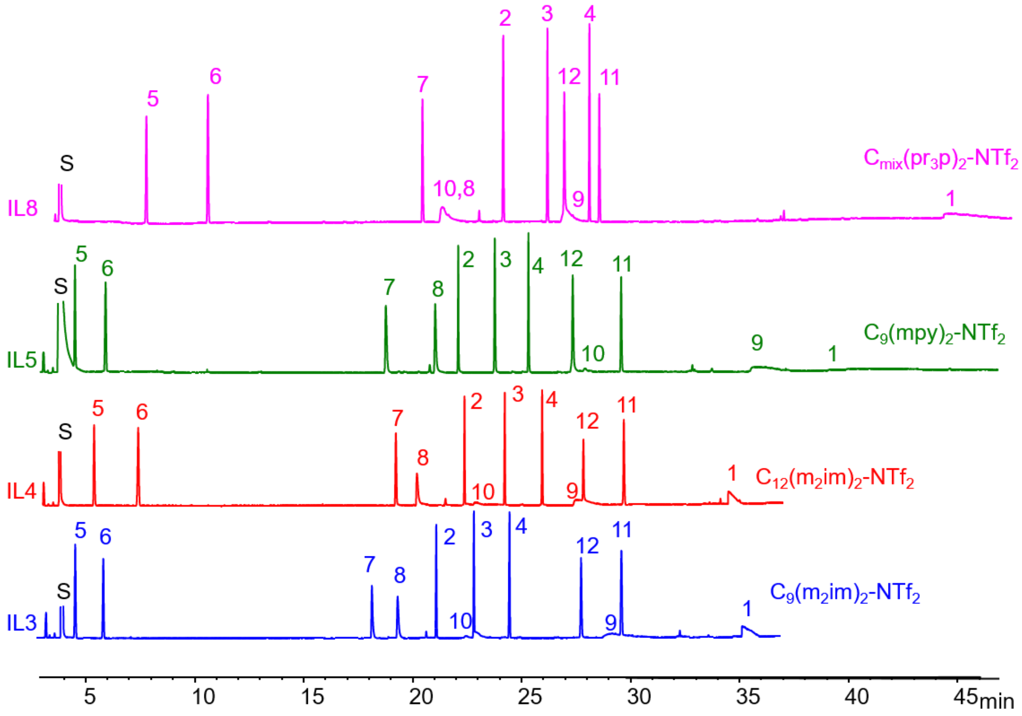

Figure 3-3 Separation of Grob test mix. 1) dicyclohexylamine 2) methyl decanoate (C10:0) 3) methyl undecanoate (C11:0 FAME) 4) methyl laurate (C12:0 FAME) 5) decane (C10) 6) undecane (C11) 7) 1-nonanal 8) 1-octanol 9) 2-ethylhexanoic acid 10) 2,3-butanediol 11) 2,6-dimethylaniline 12) 2,6-dimethylphenol S) dichloromethane. GC separation conditions: 40 °C for 5 min, 5 °C min $^{-1}$ to 200 °C; 1 mL min^{-1} He; FID

The symmetrical peaks of decane (5) and undecane (6) means that all the columns were properly produced and installed in the GC system. The FAMEs (compounds 2, 3, and 4) were well separated on all columns with symmetrical peaks and showed good separation efficiencies. The alcohols; 1-octanol (8) and 2,3-buanediol (10) are used for the evaluation of H-bonding interactions. The asymmetric peak shapes of 1-

octanol (8) on **IL3**, **IL4** and **IL5** showed presence of H-bonding sites. 1-octanol (8) and 2,3-butanediol (10) co-eluted on **IL8** column with high tailing showing the presence of strong H-bonding interactions. The acid/base pair 2-ethylhexanoic acid (9), dicyclohexylamine (1) and 2,3-butanediol (10) were either irreversibly adsorbed or eluted with high peak tailing as they were indistinguishable from the base line. 1-nonanal (7) shows adsorptive interactions independent of H-bonding and it eluted with minor tailing on all the four IL columns. 2-ethylhexnoic acid (9) and 2,3-butanediol (10) were retained longest on $C_9(mpy)_2$-NTf_2 (**IL5**) compared to the other ILs.

3.3.3 Polar Plus test mix:

Polar Plus test mix is a mixture of thirteen different polar and non-polar compounds at concentrations of 500 ppm each (see Experimental Section). The significance of the test mix is to understand the elution of polar compounds with respect to the nonpolar compounds (alkanes). The relative chromatographic behavior obtained from the analysis of Polar Plus test mix under identical conditions is shown in Figure 3-4.

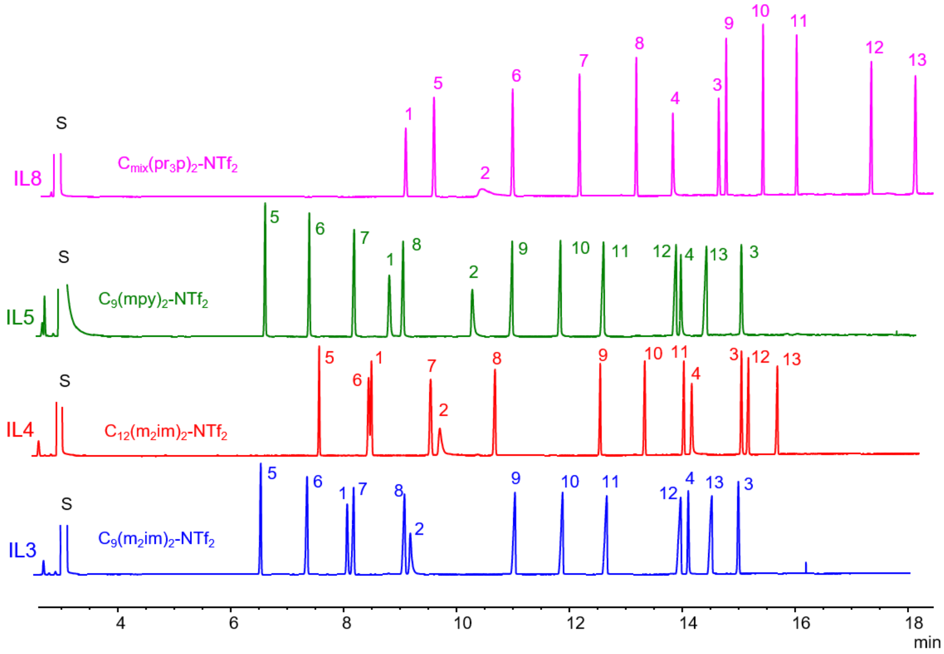

Figure 3-4 Separation of Polar Plus test mix. 1) 2-octanone 2) 1-octanol 3) 2,6-dimethylaniline 4) 2,6-dimethylphenol 5) pentadecane (C15) 6) hexadecane (C16) 7) heptadecane (C17) 8) octadecane (C18) 9) icosane (C20) 10) heneicosane (C21) 11) docosane (C22) 12) tetracosane (C24) 13) pentacosane (C25) S) dichloromethane. GC separation conditions: 60 °C for 3 min, 15 °C min $^{-1}$ to 120 °C, hold for 3 min, 15 °C min $^{-1}$ to 200 °C; 1 mL min^{-1} He; FID

2-octanone (1) showed variation in relative elution on all the stationary phases. 2-octanone (1) was less retained compared to alkanes on the phosphonium column (**IL8**). Also, the homologous series of alkanes were retained relatively longer on the phosphonium column compared to other ILs; supporting the nonpolar nature of the phosphonium IL. The order of elution of 2-octanone (1) and 1-octanol (2) with respect to the alkanes on all the columns was in accordance with the relative polarities of stationary phases (**IL5 > IL3 > IL4 > IL8**) (Refer to section 3.1 for relative polarities). Also, 2,6-dimethylaniline (3) was retained longer than the highest alkane, C25 (13), on the relatively polar $C_9(mpy)_2$-NTf_2 (**IL5**) and $C_9(m_2im)_2$-NTf_2 (**IL3**) ILs. Alkane C25 (13) was retained longer than 2,6-dimethylaniline (3) on relatively nonpolar columns $C_{12}(m_2im)_2$-NTf_2 (**IL4**) and $C_{mix}(pr_3p)_2$-NTf_2 (**IL8**). All the IL columns showed reasonable retention for both polar and nonpolar compounds. This test mix is a good example of the "dual nature" behavior of ILs; which means they can act as a polar medium to retain polar compounds and a nonpolar medium to retain nonpolar compounds.

3.3.4 PAM-HC test mix

The PAM-HC test mix is a mixture of eight polynuclear aromatic hydrocarbons (PAHs) and seven saturated higher alkanes at concentrations of 100 ppm each (see Experimental Section). The test mix was used to evaluate the relative retention of aromatic and aliphatic hydrocarbons. This test mix contains low molecular weight PAHs. The chromatograms obtained from the analysis of PAM-HC test mix are shown in Figure 3-5.

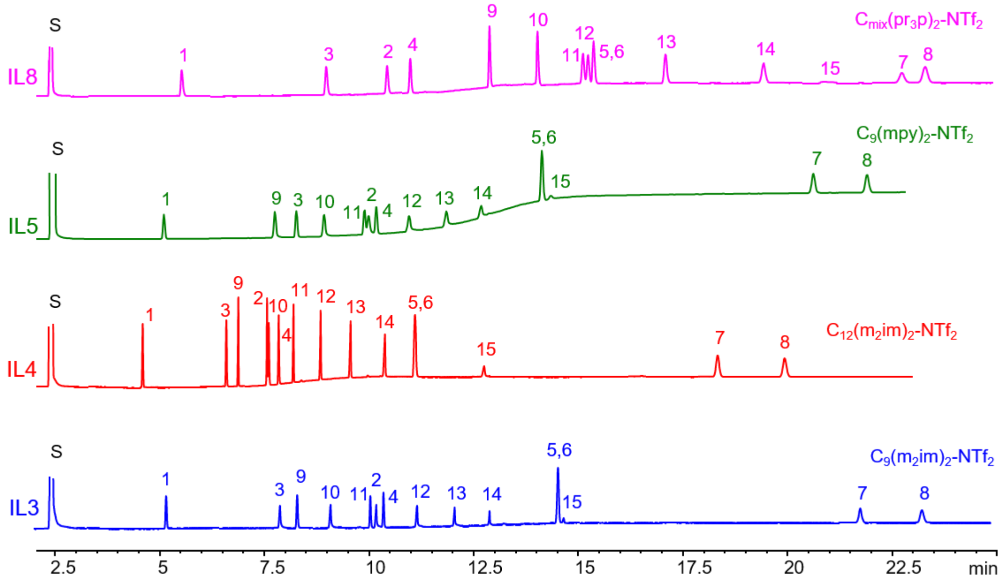

Figure 3-5 Separation of PAM-HC test mix. 1) naphthalene (MW- 128) (bp- 218 °C) 2) acenaphthylene (MW- 152) (bp- 280 °C)3) acenaphthene (MW- 154) (bp- 279 °C) 4) fluorene (MW- 166) (bp- 295 °C) 5) phenanthrene (MW- 178) (bp- 340 °C)6) anthracene (MW- 178) (bp- 340 °C)7) fluoranthene (MW- 202) (bp- 375 °C) 8) pyrene (MW- 202) (bp- 404 °C) 9) triacontane (C30) (bp- 450 °C)10) dotriacontane (C32) (bp- 467 °C)11) tetratriacontane (C34) (bp- 483 °C)12) hexatriacontane (C36) (bp- 497 °C) 13) octatriacontane (C38) (bp- 511 °C)14) tetracontane (C40) (bp- 524 °C) 15) tetratetracontane (C44) (bp- 547 °C) S) dichloromethane. GC separation conditions: 160 °C for 4 min, 10 °C min $^{-1}$ to 250 °C; 1 mL min^{-1} He; FID

Fluoranthene (7) and pyrene (8) are structural isomers and were well separated on all the IL columns. The C44 alkane (15) (bp 547 °C) has a higher boiling point than fluoranthene (7) (bp 375 °C) and pyrene (8) (bp 404 °C). But, compounds 7 and 8 were retained longer than compound 15 on all IL columns. The alkanes were relatively less retained on the **IL3**, **IL4** and **IL5** columns, while they were retained longer on **IL8**. In general, alkanes with higher boiling points eluted earlier than the low boiling PAHs. This shows the stronger interaction of PAHs with the IL stationary phases. Compound 2 (bp 280 °C) and 3 (bp 279 °C) have similar boiling points, but the relative retention of compound 2 was longer compared to compound 3. The presence of additional double bond in compound 2 could be the reason for its longer retention. Fluorene (4) showed different selectivities towards different ILs mainly affected by the polarities of ILs. The structural isomers, phenanthrene (5) and anthracene (6), were not separated on any of the four columns at the given temperature conditions (Figure 3-5).

3.3.5 Custom-PAM mix:

Custom-PAM mix is another test mix of nine polyaromatic hydrocarbons (PAHs) at concentration of 100 ppm each. It contains the high molecular weight PAHs (compared to PAM-HC test mix) and three different groups of structural isomers. One group of structural isomers is: phenanthrene (2) and anthracene (3); the second group is: benz[a]anthracene (4), chrysene (5), and triphenylene (6); and the third group of structural isomers is: benzo(b)-fluoranthene (7), benzo[k]-fluoranthene (8) and benzo[j]-fluoranthene (9). The PAHs are generated due to incomplete combustion of organic matter and they are toxic environmental pollutants.[116] The structural isomers of PAHs are difficult to separate and detect due to the high degree of overlap in their boiling points.[117] The analysis of test mix was significant to check the separation efficacy of ILs towards the high boiling structural isomers of PAHs. The analysis requires high temperatures and hence the test mix is also significant in evaluating the performance of IL stationary phases at higher temperatures (analysis done at 280 °C). The chromatograms obtained from the separation of the Custom-PAM test mix is shown in Figure 3-6.

Only the phosphonium column (**IL8**) was successful in the baseline separation (R_s = 1.6) of two structural isomers; phenanthrene (2) and anthracene (3) under the given analysis conditions (Figure 3-6). The other structural isomers; compounds 4, 5, and 6 were well separated on all of the IL columns. The separation of the benzofluoranthene structural isomers is difficult on the traditional polysiloxane based stationary phases and they typically coelute (generally, separation is carried out on phenyl and methyl substituted polysiloxanes).[118] But, the three benzofluoranthene isomers (compounds 7, 8 and 9) were well separated on all four dicationic IL columns.

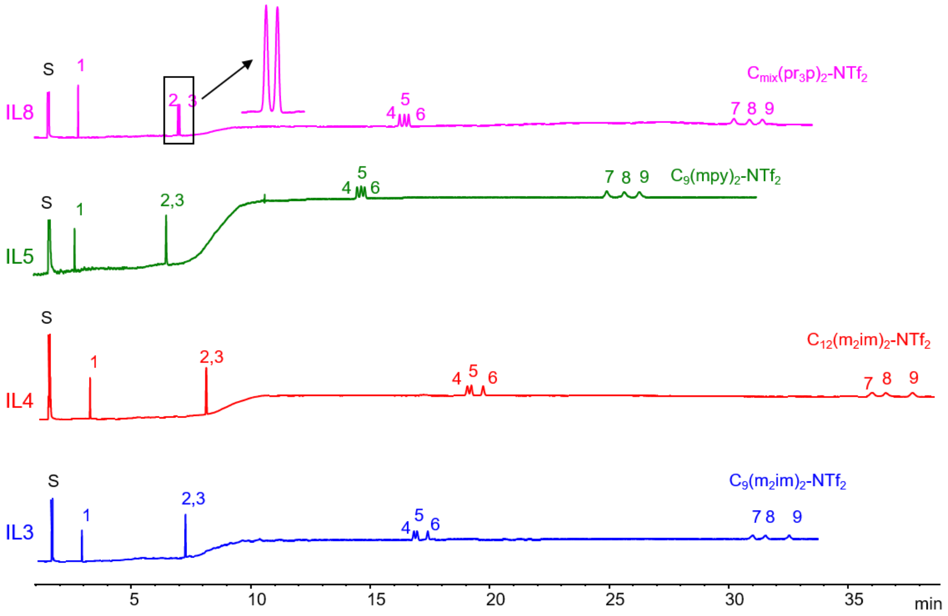

Figure 3-6 Separation of Custom-PAM test mix. GC separation conditions: 150 °C to 250 °C at 15 °C min $^{-1}$, hold for 2 min, 20 °C min $^{-1}$ to 280 °C; 1.5 mL min^{-1} He; FID

3.3.6 Ionic Liquid test mix

The Ionic Liquid test mix is a mixture of fourteen compounds with various functional groups. It contains aromatics, alkanes, FAMEs, a ketone, a sulfoxide, a lactone, an ester, and an amine (see Experimental Section). The function of this test mix is to compare the retention and selectivities of compounds with different functional groups. The separations obtained from the analysis of Ionic Liquid test mix is shown in Figure 3-7.

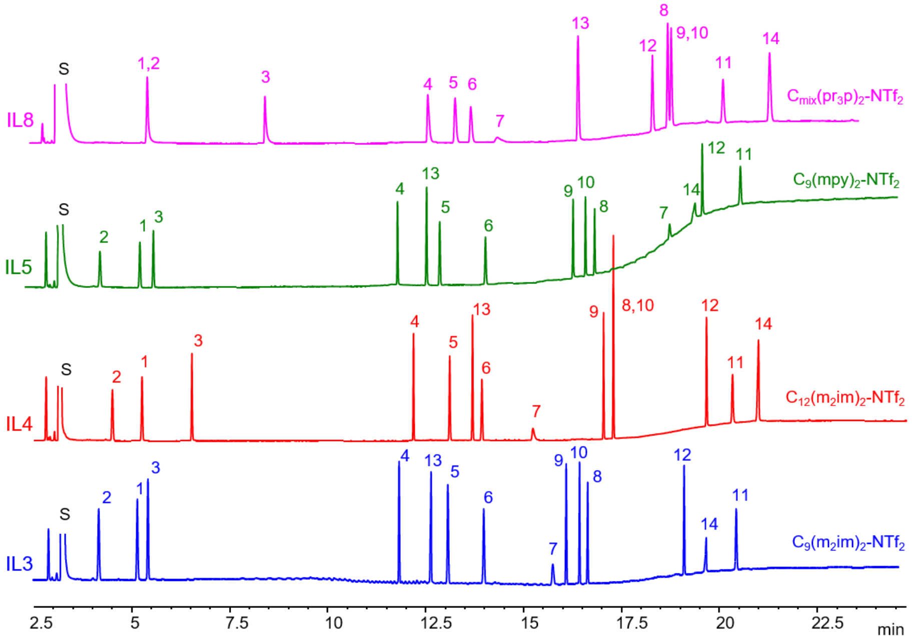

Figure 3-7 Separation of Ionic Liquid test mix. GC separation conditions: 60 °C for 4 min, 15 °C min^{-1} to 180 °C, hold for 2 min, 15 °C min^{-1} to 250 °C; 1 mL min^{-1} He; FID

The relative retention of non-polar compounds camphene (2) and tridecane (3) was observed with respect to toluene (1). Camphene (2) was less retained and elutes before toluene on nitrogen containing ILs (**IL3**, **IL4**, and **IL5**). The relative retention of tridecane (3) with respect to toluene (1) increased as the polarity of the stationary phase decreased (higher relative retention on **IL4** and **IL8** compared to **IL3** and **IL5**). The ILs $C_9(mpy)_2$ NTf_2 (**IL5**) and $C_9(m_2im)_2$-NTf_2 (**IL3**) displayed almost similar elution patterns for all the previously analyzed test mixes. However, two ILs (**IL3** and **IL5**) displayed different selectivity towards dimethylsulfoxide (7). Compound 7 (DMSO) was retained much longer on $C_9(mpy)_2$ NTf_2 (**IL5**) (k = 4.50) compared to $C_9(m_2im)_2$-NTf_2 (**IL3**) (k = 3.78). The methylpyrrolidinium cationic IL displayed increased retention for the sulfoxide (−S=O) group containing compound relative to the imidazolium and phosphonium cationic ILs. A lactone coumarin (11) (bp 301 °C) and a diester dioctyladipate (12) (bp 405 °C) displayed retention independent of their boiling points even though they both contain carbonyl groups. High boiling compound 12 (dioctyladipate) eluted before the low boiling compound 11 (coumarin) on all the IL stationary phases. The same retention pattern independent of the boiling point but dependent on polarity was observed for coumarin (11) (bp 301 °C) and C40 alkane (14) (bp 524 °C). Compound 14 was retained longer on nonpolar **IL4** and **IL8** columns while it eluted earlier than (11) on the relatively polar **IL3** and **IL5** columns.

The four IL columns displayed good performance at higher temperatures (250 °C and 280 °C) for the analyses of the Ionic Liquid test mix and both the test mixes containing PAHs. The phosphonium column $C_{mix}(pr_3p)_2$-NTf_2 (**IL8**) was observed to be the most stable and among the four ILs (showed least bleeding at 280 °C; Figure 3-6). The pyrrolidinium IL (**IL5**) was observed to be the most polar but displayed the least thermal stability (high bleeding at 280 °C; Figure 3-6). Both the imidazolium ILs displayed similar bleeding and stabilities at 280 °C (Figure 3-6).

3.4 Conclusions

In this study, we have demonstrated the effect of different IL structural features such as cation types, alkane linkage chains and anions on the polarities and selectivities of geminal dicationic ILs. The polarities of IL stationary phases were observed to increase with a decrease in the length of alkane linkage chain. Benzyl-imidazolium cationic ILs were observed to be less polar than the methyl-imidazolium ILs. The presence of an aromatic substituent (benzyl group) on position 3 of the imidazole ring lead to decrease in polarity. N-methyl substituted pyrrolidinium dicationic ILs were more polar than N-butyl substituted pyrrolidinium dicationic IL. Within the three different types of dications following trends were observed for polarity of ILs: pyrrolidinium > imidazolium > phosphonium. The comparison of analogous ILs with different anions showed that NTf_2^- anionic ILs were more polar than the $PFOS^-$ anionic ILs. The overall comparison of FAME test mix showed that $C_9(mpy)_2$-NTf_2 was the most polar while the $C_{mix}(pr_3p)_2$-NTf_2 was the least polar among all the ILs analyzed in this study.

Compounds do not elute relative to their boiling points on IL stationary phases. Also, IL columns were successful in the separation of the structural isomers of PAHs. The $C_9(m_2im)_2$-NTf_2, $C_{12}(m_2im)_2$-NTf_2, $C_9(mpy)_2$-NTf_2, and $C_{mix}(pr_3p)_2$-NTf_2 IL columns displayed good performance at high temperatures (280 °C) by separating the three benzofluoranthene isomers. The $C_{mix}(pr_3p)_2$-NTf_2 was the highlight of this study which displayed the efficient separation of anthracene and phenanthrene isomers and also displayed better thermal stability compared to other ILs. The pyrrolidinium IL $C_9(mpy)_2$-NTf_2 displayed lowest thermal stability among the four ILs. $C_9(mpy)_2$-NTf_2 and $C_9(m_2im)_2$-NTf_2 showed almost similar elution pattern for all the compounds analyzed except for dimethylsulfoxide. The pyrrolidinium column displayed higher interaction towards the sulfoxide group compared to other ILs. The IL with pyrrolidinium dication displayed stronger hydrogen bonding interactions compared to the analogous ILs with imidazolium and phosphonium dications.

Chapter 4

PHYSICOCHEMICAL PROPERTIES OF BRANCHED-CHAIN DICATIONIC IONIC LIQUIDS

Abstract

Dicationic ionic liquids (DILs) typically have higher viscosities and thermal stabilities than most conventional monocationic ionic liquids. However, due to their coulombic interactions, they often demonstrate higher melting points than conventional ILs which limit their use in many applications. Utilizing branched alkyl spacer chains between two cationic terminal groups resulted in dicationic ILs with lower melting points and therefore extended liquid ranges. A systematic investigation was conducted to determine how the position and type of substituent groups may affect the physicochemical properties of branched DILs. When compared to their linear counterparts, an increase in the kinematic viscosities and lower densities were observed for branched DILs. Thermal stability was found to be highly dependent on the position of the alkyl substituent group along with the length of the spacer chain. While the substitution on the α-carbon of a spacer chain resulted in a significant decline in the thermal stability of DILs, the effect of mid-chain substitution on their stability was negligible. The performance testing of branched DILs as gas chromatography (GC) stationary phase displayed excellent separation of geometrical isomers in BTEX mixture.

4.1 Introduction

Multidisciplinary studies on ionic liquid (IL) materials have increasingly expanded due to their exceptional characteristics, including but not limited to high liquid density, adjustable viscosity, large electrochemical windows, resistance to decomposition even at high temperatures, wide liquid phase temperature range, good chemical and electrochemical stability, and tunable solvation properties.[1,12,13,39,119] A large number of possible combinations of cations and anions provides opportunity for tuning the physicochemical properties of ionic liquids.[2] As a matter of fact, ILs with innovative characteristics have been synthesized by systematically engineering the nature and functionality of their component ions.[12,13,153,154]

Dicationic ionic liquids (DILs), are a more recent class of ILs that have drawn a great deal of attention given the broader range of their physical and chemical properties, compared to conventional ionic liquids.[7,16-18,20,108,155,156] DILs are typically comprised of two cationic head groups linked by a rigid or flexible spacer, associated with two counteranions.[17] Their features such as high viscosities, lower volatility and higher thermal stability, make DILs exceptional candidates for plethora of promising applications such as reaction media for high temperature reactions,[26,27] receptors for anion recognition,[157] ionic liquid crystals,[158] low molecular-mass gelators,[159,160] fluorescent organic salts,[161,162] additives in dye-sensitized solar cells,[163] CO_2 separation membranes,[164] high-temperature lubricants,[18,125] and exceptional separation phases.[3,15,16,37,55]

Since electrostatic interactions between the dicationic moieties and their counteranions are comparatively stronger than between singly charged ions, DILs were found to possess higher melting points than their monocationic analogs.[20] This feature considerably narrows their potential applications at low temperatures. However, this limitation can be overcome by fine-tuning the alkane linkage chain length.[165] The melting point and other physical properties can also be altered by manipulating the cationic moiety and/or counteranions. Unsymmetrical DILs can be designed containing two different cationic head groups,[108] as well as heteroanionic ILs in which two different anions are paired with the cationic portion.[155,166,167] The physical properties of unsymmetrical DILs are found to be somewhat different from the symmetrical DILs, especially regarding their melting temperature.[108] In addition, the structural variation of spacer chain between two terminal cations, can induce different physicochemical properties.[7,18,168] In this respect, one of the possible modifications to reshape the properties of DILs can be made by utilizing branched alkane spacer chains.

It is well-known that branched alkanes possess lower boiling and melting points than their linear equivalents. Despite their unique characteristics, limited studies have been devoted to the synthesis and physicochemical property evaluation of branched-chain ionic liquids.[114,169-172] Xue et al.[169] recently examined the physicochemical properties of a homologous series of monocationic branched ILs based on 1-(iso-alkyl)-3-methylimidazolium paired with bis(trifluoromethane)sulfonamide (NTf_2^-) anion and found that the melting temperature, glass transition temperature, and viscosity of these ILs are higher than their counterparts with linear substituents. However, regarding decomposition temperatures, ILs with linear alkyl side chain were found to have better thermal stability than their branched analogs.[169,170]

In order to systematically investigate the effect of branched alkane spacer chains on the physical and chemical properties of DILs, a series of ionic liquids containing methyl, dimethyl, and tert-butyl substituents on the alkane linkage chains were synthesized. The length of alkane linkage chains between the two head groups were 3-5 carbons. A number of α-branched, β-branched, and γ-branched alkane linkages were examined, to evaluate the effect of a substituent position on the physical properties of DILs. Also, the influence of double bond location on the properties of isomeric DILs was studied by comparing isobutylene and 2-butene linkages. According to our previous study, dicationic salts of dimethylimidazolium usually show high thermal stabilities (≥ 400 °C) when utilized with NTf_2^- anions.[7,173] Furthermore, due to its extensive charge delocalization and considerable flexibility around the S-N-S bond, the NTf_2^- anion is well-known to decrease the melting point of ionic compounds.[1] Thus, the combination of dimethylimidazolium cationic groups and NTf_2^- counteranions were selected for a systematic evaluation of new branched DILs. In addition, they were compared to their corresponding linear analogs. Also, it is known that the nature of cationic group has a great impact on IL properties.[173] Therefore, branched DILs comprised of methylpyrrolidinium, and tripropylphosphonium cationic head groups also were synthesized to compare their physical properties with their dimethylimidazolium analogs. The influence of spacer chain branching on physicochemical properties of DILs, including density, viscosity, melting and decomposition temperatures are presented and discussed.

4.2. Experimental

4.2.1 Materials

1,3-dibromopropane (99%), 1,4-dibromobutane (99%), 1,5-dibromopentane (97%), 1,7-dibromoheptane (97%), 1,3-dibromobutane (97%), trans-1,4-dibromo-2-butene (99%), 1-bromo-3-(2-bromoethyl)-4,4-diethylpentane, 3-bromo-2-bromomethyl-1-propene (97%), bis(trifluoromethane)sulfonamide lithium salt (99.95%), 1-methylpyrrolidine (98%), 1,2-dimethylimidazole (98%), and tripropylphosphine (97%) were purchased from Sigma-Aldrich (St. Louis, MO). 1,4-Dibromopentane (97%), 2,5-dibromohexane (97%), and 1,5-Dibromo-3-methylpentane (98+%) were obtained from

Alfa Aesar (Haverhill, MA). 1,5-dibromo-3,3-dimethylpentane (95%) was purchased from Alfa Chemistry (Holtsville, NY). 1,3-dibromo-2-methylpropane (95+%) was acquired from Oakwood Chemicals (Estill, SC). Acetonitrile, dichloromethane, methanol, and heptane were obtained from Fisher Scientific (Fair Lawn, NJ). Fused silica capillary tubing, 30-m $[3m_2(C_1py)_2C_5]^{2+}.2NTf_2^{-}$ column, and BTEX mixture were kindly provided by MilliporeSigma (Bellefonte, PA). Deionized water was produced by Synergy 185 water purification system (Millipore, Billeria, MA).

4.2.2 Synthesis

The structure of dicationic ionic liquids synthesized in this study are displayed in Figure 4-1. The synthesis of dicationic ILs involves two steps. In the first step, 1 molar equivalent of a dibromoalkane was reacted with 2 molar equivalents of either 1,2-dimethylimidazole, 1-methylpyrrolidine, or tripropylphosphine to obtain bromide salt of dication. The nucleophilic reaction was carried out in acetonitrile at 80 °C under reflux for 72 h. The solvent was evaporated by rotary evaporation, and the crude product was separated from unreacted materials by liquid-liquid extraction in water/dichloromethane (50:50). Subsequently, the vacuum drying over P_2O_5 at 40 °C for 24 hours resulted in the pure dibromo salt. The second step involved metathesis reaction to exchange the bromide ions with NTf_2^{-} anions. For this, a reaction of 1 molar equivalent of the dibromosalt with 2 molar equivalents of bis(trifluoromethane)sulfonamide lithium salt ($LiNTf_2$) was performed in water for 12 h. Following that, dichloromethane was added to the solution in order to extract NTf_2^{-} salt of the ionic liquid. The lithium bromide and excess NTf_2^{-} were removed from the nonpolar phase with successive extraction with water. Dichloromethane was removed through rotary evaporation. At last, vacuum drying over phosphorus pentoxide at 40 °C for 24 h resulted in the pure dicationic ILs with NTf_2^{-} counter anion.

4.2.3 Preparation of capillary columns

The static coating method was used to coat the ionic liquids as GC stationary phase.[174] A 20% w/v solution of IL in dichloromethane was prepared and injected to a fused silica capillary tubing. After evaporation of solvent under vacuum at 40 °C, columns with 0.20 µm film thickness were developed. Columns were then conditioned at 200 °C in the GC oven for 12 h. The column efficiency was determined by injecting naphthalene at 100 °C, and found to be between 2000 to 2500 plates/m.

***4.**2.4 Analysis methods*

4.2.4.1 Chemical characterization

Chemical characterization of all the synthesized dicationic ionic liquids were achieved by ^{1}H, and ^{13}C NMR spectrometry and mass spectrometry. The molecular weights were determined using Finnigan LXQ (Thermo Fisher Scientific, San Jose, CA) electrospray ionization mass spectrometry (ESI-MS). The ^{1}H NMR, and ^{13}C NMR spectra were recorded in dimethyl sulfoxide-d_6 and acetonitrile-d_3 on 300 MHz and 500 MHz JEOL Eclipse Plus 500 instrument (Tokyo, Japan) spectrometer at ambient temperature. Chemical shifts are reported relative to TMS. The coupling constants, J, are reported in Hz. The following abbreviations were used to designate chemical shift multiplicities: s: singlet, d: doublet, t: triplet, q: quartet, m: multiplet, br: broad. All first-order splitting patterns were assigned based on the appearance of the multiplet. When splitting patterns were difficult to interpret, assigned as m (multiplet) or br (broad).

4.2.4.2 Density and viscosity

Density was measured using 10 mL Kimble Glass specific gravity pycnometer (Vineland, NJ) at 22 °C. Heptane was used as an immiscible solvent for these measurements. Kinematic viscosity was determined using a Cannon-Manning semi-micro capillary viscometer (State College, PA).

4.2.4.3 Melting point

The melting point measurements were carried out on a Shimadzu DSC-60 (Kyoto, Kyoto Prefecture, Japan) differential scanning calorimeter (DSC). The samples (~ 10 mg) were sealed in aluminum pans and an empty aluminum pan was used as a reference. The measurements were carried out in the temperature range -120 °C to a predetermined temperature. The samples were heated at rate of 5 °C/min. Melting points for solid samples were determined using a Mel-Temp apparatus (Laboratory Devices, Cambridge, MA).

4.2.4.4. Thermogravimetric Analysis

In order to measure the thermal stability of DILs, thermogravimetric analysis was performed using Shimadzu TGA-51 Thermogravimetric Analyzer (Kyoto, Kyoto Prefecture, Japan). Around 10 mg of sample was placed in a platinum pan, and heated with ramp of 10 °C/min from room temperature to 600 °C in a nitrogen atmosphere (flow ~ 30 mL/min). The decomposition temperature was determined at 1%, 5% and 15% weight loss. The 5% weight loss corresponding to 95% w value was considered as measure of thermal stability.

4.2.4.5 Inverse GC

Agilent 6890N Gas Chromatograph (Santa Clara, CA) was employed to evaluate the thermal stability and chromatographic performance of ionic liquid stationary phases. The inverse GC experiment was carried out by ramping the column oven temperature from 100 to 450 °C at 1 °C/min. Helium was used as carrier gas at flow rate of 1 mL/min. The temperature of injection port and FID were set at 250 °C and 400 °C respectively.

4.2.5 GC application test

The performance testing of DILs as GC stationary phase was achieved by injecting 1 µL of BTEX mixture on a 30-m $[3m_2(C_1py)_2C_5]^{2+}.2NTf_2^-$ column. The oven temperature was maintained at 70 °C. Helium was used as a carrier gas at constant flow rate of 1 mL/min with split ratio of 1:100. The injector and FID temperatures were both set at 200 °C.

4.3 Results and Discussion

The physicochemical properties of DILs used in this study are summarized in Table 4-1. The following abbreviations were used in this paper relative to the type of branching; m: methyl, t-bu: tert-butyl, ene: presence of alkene group. Moreover, for the charged head groups C_1C_1im, C_1py, and $P[C_3C_3C_3]$, refer to dimethylimidazolium, methylpyrrolidinium, and tripropylphosphonium, respectively. All of the synthesized ionic liquids in this study are associated with NTf_2^- counteranions.

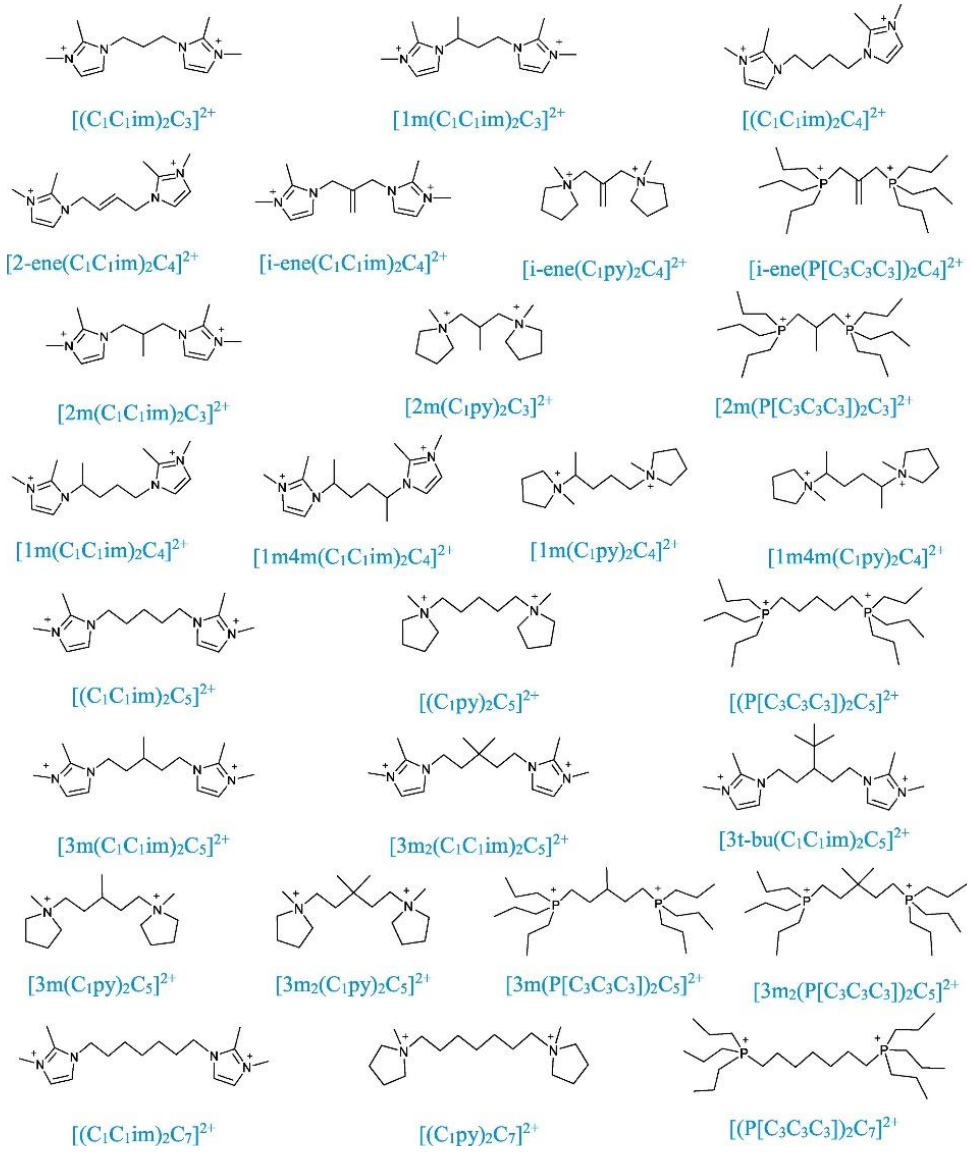

$[(C_1C_1im)_2C_3]^{2+}$ $[1m(C_1C_1im)_2C_3]^{2+}$ $[(C_1C_1im)_2C_4]^{2+}$

$[2\text{-}ene(C_1C_1im)_2C_4]^{2+}$ $[i\text{-}ene(C_1C_1im)_2C_4]^{2+}$ $[i\text{-}ene(C_1py)_2C_4]^{2+}$ $[i\text{-}ene(P[C_3C_3C_3])_2C_4]^{2+}$

$[2m(C_1C_1im)_2C_3]^{2+}$ $[2m(C_1py)_2C_3]^{2+}$ $[2m(P[C_3C_3C_3])_2C_3]^{2+}$

$[1m(C_1C_1im)_2C_4]^{2+}$ $[1m4m(C_1C_1im)_2C_4]^{2+}$ $[1m(C_1py)_2C_4]^{2+}$ $[1m4m(C_1py)_2C_4]^{2+}$

$[(C_1C_1im)_2C_5]^{2+}$ $[(C_1py)_2C_5]^{2+}$ $[(P[C_3C_3C_3])_2C_5]^{2+}$

$[3m(C_1C_1im)_2C_5]^{2+}$ $[3m_2(C_1C_1im)_2C_5]^{2+}$ $[3t\text{-}bu(C_1C_1im)_2C_5]^{2+}$

$[3m(C_1py)_2C_5]^{2+}$ $[3m_2(C_1py)_2C_5]^{2+}$ $[3m(P[C_3C_3C_3])_2C_5]^{2+}$ $[3m_2(P[C_3C_3C_3])_2C_5]^{2+}$

$[(C_1C_1im)_2C_7]^{2+}$ $[(C_1py)_2C_7]^{2+}$ $[(P[C_3C_3C_3])_2C_7]^{2+}$

Figure 4-1 Molecular structure of dicationic ionic liquids (DILs) synthesized in this study

Table 4-1 Physicochemical properties of dicationic ionic liquids containing different spacer chains

Entry	Cation Abbreviation[a]	MW (g/mol)	Melting Point[b] (°C)	Thermal Stability[c] (°C)			Density[d] (g/cm³)	Viscosity[e] (cSt)		
				99%w	95%w	85%w		30 °C	50 °C	80 °C
Dimethylimidazolium ILs										
IL1	$\mathrm{[(C_1C_1im)_2C_3]^{2+}}$	234.35	91	428	456	475	1.62	ND[f]	ND	ND
IL2	$\mathrm{[1m(C_1C_1im)_2C_3]^{2+}}$	248.37	-3	348	406	442	1.57	266	104	51
IL3	$\mathrm{[2m(C_1C_1im)_2C_3]^{2+}}$	248.37	54	398	438	478	1.55	ND	ND	79
IL4	$\mathrm{[i\text{-}ene(C_1C_1im)_2C_4]^{2+}}$	246.36	61	401	437	472	1.56	ND	ND	68
IL5	$\mathrm{[2\text{-}ene(C_1C_1im)_2C_4]^{2+}}$	246.36	134	417	447	468	1.62	ND	ND	ND
IL6	$\mathrm{[(C_1C_1im)_2C_4]^{2+}}$	248.37	122	437	453	475	1.61	ND	ND	ND
IL7	$\mathrm{[1m(C_1C_1im)_2C_4]^{2+}}$	262.40	-36	388	409	425	1.54	337	92	54
IL8	$\mathrm{[1m4m(C_1C_1im)_2C_4]^{2+}}$	276.43	-24	358	382	407	1.50	394	113	60
IL9	$\mathrm{[(C_1C_1im)_2C_5]^{2+}}$	262.40	63	389	438	477	1.60	ND	ND	83
IL10	$\mathrm{[3m(C_1C_1im)_2C_5]^{2+}}$	276.43	38	428	440	464	1.57	ND	202	88
IL11	$\mathrm{[3m_2(C_1C_1im)_2C_5]^{2+}}$	290.45	59	375	423	446	1.54	ND	ND	90
IL12	$\mathrm{[3t\text{-}bu(C_1C_1im)_2C_5]^{2+}}$	318.51	74	386	429	455	1.48	ND	ND	98
IL13	$\mathrm{[(C_1C_1im)_2C_7]^{2+}}$	290.45	54	436	463	480	1.55	ND	ND	86
N-Methylpyrrolidinium ILs										
IL14	$\mathrm{[2m(C_1py)_2C_3]^{2+}}$	226.41	31	313	373	401	1.43	ND	245	82
IL15	$\mathrm{[i\text{-}ene(C_1py)_2C_4]^{2+}}$	224.39	87	308	366	389	1.44	ND	ND	ND
IL16	$\mathrm{[1m(C_1py)_2C_4]^{2+}}$	240.43	-4	348	365	390	1.42	473	157	72
IL17	$\mathrm{[1m4m(C_1py)_2C_4]^{2+}}$	254.46	1	318	353	379	1.39	506	182	79
IL18	$\mathrm{[(C_1py)_2C_5]^{2+}}$	240.43	78	382	418	447	1.48	ND	ND	ND
IL19	$\mathrm{[3m(C_1py)_2C_5]^{2+}}$	254.46	12	382	415	459	1.43	1026	288	94
IL20	$\mathrm{[3m_2(C_1py)_2C_5]^{2+}}$	268.49	18	357	403	431	1.41	1138	312	118
IL21	$\mathrm{[(C_1py)_2C_7]^{2+}}$	268.49	68	386	428	441	1.44	ND	ND	102
Tripropylphosphonium ILs										
IL22	$\mathrm{[2m(P[C_3C_3C_3])_2C_3]^{2+}}$	376.59	38	355	402	434	1.28	ND	301	97
IL23	$\mathrm{[i\text{-}ene(P[C_3C_3C_3])_2C_4]^{2+}}$	374.57	62	323	394	429	1.30	ND	ND	88
IL24	$\mathrm{[(P[C_3C_3C_3])_2C_5]^{2+}}$	390.62	71	392	420	462	1.30	ND	ND	91
IL25	$\mathrm{[3m(P[C_3C_3C_3])_2C_5]^{2+}}$	404.64	83	384	425	448	1.29	ND	ND	ND
IL26	$\mathrm{[3m_2(P[C_3C_3C_3])_2C_5]^{2+}}$	418.67	90	396	416	443	1.25	ND	ND	ND
IL27	$\mathrm{[(P[C_3C_3C_3])_2C_7]^{2+}}$	418.67	103	382	425	447	1.28	ND	ND	ND

[a] The right part of the code refers to the spacer chain length. The spacer substituent can be m for methyl, m_2 for two methyl, and t-bu for *t*-butyl. Also, 2-eneC_4 and i-eneC_4 refers to 2-butene and isobutylene spacer chains, respectively. The cationic group is between parenthesis with C_1C_1im for 2,3-dimethylimidazolium, C_1py for N-methylpyrrolidinium, and $P[C_3C_3C_3]$ for tripropylphosphonium as suggested by Hallet and Welton.[12]

[b] Determined by peak position in DSC or obtained by Mel-Temp apparatus.

[c] Thermogravimetric analysis (TGA), 99%w refers to temperature at 1% mass loss of sample, 95%w refers to 5% mass decrease of sample, 85%w indicates 15% mass loss of sample.

[d] Measured using pycnometer.

[e] Measured using capillary viscometer.

[f] Viscosity could not be measured due to the solid phase state of compounds at certain temperatures.

ND: Not determined.

4.3.1 Melting point

A decrease in free-rotation volume and an increase in atom density changes the efficiency of crystal packing.[1] Thus, a higher degree of chain branching was found to increase the melting point of monocationic ionic liquids.[170] Conversely, dicationic ionic liquids show the opposite behavior. Similar to alkanes, branched-chain DILs are thought to have weaker van der Waals forces due to the smaller contact area between the molecules. Hence, less energy is required to overcome their intermolecular forces, leading to lower melting points of branched-chain DILs as compared to their linear-chain analogs. As indicated in Table 4-1, introducing one methyl group on the C3 linkage resulted in a large decrease in the melting point of dimethylimidazolium ILs. The melting temperature decreased from 91 °C (**IL1**) to -3 °C (**IL2**) when one α-H is substituted by a methyl group. Comparing $[1m(C_1C_1im)_2C_3]^{2+}.2NTf_2^-$ (**IL2**) and $[2m(C_1C_1im)_2C_3]^{2+}.2NTf_2^-$ (**IL3**) shows that the position of branching or molecular shape can considerably affect the phase transition temperature of branched DILs as well. The melting temperature for α-substituted isomer (**IL2**) was found to be -3 °C, whereas, the melting point for the β-substituted isomer (**IL3**) was 54 °C. In other words, the symmetry of DILs can influence their melting temperature to a great extent by providing more efficient ion-ion packing in the crystal cell.[1,108,175] Additional π-π interactions also can lead to significant increases in IL melting temperatures.[7,17] **IL4** and **IL5** contain unsaturated bonds in their alkyl spacer chains, and had higher melting points than their saturated counterparts, **IL3** and **IL6**, respectively. Also, the DIL alkene isomers had different phase transition temperatures. The $[i\text{-}ene(C_1C_1im)_2C_4]^{2+}.2NTf_2^-$ (**IL4**) had a significantly lower melting point than $[2\text{-}ene(C_1C_1im)_2C_4]^{2+}.2NTf_2^-$ (**IL5**). For the imidazolium DILs containing C4 linkages, inserting a methyl group on the α-carbon led to a large decrease in melting temperature, from 122 °C (**IL6**) to -36 °C (**IL7**). However, the melting point increased slightly to -24 °C

(**IL8**) when a second methyl group was introduced on the opposite α-carbon. Such increases have been attributed to the molecular symmetry of ionic liquids.[175] An additional contributing factor to the increased melting point of $[1m4m(C_1C_1im)_2C_4]^{2+}.2NTf_2^-$ (**IL8**) could be related to the somewhat increased dispersive interactions resulted from additional methyl group on the linkage chain.[1] Similar behavior was observed with methylpyrrolidinium DILs (**IL16** and **IL17**), where the melting point of $[1m4m(C_1py)_2C_4]^{2+}.2NTf_2^-$ was 5 °C higher than $[1m4m(C_1py)_2C_4]^{2+}.2NTf_2^-$. Comparing **IL9-IL12** shows how the introduction of one methyl, two methyl, or a tert-butyl group in the middle of the pentyl linkage can affect the melting temperatures. Similar to C3 linkage, inserting one methyl group in the middle of the C5 alkyl linkage chain resulted in formation of $[3m(C_1C_1im)_2C_5]^{2+}.2NTf_2^-$ (**IL10**) with a melting point that was 25 °C lower than $[(C_1C_1im)_2C_5]^{2+}.2NTf_2^-$ (**IL9**). However, the melting temperature gradually started increasing when a bulkier substituent was added on the C5 linkage (i.e., second methyl group (**IL11**) or a *tert*-butyl group (**IL12**), Table 4-1).

In the case of methylpyrrolidinium DILs (**IL14-IL21**) the effect of branching is more profound compared with the C5 dimethylimidazolium DILs (Table 4-1). Both 3-methylpentyl- (**IL19**) and 3,3-dimethylpentyl- (**IL20**) substituted pyrrolidinium ionic liquids show remarkably lower melting temperature than $[(C_1py)_2C_5]^{2+}.2NTf_2^-$ (**IL18**). However, the tripropylphosphonium ionic liquids do not follow the same trend as other two classes of DILs. Both $[3m(P[C_3C_3C_3])_2C_5]^{2+}.2NTf_2^-$ (**IL25**) and $[3m_2(P[C_3C_3C_3])_2C_5]^{2+}.2NTf_2^-$ (**IL26**) were found to have higher melting temperatures than $[(P[C_3C_3C_3])_2C_5]^{2+}.2NTf_2^-$ (**IL24**). It is worth noting that all the branched linkage chain DILs in this study showed lower melting points than their linear spacer chain isomers. For instance, the melting point of $[3m_2(P[C_3C_3C_3])_2C_5]^{2+}.2NTf_2^-$ (**IL26**) was found to be 13 °C lower than $[(P[C_3C_3C_3])_2C_7]^{2+}.2NTf_2^-$ (**IL27**) with the same molecular formula.

4.3.2 Density

The decrease in density with increasing the size of the cation was previously observed for both conventional and dicationic ionic liquids.[1,17,108] Branched dicationic ionic liquids had lower densities than straight chain DILs. As indicated in **Table 1**, **IL12**, bearing the bulky *tert*-butyl group, had the lowest density among all imidazolium DILs synthesized in this study. The density of $[1m(C_1C_1im)_2C_3]^{2+}.2NTf_2^-$ (**IL2**) was found to be higher than its β-substituted analog ($[2m(C_1C_1im)_2C_3]^{2+}.2NTf_2^-$, **IL3**). It can be suggested that the position of alkyl substituent (molecular symmetry) affects the van der Waals volume and packing efficiency of these isomers. DILs with methyl substituents on one α-carbon showed higher densities than DILs with methyl branching on both α-carbons (**IL7** vs. **IL8**, and **IL16** vs. **IL17**). Moreover, an increase in the length of hydrocarbon spacer chain leads to a decrease in densities of dicationic ionic liquids.[17] Thus, the DILs having C3 linkages had higher densities than analogous C4, and C5 ionic liquids. A summary of density values for the ILs used in this study is provided in Table 4-1. The density of ionic liquids also can be influenced by variation in the nature of the cationic moiety.[7] As shown in Table 4-1 dimethylimidazolium ionic liquids had greater densities than comparable methylpyrrolidinium and tripropylphosphonium ionic liquids. It has been postulated that π-π stacking interactions leads to formation of a planar structure and thereby more efficient packing of imidazolium ionic liquids.[173]

4.3.3 Viscosity

As a result of strong interionic interactions, ionic liquids usually show higher viscosities than commonly used organic fluids.[1] The high viscosities of ionic liquids narrow their applications in synthesis and extraction techniques which involve mixing and/or mass transfer operations.[11] On the other hand, highly viscous fluids would be useful for some applications, such as lubrication and stationary phases for gas-liquid chromatography.[176] The intermolecular frictional force in the ionic liquids is primarily governed by molecular shape.[177] Therefore, branched ionic liquids are expected to show different viscosities than their linear counterparts. As indicated in Table 4-1 the viscosities of branched DILs are usually larger than their straight-chain analogs. However, there are some exceptions to this experimental observation. For instance, **IL7** was found to possess lower viscosity than its straight-chain geometrical isomer **(IL9**) at 80 °C. Similar behavior was previously reported for monocationic ionic liquids.[1] In addition, the position of the branched alkyl group considerably affects the ionic liquid's viscosity. α-Substituted DILs were determined to have lower viscosities than β-substituted DILs. It was previously reported that the unsymmetrical cationic moieties lower the viscosities of ionic liquids.[1] Viscosity, like other physical properties, is influenced by the size of the pendant group. Introducing bulkier substituents such as *tert*-butyl groups (**IL12**) on the linkage chain raised the viscosity of dicationic ILs. In addition, the DILs' viscosity showed significant temperature dependency. Viscosities were decreased by increasing the temperature, due to the weakened intermolecular interactions at elevated temperatures.[178] Moreover, the viscosity of dicationic ILs also are a function of the charged head groups.[94] For DILs with the same spacer chain, the phosphonium ILs showed the highest viscosities followed by pyrrolidinium ionic liquids. The lowest kinematic viscosities were observed for imidazolium DILs probably due to their larger densities.[1]

4.3.4 Thermal stability

Conventional ILs containing linear side chains are more thermally stable than comparable branched monocationic ionic liquids.[169,170] A similar trend was observed for dicationic ionic liquids. Figure 4-2 compares thermal stabilities of DILs obtained from thermogravimetric analysis (TGA) at 5% weight loss. Compared with linear-chain DILs, thermal decomposition of DILs with branched linkage chain was usually observed at lower temperatures. As previously discussed in the melting point section, alkyl chain branching leads to disruption of packing efficiency. Meanwhile, it could also decrease the intermolecular coulombic attraction between the ions, which may lead to lower thermal stabilities of ionic liquids.[179] The decrease in thermal stability is more profound when utilizing a shorter spacer chain such as C3 or C4. In case of $[1m(C_1C_1im)_2C_3]^{2+}.2NTf_2^-$ (**IL2**), due to formation of a more stable carbocationic intermediate, the C-N bond between alkane linkage chain and imidazolium head group tends to break more readily than the β-substituted isomer (**IL3**), resulting in further instability of α-branched DILs [38,39]. By comparing $[1m(C_1C_1im)_2C_4]^{2+}.2NTf_2^-$ (**IL7**), and $[1m4m(C_1C_1im)_2C_4]^{2+}.2NTf_2^-$ (**IL8**), it was shown that inserting two methyl groups on both ends of the alkane linkage chain further decreased the thermal stability of the dicationic IL. The effect of branching on thermal decomposition of DILs containing C5 linkages was found to be small. The determined thermal stabilities of $[3m(C_1C_1im)_2C_5]^{2+}.2NTf_2^-$ (**IL10**), $[3m(C_1py)_2C_5]^{2+}.2NTf_2^-$ (**IL19**), and $[3m(P[C_3C_3C_3])_2C_5]^{2+}.2NTf_2^-$ (**IL25**) were very close to the values for their linear analogs. On the other hand, addition of another methyl group (**IL11**, **IL20**, and **IL26**) or substitution of the methyl group with a *tert*-butyl group (**IL12**) resulted in a slight decrease in the thermal stabilities of these ILs. Moreover, the nature of cationic moieties can significantly influence the thermal stabilities of ionic liquids.[1] As depicted in Figure 4-2 the presence of dimethylimidazolium charged group conferred more stability to DILs than did methylpyrrolidinium and tripropylphosphonium with the same spacer chain. The carbon-nitrogen bond between imidazolium ionic liquids is more stable than the one in pyrrolidinium ILs.[6] Also, it has been reported that the thermal stability of phosphonium ILs is slightly lower than analogous dimethylimidazolium ILs, when paired with a weakly nucleophilic anion such as NTf_2^-.[179]

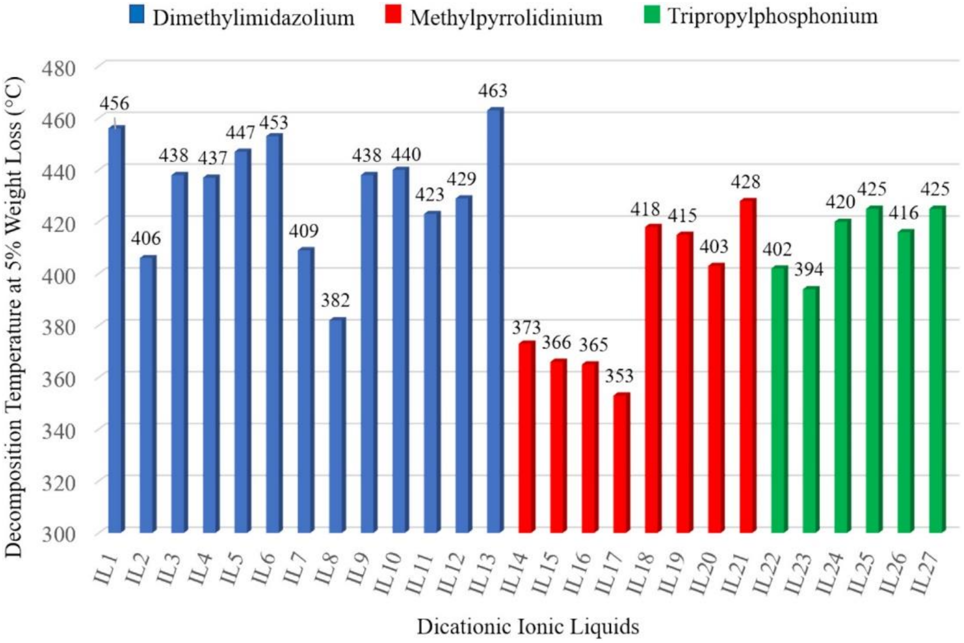

Figure 4-2 Thermal stability comparison of dicationic ionic liquids synthesized in this study. Results are obtained from 5% mass decrease of sample monitored by TGA. Temperature rate of 10 °C, under nitrogen atmosphere (flow ~30 mL/min)

The dynamic TGA experiment usually overestimates thermal stabilities. However, they can be useful to compare short-term and relative thermal stabilities of ionic liquids.[6] Alternatively, inverse gas chromatography (IGC) was utilized to obtain a more precise estimation of thermal stability of branched DILs. This method can be used to evaluate the bleeding behavior of low melting point ionic liquids.[7,15] Consequently, 14 different ILs were selected to coat on the inner surface of short capillary GC columns. The initial oven temperature was set at 100 °C and ramped with rate of 1 °C/min up to 450 °C. The slower temperature ramp of 1 °C/min provides a more accurate indication of thermal stability than fast TGA experiments. Moreover, employing the flame ionization detector (FID) enables the sensitive detection of trace volatile and/or decomposed products. The obtained data from IGC experiment is shown in Figure 4-3. In order to draw a more useful comparison with the TGA study, the decomposition temperatures were marked on each chromatogram. The marked points indicate the temperatures where column bleed started. The highest thermal stability was observed for $[3m(C_1C_1im)2C_5]^{2+\cdot}2NTf_2^{-}$ with an initial bleeding temperature of 353°C, which is considerably lower than the decomposition point determined by TGA (T95%: 440 °C). This observation can be correlated to the slower temperature ramp utilized in the IGC experiment.[7] The IGC results confirmed that the α-substituted ionic liquids tend to decompose at lower temperatures. For example, there is a 46 °C difference between thermal stability of IL2 and its β-substituted isomer, IL3. Interestingly, substitution of the 3-methylpentyl (IL10) linkage by a 3,3-dimethylpentyl (IL11) spacer chain caused a tremendous drop (~40 °C) in the thermal stability of dimethylimidazolium ionic liquids. This substantial difference in thermal stability was not observed in the TGA experiment. Thermal stabilities of methylpyrrolidinium DILs with 2-methylpropyl (IL14) and 3-methylpentyl (IL19) linkages were found to be about 40 °C lower than analogous dimethylimidazolium DILs (IL3, and IL10). However, there was not a significant difference between stabilities of $[3m_2(C_1C_1im)_2C_5]^{2+}.2NTf_2^{-}$ (IL11) and $[3m_2(C_1py)_2C_5]^{2+}.2NTf_2^{-}$ (IL20) when probed by inverse GC. When comparing DILs containing 2-methylpropyl (IL3, IL14, and IL22) or isobutylene (IL5, IL15, and IL23) with different cationic head groups, the following trend can be observed for their thermal stabilities; $C_1C_1im > P[C_3C_3C_3] > C_1py$.

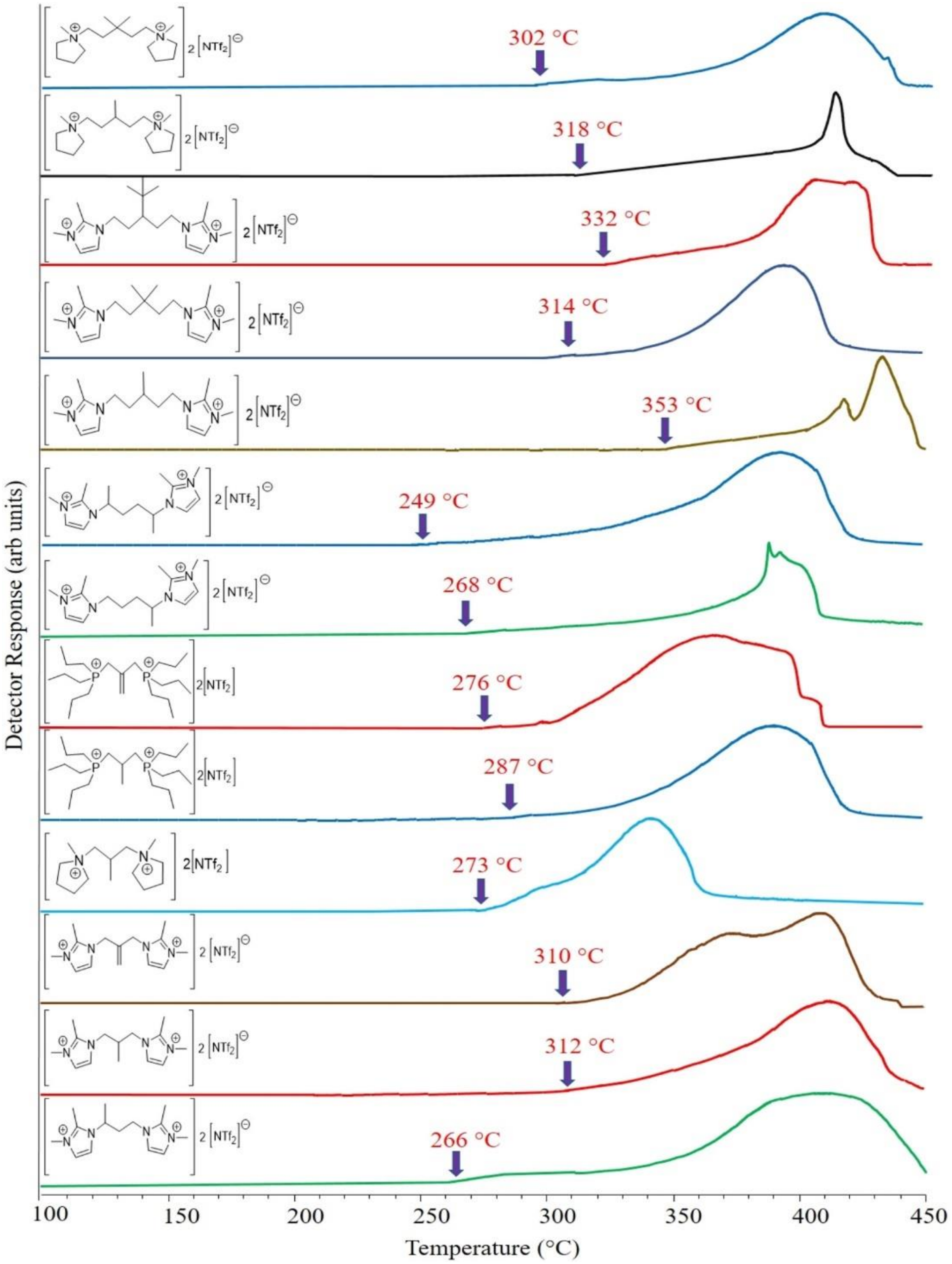

Figure 4-3 Thermal stability diagram of 13 selected DILs acquired from inverse GC-FID. Oven temperature was set at 100 °C and ramped up to 450 °C by rate of 1 °C/min. Helium was used as carrier gas @ 1 mL/min

4.3.5 Chromatographic performance

Designing the low melting point materials with considerably high thermal stability is one of the major challenges in making novel GC stationary phases. In other words, the coated materials should maintain a stable liquid state over a wide range of temperatures.[15] In addition, large viscosities at high temperatures are required to maintain coating efficiencies.[11,15] Dicationic ionic liquids have been found to possess such properties and shown to produce efficient and effective separations.[15] Unlike traditional stationary phases, IL-based stationary phases show multiple solvation interactions and provide unique selectivities toward a variety of compounds.[165] As discussed previously, branching on the alkyl linkage chain lowers the melting point of dicationic ILs. Also, some of the branched DILs showed similar thermal stability and higher viscosities than their linear analogs. Therefore, they can be utilized as effective GC stationary phases. Most recently, we reported an unprecedented GC separation of *cis* and *trans* fatty acid isomers on branched-chain dicationic ionic liquid columns.[55]

In environmental studies, it is very crucial to effectively determine and quantify each component in the BTEX mixture due to their potential health risks.[180] However, it is often difficult to achieve baseline separation of aromatic isomers on traditional GC columns, especially in the case of ethylbenzene, *m*-xylene, and *p*-xylene. A 30-m $[3m_2(C_1py)_2C_5]^{2+}.2NTf_2^-$ column was employed to evaluate the selectivity of branched-chain IL-based columns toward separation of BTEX components. Figure 4-4 shows an excellent separation of the BTEX mixture on the $[3m_2(C_1py)_2C_5]^{2+}.2NTf_2^-$ stationary phase. Baseline separation of *m*- and *p*-xylene was achieved at 70 °C, indicating the great selectivity of this stationary phase for separation of positional isomers. The details of chromatographic conditions were summarized in the experimental section.

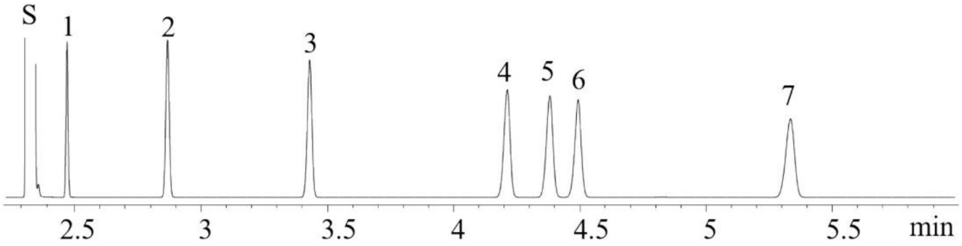

Figure 4-4 Separation of structural isomers of BTEX mixture on the $[3m_2(C_1py)_2C_5]^{2+}.2NTf_2^-$ IL column (30 m × 0.25 mm i.d.). S) hexane, 1) nonane, 2) benzene, 3) toluene, 4) ethylbenzene, 5) *p*-xylene, 6) *m*-xylene, 7) *o*-xylene. GC separation conditions: 70 °C, isothermal, 1 mL/min He; FID

4.4 Conclusions

By synthesizing 18 different branched-chain DILs and comparing their properties with their linear counterparts, we have shown how the inclusion of alkyl substituents on the dicationic ionic liquids spacer chains can be used to change and “tune” their physicochemical properties. In contrast to branched monocationic ionic liquids, branched-chain DILs were found to possess lower melting points than analogous linear-chain DILs. Dicationic ILs containing branched alkyl linkage chain have higher viscosities and lower densities than their linear analogs. Thermal stabilities of branched-chain DILs are significantly influenced by the position of alkyl substituent and the symmetry of the dicationic moiety. The α-methyl substituted DILs with propyl linkages had considerably lower thermal stabilities than 2-methylpropyl containing DILs. Branched-chain DILs with short linkage chains (C3, C4) exhibited lower thermal stabilities than their linear analogs. However, the homothetic mid-chain methyl substituted DILs with C5 linkage showed similar thermal stabilities to their unbranched counterparts. The effect of the cationic moiety on the physicochemical properties of DILs was determined to be even more significant than spacer chain branching. For instance, DILs containing phosphonium cationic moiety have larger viscosities and lower densities than nitrogen-based ionic liquids. The remarkable selectivity of branched-chain dicationic ILs as GC stationary phase was demonstrated by the complete separation of a BTEX mixture. The $[3m_2(C_1py)_2C_5]^{2+}.2NTf_2^-$ column was successfully used to distinguish between *m*- and *p*-xylene isomers which are difficult to separate on conventional GC columns.

Chapter 5

BRANCHED-CHAIN DICATIONIC IONIC LIQUIDS FOR FATTY ACID METHYL ESTER ASSESSMENT BY GAS CHROMATOGRAPHY

Abstract

Twelve bis- or dicationic ionic liquids (ILs) including eight based on imidazolium, a single one based on phosphonium and three based on pyrrolidinium cationic units were prepared with the bis(trifluoromethyl sulfonyl) imide anion. The two identical cationic moieties were attached by different alkyl spacers having 3 or 5 carbons and differing alkyl substituents attached to the spacer. The SLB-IL111 column, as the most polar commercial stationary phase known, was included in the study for comparison. Isothermal separations of a rapeseed oil fatty acid methyl ester (FAME) sample were used to study and compare the 12 IL-based column performances and selectivites. The retention times of the most retained methyl esters of lignoceric (C24:0) and erucic (C22:1) acids were used to estimate the IL polarity. The phosphonium dicationic IL column was, by far, the least polar. Imidazolium based dicationic IL columns were the most polar. Polarity and selectivity for the FAME separation were somewhat related. The separation of a 37-FAME standard mixture allowed investigation of selectivity variations observed on the 12 IL-based columns under temperature gradients up to 230 °C. The remarkable selectivity of the IL-based columns is demonstrated by the detailed analysis of the cis/trans C18:1 isomers of a partially hydrogenated vegetable oil sample on 30 m columns, separations competing with that done following an “official method” performed on a 100 m column.

5.1 Introduction

Ionic liquids (ILs) are innovative fluids that have found applications in many branches of chemistry.[1,11,119] Thanks to their extremely low vapor pressure and high thermal stability, they were very successfully used as stationary phases in gas chromatography (GC).[15,28,181,182] The IL-based GC stationary phases turned out to be remarkably polar and thermally stable phases having a unique selectivity not seen before with molecular GC stationary phases.[15] Bis- or di-cationic imidazolium based[5] or phosphonium based[94] ILs, showed decomposition temperatures significantly higher than monocationic traditional ILs. These dicationic ILs are constitutive of successful and commercially available polar GC capillary columns. The commercially available IL-based capillary GC columns are polar stationary phases with polarity ranging from a McReynolds constant of 2666 for SLB-IL60 to the most polar SLB-IL111 with a McReynolds constant of 5150 with working temperature ranges between 50 and 270 °C. [57,146] Ionic liquids can undergo multiple types of solvation interactions and provide unique selectivity for separation of variety of compounds.[15] They have been effectively utilized for the analysis of flavors and fragrances,[142,146,183,184] ethanol,[34,36] water,[29-33] and fatty acids (FA),[45-48,56,57,60-64,69,71,72,81,82,88,185-192] in food as well as pharmaceutical samples.

Analysis of fatty acids (FAs) is important, especially in food industry, because of their bio-functional significance in living organisms.[47] FAs are categorized as short chain FAs (less than 6 carbons), medium chain FAs (with 6 to 12 carbons) and long-chain FAs with more than 12 carbons in the alkyl chain length. Further, there are saturated FAs and unsaturated FAs. Unsaturated FAs, depending on their chain length, can have up to six double bonds with possible *cis-trans* configurations making a very large number of geometrical isomers.[48] GC is the preferred technique for the analysis of fatty acids when derivatized as methyl esters (FAMEs). The IL-based commercially available capillary columns demonstrated an outstanding efficacy for this task. The main results were that the FAME retention times decreased with increasing IL polarity, but unsaturated FAMEs were retained longer compared to their saturated counterparts.[48,57] In fact, ionic liquid columns exhibit higher polarity and complementary selectivity compared to traditional GC stationary phases. IL phases are particularly adept at separating *cis* and *trans* FAME isomers.[46,57,62] Their dipolar nature is able to polarize the unsaturated FAME groups which help them to distinguish between such fatty acid isomers.

The retention properties of dicationic IL-based stationary phases are primarily governed by their molecular structure.[47] By performing proper structural modification on the cationic moieties, spacer chain, or counteranions, the physico-chemical properties of dicationic ILs, melting point, viscosity or thermal stability, can be tuned.[7] However, different ILs may have different selectivies and polarities when used as GC stationary phase. In our recent investigations on the dicationic ILs properties, when used as stationary phases in GC, we focused on influences of the cationic head group and the anionic counterion.[15] In this work, we showed how structural variation on the alkyl linkage chain can affect the polarity and selectivity of dicationic ionic liquids. Twelve branched-chain dicationic ionic liquids based on imidazolium, pyrrolidinium, and phosphonium head groups paired with the same bis(trifluoromethyl sulfonyl) imide anion were specially synthesized and coated on capillary columns of identical geometry. Their capabilities in separating FAMEs were evaluated and compared to the results obtained with the SLB-IL 111 column, which is known to be very effective for FAME analyses and is the most polar commercial GC stationary phase. Different FAME test mixtures were examined on the 12 columns focusing on their selectivity.

5.2 Experimental

5.2.1 Chemicals and columns

The Supelco 37 component FAME mix (CRM47885), *cis-trans* isomer standard (N08105), and rapeseed oil mix (N08657) were kindly provided by Supelco (Bellefonte, PA). The individual C18:1 FAME isomers were purchased from Millipore-Sigma (ex-Sigma-Aldrich, St. Louis, MO). The ionic liquids used for stationary phases in this study were synthesized in our laboratory. The whole synthesis processes and characterization of physicochemical properties of these branched-chain ILs is reported elsewhere.[9] The IL abbreviation system presented in Table 5-1 was defined by Hallet and Welton.[12]

Basically, the focus was set on the spacer linking the two charged head groups of the dicationic ILs. IL1 to IL5 were prepared with a propyl (three carbon) spacer and seven ILs, IL6 to IL12, were made with a pentyl (five carbon) spacer inserted in between two identical charged groups as summarized in Table 5-1 IL6 is the known stationary phase of the commercially available SLB-IL111 (Supelco, Millipore-Sigma). All newly synthesized dicationic ILs were associated with bis(trifluoromethyl sulfonyl) imide anions, $N(SO_2CF_3)_2^-$. The dicationic ILs were coated on fused silica capillary columns with dimension 30 m x 0.25 mm i.d. and a film thickness of 0.20 µm.

The results were compared with the commercially available SLB-IL111 capillary column of the same 30 m x 0.25 mm i.d. and 0.20 µm film thickness (IL6 in Table 5-1). The listed polarity values were roughly estimated using the retention times of lignoceric acid (C24:0) and erucic acid (C22:1) whose retention times were found related to the McReynolds constants of IL-based GC columns. All the IL coated columns along with a SP-2560 column (bis-cyanopropyl polysiloxane, 100 m x 0.25 mm i.d., 0.20 µm) were provided by Supelco (Millipore-Sigma, Bellefonte, PA).

5.2.2 Instrumentation

The gas chromatographic analyses were performed using an Agilent 6890N (Agilent, Palo Alto, CA, USA) gas chromatograph equipped with a flame ionization detector. An Agilent ChemStation data processing unit was used for processing and storing the chromatograms. Helium was used as the carrier gas at a constant flow rate of 1 mL/min. The typical injection volume was 1 µL using a split ratio of 100:1. The injection port and FID temperatures were set at 250 °C. Each injection was made in triplicate. The 30 m column efficiencies were determined by injecting naphthalene at 110 °C and were all in the 120,000-plate range or ~4000 plate/m or ~250 µm (one column diameter) height equivalent to a theoretical plate. The analyses made with the rapeseed oil mix were performed isothermally at 180 °C. Analyses of the Supelco 37-FAME mix were made on all 12 IL-based columns using the same temperature program: the initial oven temperature was set at 70 °C hold for 2 min, then a 10 °C/min ramp was started, up to 180°C, hold for 1 min, then a second ramp of 4°C/min followed up to 280 °C that was maintain for 6 min. The *cis-trans* isomer standard was separated isothermally at 130 °C, and 175 °C, on the 30 m, and 100 m columns, respectively.

Table 5-1 Structure and polarity estimation of the 12 dicationic-NTf_2 ionic liquids used to prepare 30 m x 250 µm capillary columns.

Entry	Cation Abbreviation[a]	Cation Structure		m.w.	Polarity[b]
		Molecular Model	Formula		
IL1	$2mC_3(mim)_2$		$C_{12}H_{20}N_4$	220.3	5400 (117)
IL2	$2mC_3(m_2im)_2$	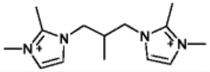	$C_{14}H_{24}N_4$	248.3	5080 (109)
IL3	$2mC_3(mpy)_2$	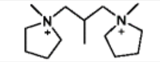	$C_{14}H_{30}N_2$	226.4	4360 (93)
IL4	$2mC_3(pr_3p)_2$	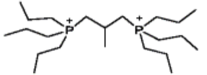	$C_{22}H_{50}P_2$	376.6	2700 (62)
IL5	i-ene$C_4(m_2im)_2$	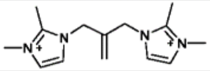	$C_{14}H_{22}N_4$	246.4	5500 (119)
IL6	$C_5(m_2im)_2$ (SLB-IL 111)	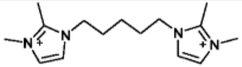	$C_{15}H_{26}N_4$	262.4	5150 (111)
IL7	$3mC_5(mim)_2$	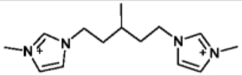	$C_{14}H_{24}N_4$	248.4	5200 (112)
IL8	$3mC_5(m_2im)_2$	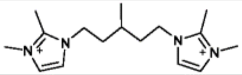	$C_{16}H_{28}N_4$	276.4	5200 (112)
IL9	$3m_2C_5(m_2im)_2$		$C_{17}H_{30}N_4$	290.4	4460 (95)
IL10	$3t\text{-}buC_5(m_2im)_2$	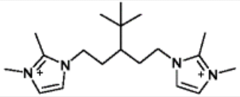	$C_{19}H_{34}N_4$	318.5	4550 (98)
IL11	$3mC_5(mpy)_2$	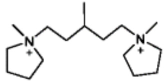	$C_{16}H_{34}N_2$	254.5	5040 (109)
IL12	$3m_2C_5(mpy)_2$		$C_{17}H_{36}N_2$	268.5	4230 (90)

[a] The left part of the code refers to the spacer. The first number indicates the position of the substituent on the spacer chain whose length is given by the carbon number n. The spacer substituent can be m for methyl, m_2 for two methyl, and t-bu for *t*-butyl. Also, i-eneC_4 refers to isobutylene spacer chain. The cationic group is between parenthesis with mim for 3-methylimidazolium, $m_2$im for 2,3-dimethylimidazolium, mpy for N-methylpyrrolidinium, and ppr_3 for tripropylphosphonium.[12]

[b] The first polarity value is a rough estimate of the global McReynolds constant obtained using the C24:0 and C22:1 retention times and standardizing with known columns, the value in parenthesis corresponds to the polarity number defined by Ragonese and Mondello.[146]

5.3 Results and discussion

5.3.1 Polarity and selectivity with isothermal FAME separations

5.3.1.1 Polarity and FAME retention

Polarity and selectivity changes observed on all 12 dicationic IL-based columns were evaluated using the rapeseed oil test mixture (N08657). This mixture of known composition was injected utilizing the same experimental conditions, i.e. isothermal 180 °C with a constant He, 1 mL/min flow. Given past results that showed the elution of FAMEs was faster on more polar IL-based stationary phases,[15] the retention times of the lignoceric (tetracosanoic) acid, C24:0, and erucic acid, C22:1, were used to obtain a rough estimate of the McReynolds constants of the new IL stationary phases. Using this value, the polarity number (PN) defined by Ragonese et al.[146] was calculated and reported in Table 5-1. These polarity values derived from the C24:0/C22:1 retention times are a rough approximation, but they allow for a rapid estimation of the polarity differences between the newly prepared ILs. **IL6** is marketed by Millipore-Sigma under the trade name SLB-IL111 due to its polarity number of 111.

The least polar dicationic stationary phase is the unique phosphonium based **IL4**, containing neither double bond nor π electrons. No other IL in this group has such a low polarity (PN 62). Conversely, the most polar IL is the imidazolium based **IL5**, the only IL containing a double bond in its spacer (Table 5-1). However, with its PN 119, **IL5** is close to other imidazolium-based compounds such as **IL1** (PN 117), **IL7** and **IL8** (both with PN 112), or **IL6** (SLB-IL 111, PN 111).

The changes made on the spacer chain structure have different influences on the IL polarity. **IL1** with a 2-methylpropyl spacer has a high polarity, the homothetic **IL7** with a pentyl spacer is slightly less polar. The same trend is not observed between **IL2** (PN 109) and **IL8** (PN 112), the second one, with a pentyl spacer, being slightly more polar than its propyl equivalent. Comparing **IL3** (PN 93), a methylpyrrolidinium dicationic IL with a propyl spacer and the similar **IL11** (PN 109) that has a pentyl spacer, the latter is significantly more polar. The addition of two methyl groups on the C_2 position of the imidazolium rings has a limited effect on the IL polarity but a tremendous effect on its thermal stability.[7] The imidazolium hydrogen at position 2 is slightly acidic and will be cleaved upon heating much more easily than a methyl group.[173] A methyl group added in the middle of the spacer also does not affect much the IL polarity. **ILs 6**, **7** and **8** have a similar polarity (Table 5-1). However, adding a second methyl group in the middle of the spacer chain (**IL 9** and **IL12**) significantly decreases the IL polarity. The bulky *t*-butyl group added to the pentyl spacer (**IL10**) also reduced the polarity as might be expected. The polarity of IL stationary phases decreases by increasing the van der Waals dispersion interactions.[15]

5.3.1.2 Selectivity observing two critical FAME pairs

The selectivity of the newly synthesized dicationic IL GC stationary phases was evaluated by studying the linoleic/arachidic and linolenic/behenic FAME separation (C18:2/C20:0 and C18:3/C22:0, respectively). The C18:2/C20:0 couple was selected due to the close elution of these two FAMEs with unpredictable elution order. The C18:3/C22:0 couple was also difficult to separate with coelution on several columns. However, when separation is observed, C22:0 always eluted last. Figure 5-1A shows the selectivity factors obtained for these two separations. The columns are aligned (from left to right) from most polar (**IL5**) to least polar (**IL4**).

Since the selectivity factor is the ratio of the retention factor of the more retained compound to that of the less retained compound, it does not give information on the elution order. Therefore, another way to study the column selectivity is to use the equivalent chain length (ECL) difference between compounds. The ECL value is used for unsaturated FAMEs. It corresponds to the theoretical fractional saturated chain length that would produce the same retention than that observed for the unsaturated FAME. The ECL value is calculated using the two saturated FAMEs that bracket the peak of the unsaturated FAME.[58] The following equation was used to calculate the ECL values in this study:

$$ECL(C_n : x) = n + 2\frac{\log(RRT(C_n : x) - \log(RRT(C_n : 0)}{\log(RRT(C_{n+2} : 0) - \log(RRT(C_n : 0)} \qquad (5\text{-}1)$$

in which *n* is the FAME chain length, *x* is the number of double bonds and RRT is the relative retention time compared to $C_n : 0$. Figure 5-1B shows the bar plot of the FAME ECL difference. The magnitude of the bar is linked to selectivity with the sign indicating the retention order. All bars are positive for the C22:0/C18:3 separations as seen on the chromatograms: C22:0 is more (or equally) retained to C18:3.

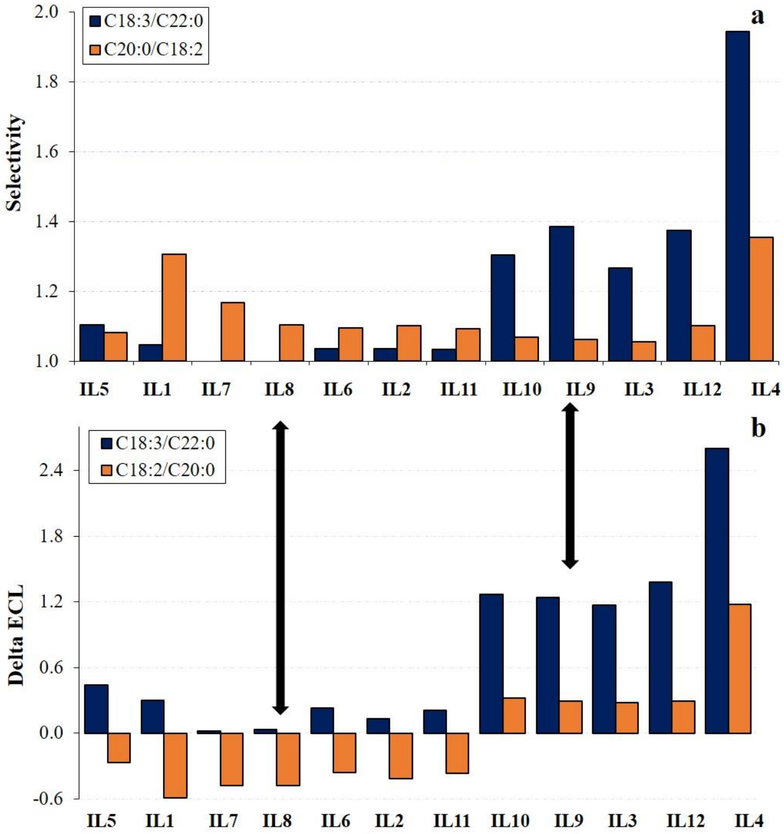

Figure 5-1 Comparison of the selectivity obtained with the dicationic IL-based GC columns in the separation of the methyl esters of linoleic acid and arachidic acid (C18:2 and C20:0) and linolenic acid and behenic acid (C18:3 and C22:0). **A** shows the selectivity factors (ratio of the higher retention factor over the lower one). **B** presents the equivalent chain length differences. The vertical arrows indicate the two columns whose chromatograms are shown in Figure 5-2. The columns are sorted by decreasing polarity order with the most polar IL5 on the left (see Table 1). Columns 30 m x 250 µm, film thickness 20 µm, helium carrier gas @ 1 mL/min, 180°C

To illustrate this point, Figure 5-2 shows the chromatograms obtained with **IL8** (Figure 5-2A) and **IL9** (Figure 5-2B) with vertical arrows pointing to the C22:0 and C18:3 peak positions. For the C20:0/C18:2 separations, Figure 5-1B shows a negative bar for **IL8** since the C18:2 FAME elutes after C20:0 (Figure 5-2A). On the contrary, the positive bar **for IL9** corresponds to the elution of C20:0 after C18:2 as seen in Figure 5-2B. For the C18:3/C22:0 pair, the selectivity difference induced by the simple addition of a methyl group in the middle of the C_5 linker is striking (arrows of Fig. 2). The two FAMEs are coeluted on **IL8 (**Figure 5-2A). The same FAMEs elute 1.5 min apart on **IL9** (Figure 5-2B).

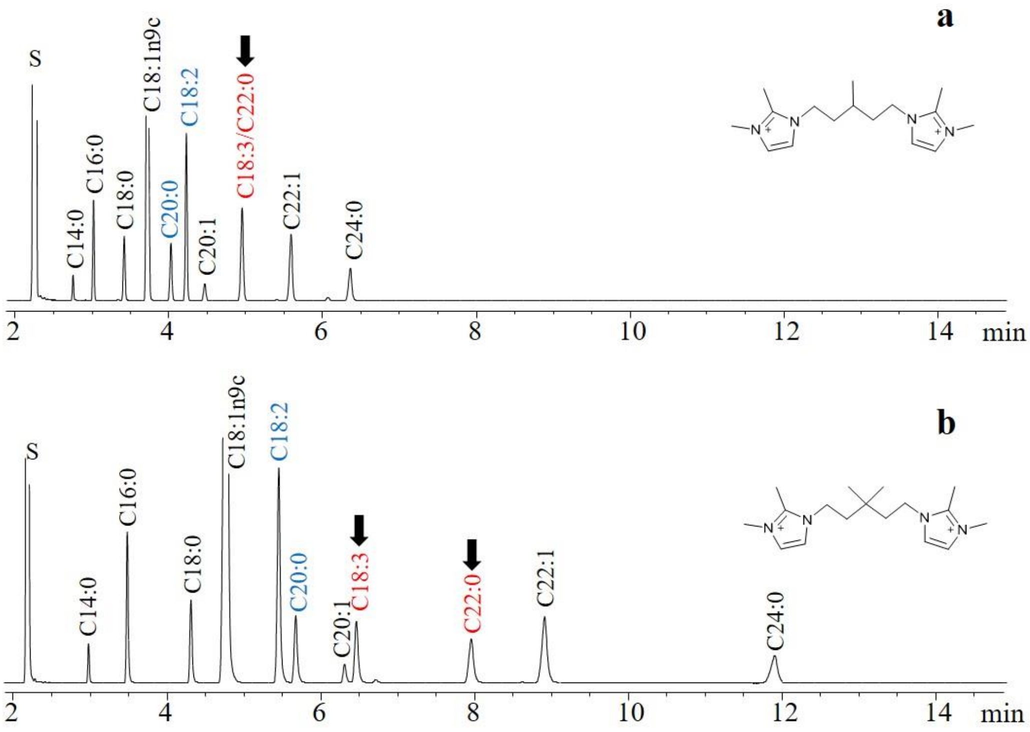

Figure 5-2 Chromatogram of the rapeseed FAME mixture N08657 on the $3m_2C_5(m_2im)_2$ **IL8** (**A**) and $3mC_5(mim)_2$ **IL9** (**B**) capillary columns (30 m x 250 µm, film thickness 20 µm)

The results presented in Figure 5-1, either selectivity (**a**) or ECL difference (**b**) are very coherent: **IL4**, the only phosphonium based IL of this series, stands out for these two pairs of peaks. The long retention times obtained with this least polar stationary phase (PN 62) produce separation for the two pairs that are minutes apart. The second-best selectivity for the C18:2/C20:0 pair is obtained on **IL1** or 2mC$_3$(mim)$_2$ which also is the second most polar column of the set with a polarity number of 117 (Table 1). The second-best selectivity for the C18:3/C22:0 pair is obtained on **IL9** or 3m$_2$C$_5$(m$_2$im)$_2$ which has a polarity number of 95. There is not a strong relationship between polarity and selectivity for these two selected FAME pairs. The C18:2/C20:0 pair seems to be better separated by more polar columns except by the most and least polar ones: the most polar **IL5** separates poorly and the least polar **IL4** is the best (**Fig. 1**). The C18:3/C22:0 pair seems to be better separated by the least polar columns, here also, with a huge variation (dark bars in Figure 5-1).

5.3.2 Polarity and selectivity with gradient FAME separations

The CRM47885 test mix (see Materials and methods) contains 37 different fatty acids from the methyl esters of butyric acid (C4:0) to nervonic acid (C24:1) with a variety of unsaturated FAMEs including *cis* and *trans* isomers. For comparison purposes, the temperature gradient described in the experimental section was used for all columns. In these experimental conditions, the retention time of the most retained FAME, C24:1, decreased as the polarity of the column increased, being 29.02 min on the least polar **IL4**, 2mC$_3$(ppr$_3$)$_2$, column and 16.40 min on the most polar **IL5**, i-eneC$_4$(m$_2$im)$_2$, column.

The selectivity factor of four FAME couples was evaluated. The four pairs were: the *cis* and *trans* C18:1n9 and C18:2n6 pairs, the C20:3n3/C20:3n6, and the C20:3n3/C22:1n9 pairs. A distinctive characterization of the IL-based stationary phases found in FAME separation was their ability to elute *trans* isomers before *cis* isomers.[57] This observation was fully confirmed on all new dicationic IL-based columns tested. There was no elution order reversal for the three first pairs on all 12 columns. An elution order inversion was observed for the C20:3n3/C22:1n9 pair, the C22:1n9 FAME eluted first on the extremely polar columns (by definition; PN > 100) whereas, the C20:3n3 FAME eluted first on the least polar columns (PN < 100, Table 1). The selectivity factors are given in Figure 5-3. The two *cis/trans* separations were observed on all IL columns tested with baseline separation and always with the *cis* isomer eluting after the *trans*.

The double bond position in the chain influences the FAME retention behavior. On most GC columns, the n3 or omega 3 FAMEs are more retained than the n6 or omega 6 isomers .[47] This retention difference was observed on all 12 IL-based columns. The separations of the C20:3n3 and C20:3n6 isomers were completed with selectivity factors between 1.02 and 1.04 (Figure 5-3).

A higher variation in selectivity is observed with the C20:3n3 and C22:1n9. These two FAMEs were not separated by **IL10**, $3t\text{-buC}_5(\text{m}_2\text{im})_2$, and barely by **IL11**, $3\text{mC}_5(\text{mpy})_2$. **IL12**, $3\text{m}_2\text{C}_5(\text{mpy})_2$, was more efficient separating this pair. **IL11** and **IL12** are two pyridinium-based dicationic ILs differing by a methyl group in the middle of the C_5 linker confirming the observation made with **IL8** and **IL9** (Figure 5-2) on significant selectivity changes induced by this extra methyl group.

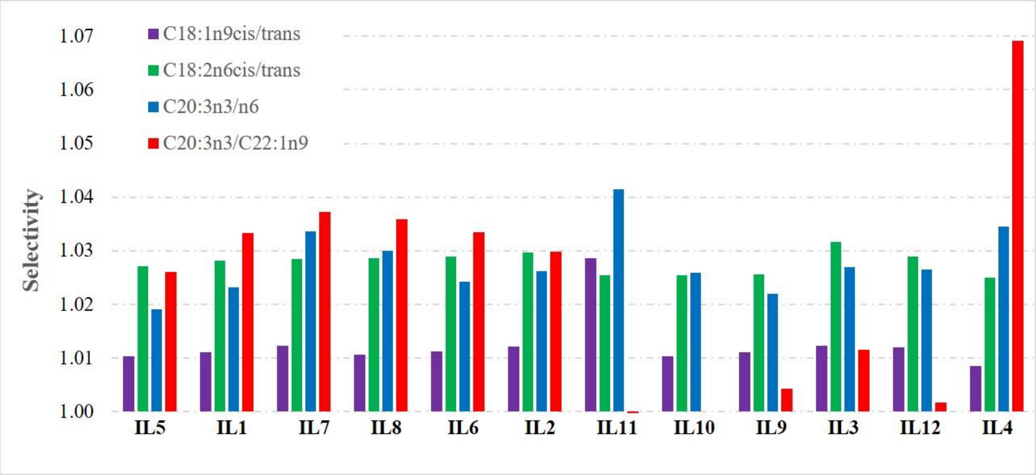

Figure 5-3 Comparison of the selectivity obtained with the dicationic IL-based GC columns in the separation of the methyl esters of the cis and trans isomers of C18:1n9 (oleic and elaidic acids), cis and trans isomers of C18:2n6 (linoleic acid), C20:3n3 and n6, and C20:3n3 and C22:1n9 (erucic acid). The columns are sorted by decreasing polarity order with the most polar IL5 on the left. Columns 30 m x 250 µm, film thickness 20 µm, helium carrier gas @ 1 mL/min, 180 °C

5.3.2.1 Effect of different substituents on the linker

To gain more information on the effect of substituents added on the linker**,** Figure 5-4 shows the selectivity variations induced by simply changing the size of the groups attached in the middle of the C_5 spacer. **IL8**, **9** and **10** are dimethylimidazolium cations attached by a pentyl spacer with a methyl group on the third carbon (**IL8**) or two methyl groups (**IL9**) or a *t*-butyl group (**IL10**). The major differences in elution order and selectivity of these columns are summarized here.

Comparing chromatogram of **IL8** (Figure 5-4A) and **IL9** (Figure 5-4B) shows the dramatic changes in both polarity and selectivity produced by a simple methyl group addition as already observed in isothermal conditions (Figure 5-2). The retention time of the last eluting C22:6 is 19.75 min on **IL8** and 21.87 min on **IL9** roughly corresponding to polarity numbers of respectively 112 and 95 (Table 1). The three pairs C16:0 and C15:1, C17:0 and C16:1, and C18:0 and C17:1 overlap on **IL8**, while they are baseline separated on **IL9**. C21:0 coelute with C18:3n6 on **IL8** when they are 0.7 min apart on **IL9**. The change in elution order between C24:1 and C20:5 is striking. Eicosapentaenoate (C20:5) elutes between C23:0 and C24:0 markers on **IL9**. However, it is retained after the C24:0 marker on the highly polar **IL8** column becoming the last-but-one eluting FAMEs (**Fig. 4b**). Moreover, on the extremely polar **IL8** (PN = 112), C22:1 eluted before C20:3n6, while was more retained and eluted after both C20:3n6 and C20:3n3 on the less polar stationary phases, **IL9**, with a PN of only 95 (Table 1).

On the other hand, the chromatograms obtained with **IL9** and IL10 (Figure 5-4C) are very similar. Changing the two methyl groups for a four-carbon *t*-butyl group in the middle of the pentyl spacer chain does not make great difference in both polarity and selectivity. The major difference is the baseline separation of C20:4 on **IL10**, while it overlapped with C20:3n3 on **IL9 (**Figure 5-4). Also, the partial separation of C20:1 and C18:3n3 on **IL9** is lost on **IL10** that shows a single peak for the two FAMEs (Figure 5-4C).

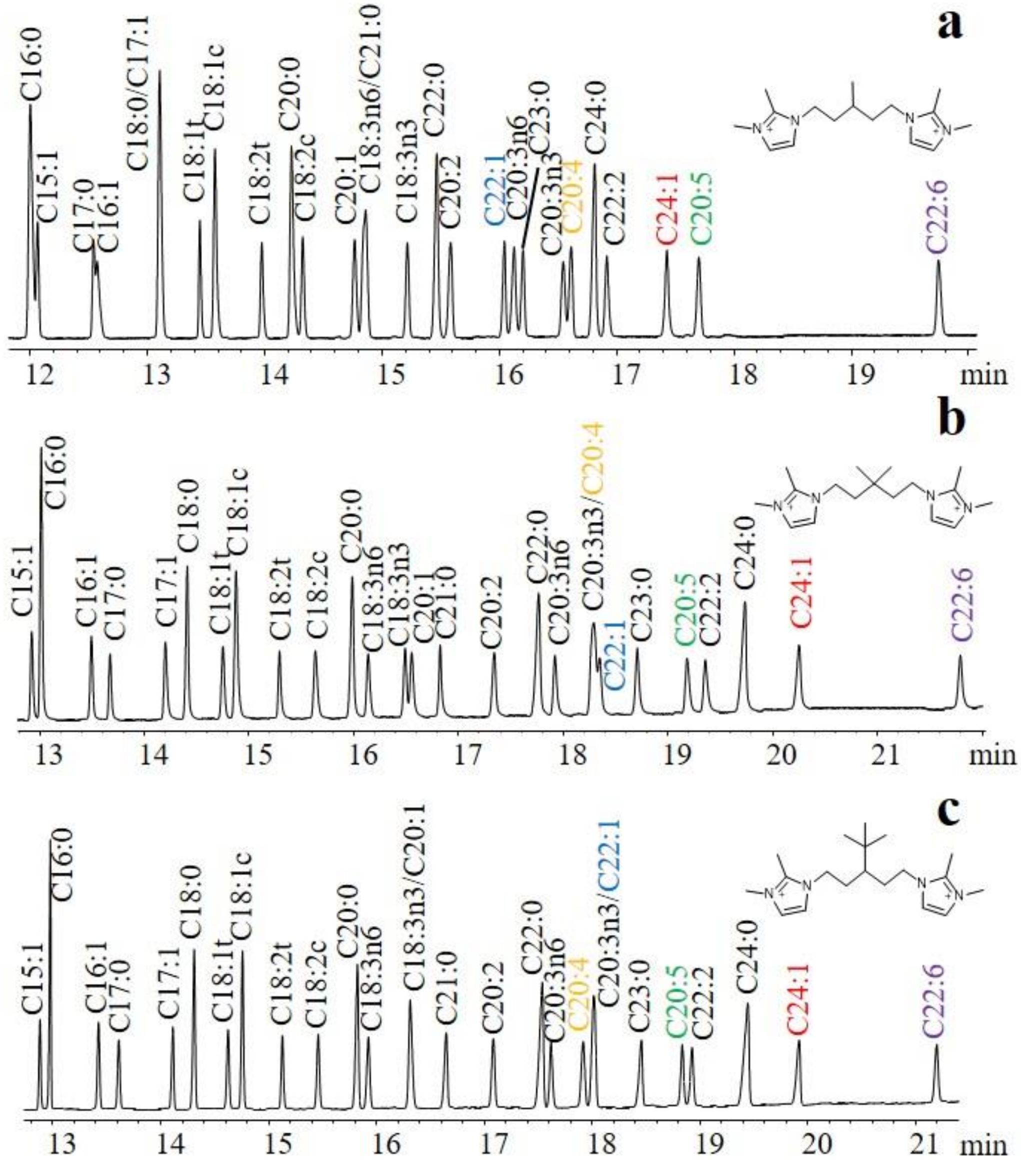

Figure 5-4 Effect of changes in the C5 spacer branching attaching dimethyl-imidazolium cations used as GC stationary phases on the 37 FAME mix separations. A $3mC_5(m_2im)_2$ IL8, B $3m_2C_5(m_2im)_2$ IL9, C $3t\text{-}buC_5(m_2im)_2$ IL10. Columns 30 m x 250 µm, 0.2 µm film thickness. Helium at 1 mL/min constant flow. Temperature gradient: 70 °C for 2 min, 10 °C/min up to 180 °C hold for 1 min, 4 °C/min up to 230 °C hold for 6 min

5.3.2.2 Effect of the cationic moieties

Figure 5-5 compares the chromatograms of the same 37 FAME mix (CRM47885) obtained with the same gradient temperature on IL-based columns which have the same 2-methyl propyl spacer linking two methylimidazolium (Figure 5-5A), N-methylpyrrolidinium (Figure 5-5B), and tripropylphosphonium (Figure 5-5C) cationic moieties. Major differences in both polarity and selectivity are evidenced. First, the change in polarity is seen in the different retention times of saturated FAMEs. The retention times of C24:0, methyl lignocerate, are 15.96 min, 20.24 min, and 28.30 min on **IL1**, **IL3** and **IL4**, respectively. These retention times are coherent with the isothermal polarity numbers that were respectively 119, 93, and 62 (Table 1). Next, the changes in selectivity are remarkable. Eicosapentaenoate (C20:5) elutes 26 s after nervonate (C24.1) on the polar **IL1**. The elution order is reversed on **IL3** with C24:1 eluting 75 s after C20:5. The C24:1-C20:5 retention difference reaches a substantial 295 s on the less polar **IL4** (Figure 5-5C). The elution of C22:6 right before C24:0 on IL4 indicates that the separation mechanism of phosphonium ILs is mostly dominated by dispersive interactions.[94] Whereas, some induced dipole-dipole and π-π interactions on the imidazolium and pyrrolidinium ILs result in an increased retention of the polarizable analytes that have a higher degree of unsaturation.[15] Therefore, the docosahexaenoate FAME (C22:6) eluted last on **IL1** and **IL3** columns.

More selectivity changes are seen in the Figure 5-5 chromatograms such as the elution of C18:3n6 and C20:1, that are almost coeluting on **IL1** at 14 min retention time, and 47 s (around 17 min r.t.) and 124 s apart (between 20 and 22 min r.t.) on **IL3** and **IL4**, respectively. Unexpectedly, C20:3n3 is often more retained than C20:4n6. This elution order was observed because the position of the three unsaturated bonds close to the fatty chain end in C20:3n3, generates a stronger dipole moment than the four double bonds in the middle of the C20:4n6 fatty chain. It is only on a highly polar column such as **IL1** and **IL8** that the retention order is substantially influenced by the degree of unsaturation rather than the position of the double bond. While C20:3n3 and C20:4n6 coeluted on **IL1** and **IL3**, baseline separation of this critical pair was achieved on the medium polarity column, **IL4** (Figure 5-5C).

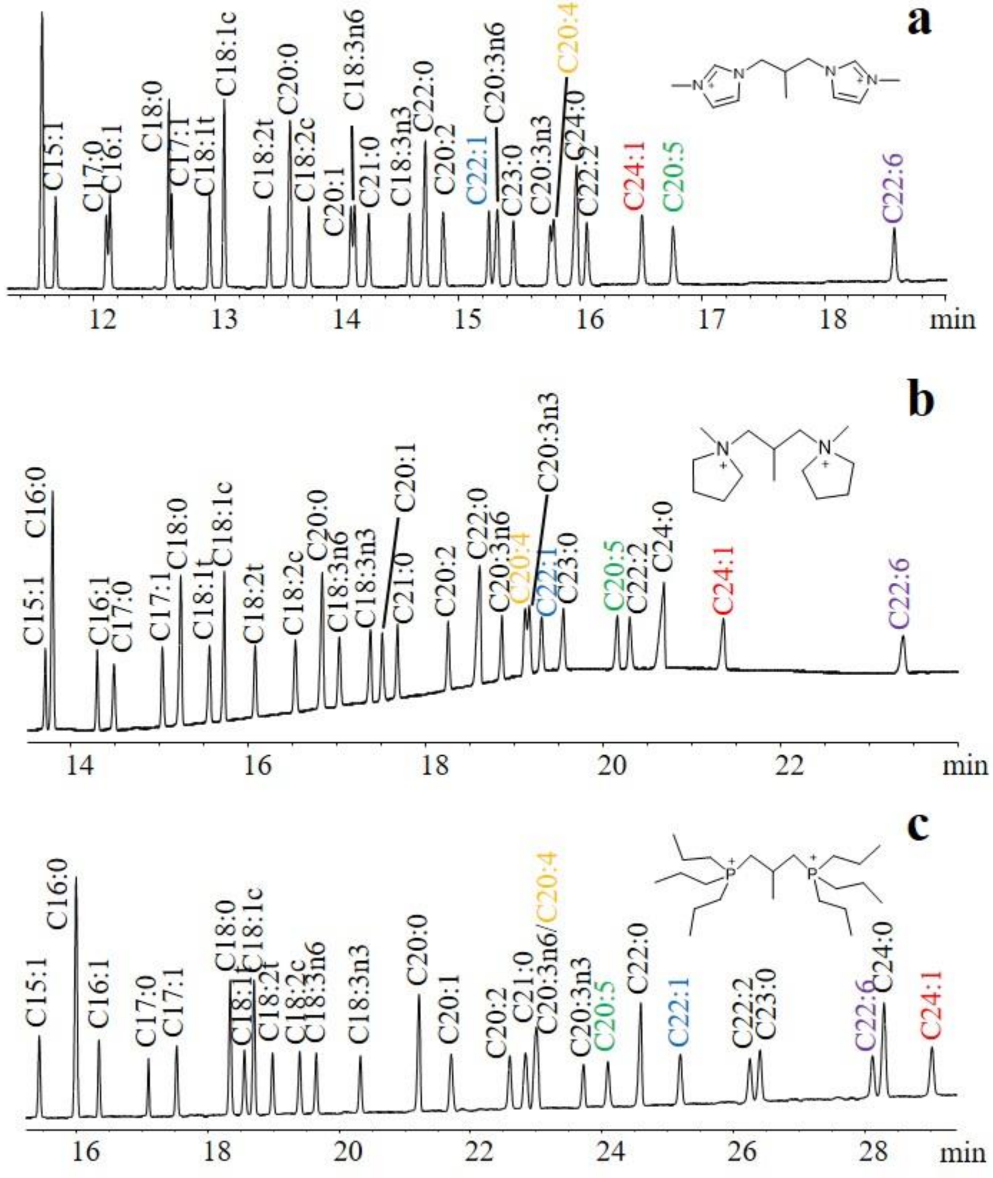

Figure 5-5 Chromatograms of the 37 FAME mix obtained with dicationic IL with a methyl-2-propyl spacer and, A methylimidazolium cation (IL1); B N-methylpyrrolidinium cation (IL3); C tripropylphosphonium cation (IL4). Columns 30 m x 250 µm, 0.2 µm film thickness. Helium at 1 mL/min constant flow. Temperature gradient: 70 °C for 2 min, 10 °C/min up to 180 °C hold for 1 min, 4 °C/min up to 230 °C hold for 6 min

It was recently found that the thermal stability of pyrrolidinium ionic liquids was lower than imidazolium and phosphonium ILs.[7,15] A baseline increase is observed with **IL3** (Figure 5-5B) starting at 180 °C (around 16 min). This was due to some thermal bleed of the **IL3** stationary phase. The other IL-based stationary phases do not show such baseline change up to 230 °C, the final temperature of the programmed ramp for the 37 FAME mix.

5.3.3 Cis and trans FAME analysis

The vast majority of naturally occurring unsaturated fatty acids are *cis* isomers. Fatty acids with *cis* configuration are found to be metabolized more efficiently than *trans*-FAs in the human body.[50] In fact, the increased intake of *trans*-FA increases the risk of cardiovascular disease.[62] Therefore, the determination of *trans* fats in food products is of the utmost importance and is often required by regulatory authorities.[50] The official American Oil Chemist Society method (Ce 1h-05) for this analysis suggests the use of a 100 m SP-2560 capillary column operated at 180°C.[49] The SP-2560 column contains the polar biscyanopropyl polysiloxane polymer and can be operated up to 250 °C. Using the *cis-trans* isomer standard (N08105) developed by Delmonte et al. from partially hydrogenated vegetable oil ,[50,70] the efficacy of the *cis-trans* mix separation on a 100 m **IL12** ($3m_2C_5(mpy)_2$) column (Figure 5-6A) was compared to the results obtained with a 100 m SP-2560 column (Figure 5-6B). On both columns, the *trans* isomers are eluting before their *cis* isomers, both being more retained as the double bond is located further down the alkyl chain. The first eluting C18:1 isomers (double bond closer to the methyl ester group) are significantly better separated by the **IL12** column as shown by the enlargements (Figure 5-6C) with identification of the isomers obtained using the available standards and estimating the intermediates. The 10t, 11t, and 10c isomers are quantifiable with the **IL12** column separation and not with the SP-2560 (Figure 5-6D). Separation of vaccenic acid (C18:1Δ11t) is important because of its relatively high percentage in ruminant fats.[52] Moreover, the methyl oleate (C18:1Δ9c), one of the most abundant naturally occurring fatty acids, was perfectly separated from the other isomers on **IL12** column; whereas, it was coeluted with the 15t isomer on the SP 2560 column.

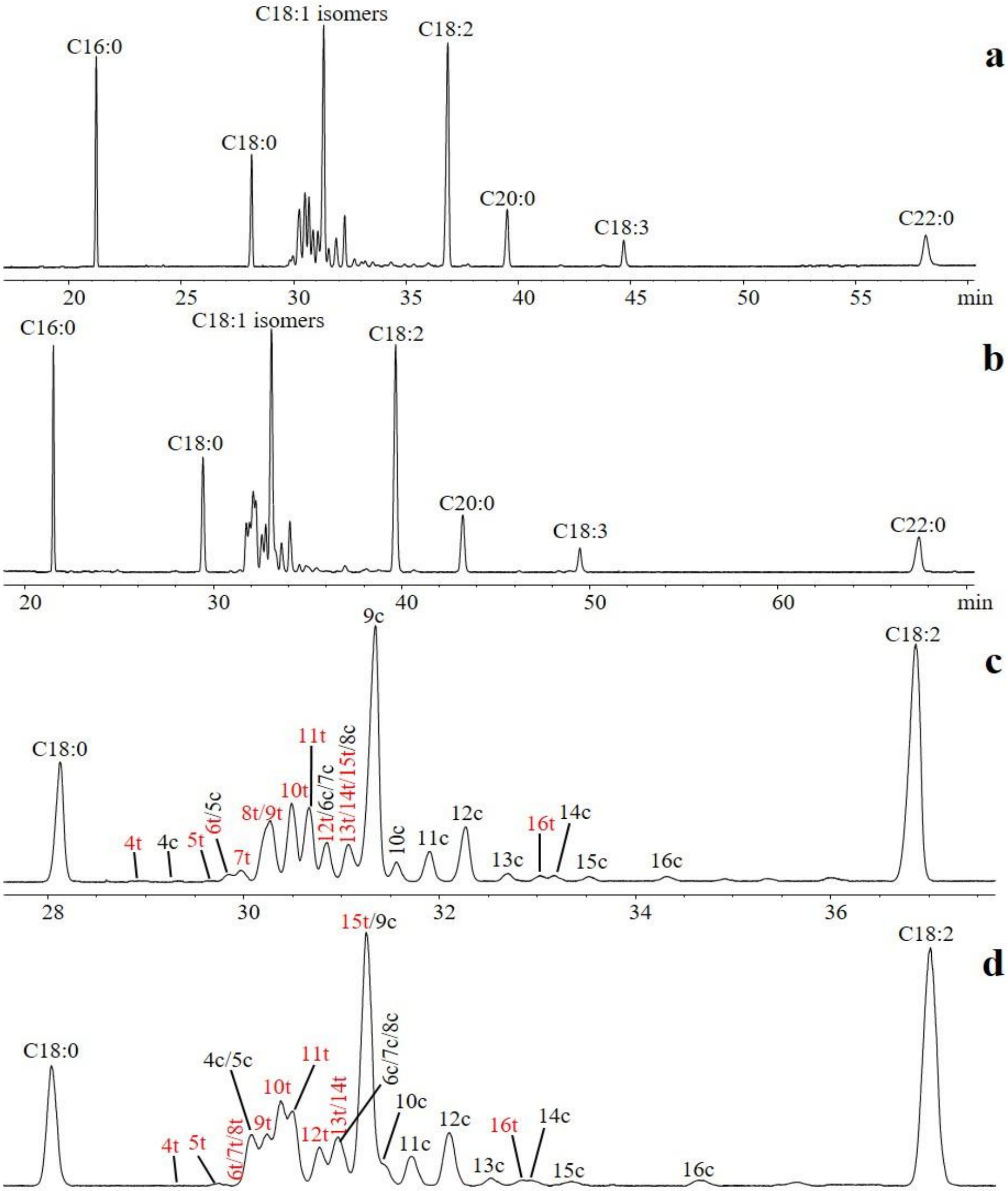

Figure 5-6 Chromatograms for detailed analysis of C18:1 cis-trans mixture of partially hydrogenated vegetable oil (PHVO) on: A 100 m x 250 µm IL12 column, B 100 m x 250 µm SP-2560 column. The C18:1 isomer region is enlarged with peak identification for C IL12 column and D SP-2560 column. Isothermal @ 175°C, He 1 mL/min constant flow

The expensive and fragile 100 m long column of the official test could be replaced by the commercial 30 m SLB-IL111, **IL6** in our series, in many cases. A detailed analysis of the C18:1 cis-trans isomers was performed on a 30 m commercial **IL6** column at 130°C as shown by the Figure 5-7A. The 30 m **IL12** column was also tested for this *cis-trans* analysis (Figure 5-7B). The 14t and 10c isomers are well separated by the **IL12** column and not by the **IL6** (SLB-IL111) column. Also, the 10c and 15t compounds were sufficiently separated on **IL12**, while they coeluted on **IL6**. However, SLB-IL111 demonstrated an excellent separation of 11t and 12t that could not be obtained on the **IL12** column. These two 30 m columns compete well with the 100 m SP-2560 column for the C18:1 *cis-trans* isomers separation demonstrating the remarkable selectivity provided by IL-based capillary columns.

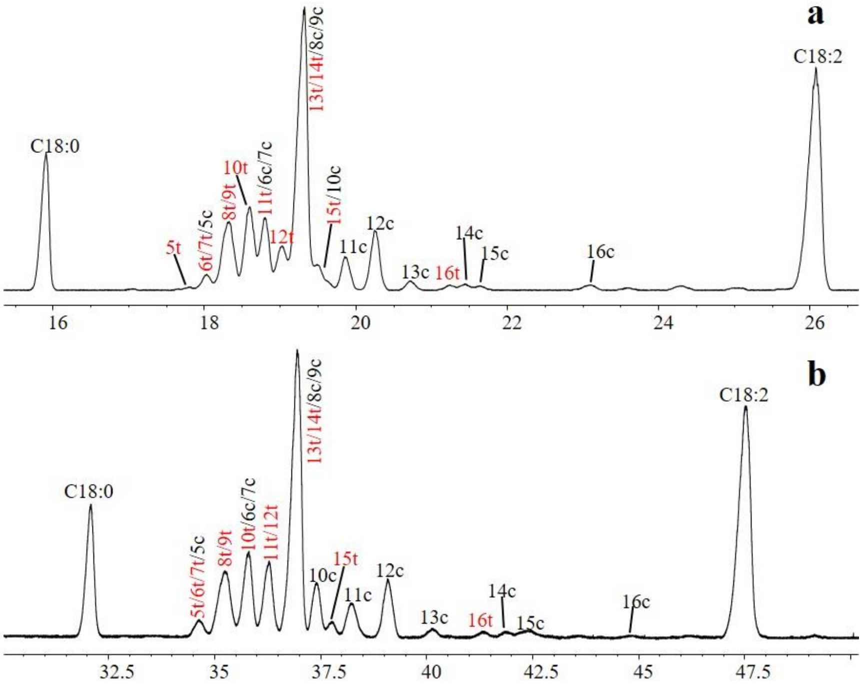

Figure 5-7 Chromatograms of the N08105 detailed analysis of C18:1 cis-trans mixture of partially hydrogenated vegetable oil (PHVO) on: A 30 m x 250 µm SLB-IL111 (IL6) commercial column, and B 30 m x 250 µm IL12 (3m$_2$C$_5$(mpy)$_2$) column. The C18:1 isomer region is enlarged with peak identification for the two separations. Oven temperature constant 130°C, helium 1 mL/min constant flow

5.4 Conclusions

The newly synthesized branched chain dicationic ionic liquids used as stationary phase in capillary GC columns confirmed the efficacy of this type of column in the separation of FAMEs. Structural variation on the alkyl spacer chain was determined to alter considerably both polarity and selectivity toward FAME separations. Adding non-polar alkyl groups decreased the IL polarity with variable effect on FAME selectivity. Introducing a double bond to the spacer chain engendered stronger polarizable interactions. As a result, **IL5** (i-eneC$_4$(m$_2$im)$_2$) showed the highest polarity in our series. The nature of the cationic group, either imidazolium, pyrrolidinium, or phosphonium, also was found to have profound impact on both polarity and selectivity of the stationary phases. The dicationic phosphonium **IL4** (2mC$_3$(pr$_3$p)$_2$) had a significantly lower polarity than all other dicationic ILs in this study. The pyrrolidinium ILs were less polar than their imidazolium counterpart with the same alkyl spacer. The remarkable selectivity of the dicationic IL capillary column is demonstrated by the separation of the *cis-trans* isomers of a partially hydrogenated vegetable oil sample. The *cis-trans* separations obtained on 30 m columns by the commercially available SLB-IL111 and **IL12** (3m$_2$C$_5$(mpy)$_2$) of our set could compete with the official method separation performed on the AOCS recommended SP-2560 100 m column.

Chapter 6

VARIATION OF ANIONIC MOIETIES OF DICATIONIC IONIC LIQUID GC STATIONARY PHASES: EFFECT ON STABILITY AND SELECTIVITY

Abstract

Dicationic ionic liquids (DILs) are more and more accepted as a new class of high temperature and polar stationary phases for gas chromatography (GC). This study deals with the effect of seven different fluorosulfonyl derivatized anions associated with two dications: 1,3-di(3-methylimidazolium)-2-methylpropane [$2mC_3(mim)_2$], and 1,3-di(3-methylimidazolium)-isobutene [i-ene$C_4(mim)_2$]. Thermophysical properties of the 14 synthesized DILs were evaluated in terms of melting point, viscosity, and thermal stability. The optimal physicochemical properties of 13 DILs allowed preparing 13 GC capillary columns. Accordingly, the polarity and selectivity of the DILs were evaluated by determining the Rohrschneider-McReynolds constants and the equivalent chain lengths of C18 fatty acid methyl esters (FAMEs). The symmetrical fluoroalkylsulfonyl and the trifluorosulfonate anions seem to produce the most polar DILs. Compared to classical polyethyleneglycol phases, the DILs showed substantially decreased retention of apolar compounds and a much stronger retention of the polar ones. Unique selectivities were observed with unsaturated FAMEs, polyaromatic hydrocarbons, and bacterial specific FAMEs. The two applications presented included a biodiesel and bacterial FAME analyses.

6.1 Introduction

Classical polar materials used as stationary phases in gas chromatography (GC) were traditionally significantly less thermally stable than their apolar polysiloxane counterparts. For decades, polar capillary GC columns were based on polyethylene glycol (Carbowax), poly(cyanopropyl)siloxane or tris-cyanoethoxypropane with maximum working temperatures well below 250°C. Due to their polar nature as molten salts, extremely low vapor pressure and high thermal stability, ionic liquids (ILs) were immediately used as polar GC stationary phases that could be used at temperatures at or above 250°C.[5,28,181,182,193] Improvements were made towards IL thermal stability, polarity and selectivity by the release of new dicationic IL or DILs.[194] These DILs turn to be so reliable that several IL- or DIL-based capillary GC columns are now commercially available, having a wide range of McReynolds polarity, from 2624 (SLB-IL59) to 4938 (SLB-IL111). These IL-based commercial columns were found to be a breakthrough in polar GC capillary columns allowing separations not possible before.

It was demonstrated that the GC retention properties of DILs were governed by their molecular structures.[47] In recent studies, the effect of structural modifications of the linkage chain between the two cationic head groups of NTf_2 DILs was examined.[7,9,15,55] DILs with branched-chain alkyl spacer chains have significant lower melting points but similar viscosities to DILs with linear alkyl spacers, making them promising candidates to be coated as GC stationary phases.[9] With the identical cationic terminals and charge balancing anions, the thermal stabilities of branched-chain DILs are tremendously influenced by the alkyl substituent position. The mid-chain methyl and methylene substituted DILs showed very close thermal stabilities to their linear chain analogs.[6] Fatty acid methyl esters (FAMEs) were used to evaluate the polarity and selectivity of these structurally-tuned DILs as GC stationary phases.[55] It was found that the FAME retention was dependent on the polarity of the IL: the more polar IL-based columns showing less FAME retention.[43] Also the IL-based capillary GC columns were found superior to classical polar GC columns in differentiating *cis-trans* FAME isomers.[55]

The bis-(trifluoromethyl)sulfonylimide (NTf_2) anion is almost exclusively associated with the different cationic entities making the DILs used to prepare the commercial GC columns.[47] This anion was selected because it produced ILs with appropriate melting points, viscosities, and thermal stabilities compared to triflate, dicyanamide, halogens, tetrafluoroborate or hexafluorophosphate anions.[195] Successful applications of ILs containing NTf_2 anions in GC analysis motivates a search for new types of low-coordinating anions. Three major strategies can be employed on the modification of these anions:[196] i) enlarging or shortening the perfluoroalkyl chains in the anion; ii) introducing asymmetry in the imide anion; and iii) using the triflide CTf_3, the carbon based analogous anion. The nonaflate (NfO) and bis(pentafluoromethanesulfonyl)imide (NPf_2) anions can be considered as elongated versions of triflate (TfO) and NTf_2 anions, respectively. Similarly, the bis(fluorosulfonyl)imide (Nf_2) anion is the short version of the NTf_2 anion. The fluorosulfonyl-NTf anion is a nonsymmetrical version of NTf_2.

This work focuses on the characterization of fourteen new DILs with seven different sulfo-fluorinated anions and two branched-chain dications that were found to have the best physicochemical properties in previous studies.[9,55] The influence of the seven different anions on the thermophysical properties of the DILs is investigated. Capillary columns were prepared with the newly synthesized DILs and examined with different samples including polyaromatic hydrocarbons (PAHs) and FAMEs from various origins.

6.2 Experimental

6.2.1. Chemicals and standards

The starting salt materials: potassium tris(trifluoromethanesulfonyl)methide (>98%) and potassium (fluorosulfonyl)(trifluoromethanesulfonyl)imide (>98%) were purchased from TCI Chemicals (Portland, OR). Potassium bis(fluorosulfonyl)imide was obtained from Strem Chemicals (Newburyport, MA). Bis(trifluoromethyl) sulfonimide lithium salt (99.95%), silver trifluoromethanesulfonate (≥99%), 3-bromo-2-bromomethyl-1-propene (97%), 1-methylimidazole (≥99%), and potassium nonafluoro-1-butanesulfonate (98%) as well as 14 polyaromatic hydrocarbon (PAH) compounds with low and medium molecular weights: naphthalene, biphenyl, biphenylene, acenaphthene, acenaphthylene, fluorene, phenanthrene, anthracene, fluoranthene, pyrene, benzo[c]phenanthrene, benz[a]anthracene, chrysene, and triphenylene were acquired from Millipore Sigma-Aldrich (St. Louis, MO). Lithium bis(pentafluoromethanesulfonyl)imide (98+%) and 1,3-dibromo-2-methylpropane (95+%) were purchased from Oakwood Chemicals (Estill, SC). The solvents: acetonitrile, dichloromethane, methyl formate, methanol, tetrahydrofuran, and heptane were obtained from Fisher Scientific (Fair Lawn, NJ).

A qualitative retention time index standard containing C7-C33 *n*-alkanes was purchased from Restek (Bellefonte, PA), and used to determine Kovats retention indices (KRI). Three FAME mixtures were used: i) a standard mix of unsaturated oleate (C18:1n9c), linoleate (C18:2n6) and linolenate (C18:3n3), along with saturated even carbon FAMEs containing stearate (C18:0), arachidate (C20:0), behenate (C22:0), and lingocerate (C24:0) methyl esters was prepared at 5 mg/mL for equivalent chain number (ECL) determination, ii) a standard mixture of B20 blend (diesel/biodiesel 80:20) was purchased from Restek (Bellefonte, PA), and iii) a mixture of bacterial fatty acid methyl esters (BAMEs) with a 10 mg/mL total concentration in methyl caproate (C6:0) was obtained from Supelco (Millipore Sigma, Bellefonte, PA).

6.2.2 Dicationic ionic liquid synthesis

The two dications selected from our recent studies were 1,3-di(3-methylimidazolium)-2-methyl-propane, named 2mC$_3$(mim)$_2$, and 1,3-di(3-methylimidazolium)-isobutene, named i-eneC$_4$(mim)$_2$. Their syntheses were achieved in two steps. In the first step, 1 molar equivalent of 1,3-dibromo-2-methylpropane, for 2mC$_3$(mim)$_2$, or 3-bromo-2-bromomethyl-1-propene, for i-eneC$_4$(mim)$_2$, was reacted with 2 molar equivalents of 1-methylimidazole to obtain the corresponding dibromo salt. The nucleophilic reaction was performed in acetonitrile at 90 °C in a sealed flask for 72 h. The rotary evaporation of solvent, followed by successive liquid-liquid extraction using water/dichloromethane (50:50), resulted in pure dicationic dibromo salts that were kept under vacuum in an oven at 40°C to dry over P_2O_5 for at least 12 h.

The second step is a metathesis reaction entailed to exchange of the bromide ions for the desired anions. The metathesis reaction is simply done reacting 2 molar equivalents of a lithium or potassium salt of the intended anion with 1 molar equivalent of the dicationic bromide salt in methanol for 12 h at room temperature. Subsequently, methanol was removed through rotary evaporation. The crude DIL product was purified using a biphasic water/dichloromethane (50:50) extraction to remove the lithium or potassium bromide salt and unreacted starting materials in the upper aqueous phase and the DIL in the lower dichloromethane phase. Lastly, dichloromethane was evaporated in a rotary evaporator, and the final DIL product was placed in a vacuum oven at 40 °C for 24 h to ensure complete dryness.

The water solubility of the DIL triflates imposed a slightly different procedure. A reaction of 1 molar equivalent of the dibromo salt with exactly 2 molar equivalent of silver trifluoromethanesufonate was carried out in ethanol for 12 h with the precipitation of silver bromide. The crude DIL product was collected by filtering out the solution and evaporating ethanol through rotary evaporation. The triflate DIL was washed with water 3 times to remove any unreacted bromide salt and placed in the vacuum oven to dry over P_2O_5 at 40 °C for 12 h. A dark color of the triflate-based DIL indicated the presence of residual silver in the matrix. In this case, the IL must be re-synthesized since there was no mean to remove the silver ions.

6.2.3. Dicationic ionic liquid characterization

Table 6-1 lists the fourteen DIL structures as well as some thermophysical properties.

6.2.3.1 Structural identification

The mass spectra along with ^{1}H, and ^{13}C NMR spectra of all DILs were acquired to confirm their purity and chemical structure. The molecular weights were determined using a Finnigan LXQ (Thermo Fisher Scientific, San Jose, CA) electrospray ionization mass spectrometry (ESI-MS). The ^{1}H NMR, and ^{13}C NMR spectra were recorded in dimethyl sulfoxide-d_6 on a 500 MHz JEOL Eclipse Plus 500 instrument (Tokyo, Japan) NMR spectrometer at ambient temperature.

6.2.3.2 Thermophysical properties

A Cannon-Manning semi-micro capillary viscometer (State College, PA) was used to measure kinematic viscosity. Viscosities were recorded at 30 °C, 50 °C, and 80 °C. A Shimadzu DSC-60 (Kyoto, Kyoto Prefecture, Japan) differential scanning calorimeter (DSC) was used to measure the melting point of synthesized ionic liquids. The samples (~ 5 mg) were sealed in aluminum pans and an empty aluminum pan was used as a reference. The measurements were carried out in the temperature range -50

°C to a predetermined temperature. Liquid nitrogen was used to maintain low temperatures. The samples were heated at rate of 5 °C/min. Thermogravimetric analyses (TGA) were carried out using a Shimadzu TGA-51 Thermogravimetric Analyzer to determine the thermal stabilities of synthesized ionic liquids. Roughly 10 mg of sample was weighed and placed in a platinum pan and heated raising the temperature from room temperature to 600 °C at a rate of 1 °C/min under a 25 mL/min N_2 inert circulating atmosphere. The $T_{5\%}$ decomposition temperature was determined at 5% weight loss.

Further information on thermal stability of DILs was obtained through inverse GC experiments. DIL coated capillary columns (3-m × 0.25 mm × 0.20 µm) were prepared as will be described thereafter. The 3-m columns were installed in a GC oven, connected to a flame ionization detector (FID) and flown by a 1 mL/min He gas making a 34 cm/s average gas velocity. The FID signal was recorded as zero as long nothing was released by the column. Raising the oven temperature from 100 to 450 °C at 1 °C/min produced a level change in the flat baseline. This recorded FID signal change corresponded to some bleeding material coming from the capillary column. The initial bleeding temperature was recorded for each column and taken as another value for the DIL decomposition temperature.

6.2.4 Chromatographic conditions

6.2.4.1 Capillary column preparation

The coating of the capillary columns with a DIL film was carried out using the static coating method. Briefly, a 20% w/v solution of the selected DIL in dichloromethane was prepared and filled-up into a 30-m fused silica capillary tubing of 250 µm internal diameter. The DILs with triflate anions were dissolved in a binary solvent mixture of dichloromethane/methyl formate (50:50) to improve their solubility. After closing one side of the filled capillary, the solvent was evaporated at 40 °C putting the other side under vacuum. This resulted in development of capillary columns with 0.20 µm DIL film thickness. The capillary columns were then conditioned at 200 °C in the GC oven for 12 h under He circulation. Naphthalene was injected to each column at 110 °C to evaluate their efficiencies. The DIL coated columns showed efficiency ranging between 2500 to 4000 plates/m. In other words, the height equivalent to a theoretical plate (HETP) ranged between 250 and 400 µm (or 1 < HETP < 1.6 column diameter).

The Squalane, Supelcowax® 10, Omegawax® 250, SLB®-5ms, SLB®-IL59, SLB®-IL100, and SLB®-IL111 were kindly provided by Supelco (Millipore Sigma). All columns were 30 m × 0.25 mm capillary with 0.20 µm film thickness.

6.2.4.2 Instrumentation

The gas chromatographic analyses were carried out on an Agilent 6890N (Agilent, Palo Alto, CA, USA) gas chromatograph equipped with a FID. An Agilent ChemStation data processing unit was used for processing and storing the chromatograms. Helium was used as carrier gas for all analyses.

6.2.4.3 Determination of Kovats retention indices (KTI) and McReynolds constants

A qualitative retention time index standard containing C7-C33 *n*-alkanes was purchased from Restek (Bellefonte, PA), and used to determine the KRIs of the representative McReynolds probes, benzene, n-butanol, 2-pentanone, nitropropane and pyridine, and three unsaturated FAMEs (C18:1, C18:2, and C18:3). Due to solutes overlapping with the injection solvent, the injection of neat probe molecules as well as C5-C12 alkanes were performed in the headspace mode using a 7 µm polydimethylsiloxane solid-phase microextraction (SPME) fiber (Millipore Sigma).

Analyses were performed isothermally at 120 °C. The average helium velocity of 40 cm/s was used for consistency of analyses conditions. Manual GC injection was used to determine the Equivalent Chain Length (ECL) values of C18:1, C18:2, and C18:3 at 3 different temperatures (120 °C, 150 °C, and 180 °C).

6.2.4.4 Fatty acid methyl ester and polyaromatic hydrocarbon applications

To study the selectivity of new stationary phases, FAMEs and PAHs were analyzed on the 30 m capillary columns. A split ratio of 100:1 was used in all injections. The temperature programming for analyses of biodiesel was starting at 50 °C with a 9 °C/min ramp up to 220 °C, held for 30 min to insure elution of all compounds. Helium was used as carrier gas with flow rate of 1.5 mL/min. FAMEs in bacteria, called BAMEs, were analyzed with a gentler temperature programming with a 5 °C/min ramp and a lower helium flow rate of 1 mL/min. For the PAH analysis, a mixture containing 14 compounds was prepared in THF and stored at 4 °C prior to analysis. The gradient temperature program was started at 140 °C with a ramp of 12 °C/min till 240 °C, held for 30 min. Helium flow rate of 1.5 mL/min was used for analysis of PAHs. When PAHs were analyzed with SLB-5ms column, the ramp was raised to 300°C.

Table 6-1 Thermophysical properties of branched-chain dicationic ionic liquids containing different sulfo-fluorinated anions

Anion structure	code	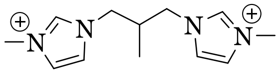 **2mC$_3$(mim)$_2$**							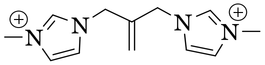 **i-eneC$_4$(mim)$_2$**						
		Melting point (°C)[a]	**Thermal stability (°C)**		**Viscosity (cSt)[d]**				**Melting point (°C)[a]**	**Thermal stability (°C)**		**Viscosity (cSt)[d]**			
			$T_{5\%}$[b]	**T_{IGC}[c]**	**30 °C**	**50 °C**	**80 °C**	**120°C**		**$T_{5\%}$[b]**	**T_{IGC}[c]**	**30 °C**	**50 °C**	**80 °C**	**120°C**
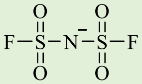 $\mathrm{F{-}S(O)_2{-}N^{-}{-}S(O)_2{-}F}$	**Nf_2**	-23	232	231	348	98	47	17	-14	231	235	324	85	42	15
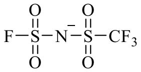 $\mathrm{F{-}S(O)_2{-}N^{-}{-}S(O)_2{-}CF_3}$	**fNTf**	-32	307	268	440	124	61	22	-21	309	270	432	109	56	20
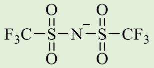 $\mathrm{F_3C{-}S(O)_2{-}N^{-}{-}S(O)_2{-}CF_3}$	**NTf_2**	-7	388	316	507	151	68	24	3	389	310	495	142	62	21
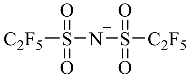 $\mathrm{C_2F_5{-}S(O)_2{-}N^{-}{-}S(O)_2{-}C_2F_5}$	**NPf_2**	24	378	319	588	174	76	26	27	381	312	564	164	72	25
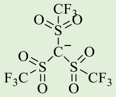	**CTf_3**	29	375	315	614	182	80	27	35	374	312	604	170	78	27
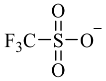 $\mathrm{F_3C{-}S(O)_2{-}O^{-}}$	**TfO**	19	332	244	672	210	86	30	31	327	252	656	198	80	28
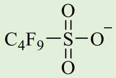 $\mathrm{C_4F_9{-}S(O)_2{-}O^{-}}$	**NfO**	36	340	279	solid	278	97	33	88	336	ND[e]	solid	solid		solid

[a] Determined by peak position in DSC.

[b] $T_{5\%}$ refers to temperature at 5% mass loss of sample in TGA.

[c] T_{IGC} is the temperature at which an initial column bleed was observed.

[d] capillary viscometer measurement except for 120°C obtained with the Walther eq. (1).

[e] Restricted GC application due to the high melting temperature. ND: Not determine

6.3 Results and discussion

6.3.1 Physicochemical properties of the newly synthesized DILs

Table 6.1 lists the chemical structure and adopted abbreviations, along with the thermophysical properties of 14 newly synthesized DILs with fluorosulfonyl derivatized anions. Melting point, viscosity and thermal stability are the physicochemical properties of interest for gas chromatographic applications.

Previously, it was shown that dicationic ILs containing the i-eneC4 alkyl spacer chain have higher phase transition temperatures as compared to DILs with $2mC_3$ linkage due to additional π-π interactions.[9] Generally, an increase in the anion's perfluoroalkyl chain results in increasing the melting point of conventional monocationic ionic liquids. A similar trend was observed in this study, where NTf_2 and TfO containing DILs showed lower melting temperatures than their enlarged perfluoroalkyl chain derivatives, NPf_2 and NfO, respectively. I-$eneC_4(mim)_2$.2NfO with its 88 °C m.p. stands apart from all other DILs as it had a much higher melting point. This was a problem since it precluded the capillary coating procedure so no GC column with this DIL could be prepared. DILs with Nf_2 and unsymmetrical fNTf anions were found to have the lowest melting points as well as viscosities. Decreased van der Waals interactions resulted from shorter fluorinated chain leads to a decrease in the viscosity and melting point of the respective ILs.[196]

The DIL viscosities at 80 °C were between 42 and 97 cSt in kinematic units (Table 6-1). The 30 °C, 50 °C and 80 °C kinematic viscosity values could be fitted well by the Walther formula:[197]

$$\log[\log(\nu + 0.8)] = A + B\log(T) \tag{6-1}$$

in which v is the kinematic viscosity in cSt, T is the absolute temperature in Kelvin and A and B are constants of the liquid studied. The A and B constants were very consistent for all DILs with slopes B between -2.44 and -2.76, and with intercepts A between 6.5 and 7.2 with regression coefficients higher than 0.95. These A and B values were used to calculate the DIL viscosities at 120 °C since this temperature is commonly used in GC experiments. The 120 °C viscosity values were between 15 and 30 cSt (or 22 and 45 cP) as listed in Table 6-1. A minor effect of the cation is seen with the alkane spaced cation DILs being slightly more viscous than the alkene spaced DILs. The anion has a more pronounced effect with the bis(fluorosulfonyl)imide (Nf_2) and the perfluorobutylsulfonate or nonaflate (NfO) anions producing respectively the lowest and the highest viscosities (Table 6-1).

The thermal stability temperature obtained by inverse GC were between 40 °C and 70 °C lower than the $T_{5\%}$ obtained by TGA for all but one set of DILs. The two Nf_2 salts produced $T_{5\%}$ and T_{IGC} stability thermal values that were similar (Table 6-1). This may be related to the fact that the Nf_2 anion produced the two ILs with the lowest overall thermal stability (231 °C-235 °C). There was no cation effect on thermal stability; the two sets of DILs have the same thermal stability temperatures depending only on the anion (Table 6-1). Recently, we demonstrated that substitution on the central carbon have negligible impact on thermal stability of branched-chain dicationic ionic liquids. Three anions, NTf_2, NPf_2, and CTf_3 gave the highest thermal stability with $T_{5\%}$ around 380 °C or TIGC around 315 °C. The relatively low thermal stability of TfO and NfO containing DILs could be attributed to the significant nucleophilicity of sulfonate-based anions.

6.3.2 Rohrschneider-McReynolds polarity

In order to characterize and to compare different materials used as GC stationary phases, Rohrschneider and McReynolds developed a system based on the retention of several probe molecules.[42] The most informative of these probes are benzene for π-π interaction: index X, 1-butanol for H-bond: Y, 2-pentanone for dipole interaction: Z, nitropropane for polar interaction: U, and pyridine for basic interaction: S. The KRIs of the five solutes are determined using the DIL coated capillary columns at 120 °C and an average He velocity of 40 cm/s. For each solute, the X´, Y´, Z´, U´ and S´ values listed in Table 6-2 are obtained by subtracting the KRI obtained on a squalane apolar column to the DIL Kovats index in the same conditions. The global polarity Pt is simply the sum of the five polarity values and the polarity number, PN, is obtained as:[80,146]

$$PN = \left(\frac{Pt}{P_{SLB-IL100}} \right) x\,100 \qquad (6\text{-}2)$$

in which PSLB-IL 100 is the global polarity of a 1,9-di(3-vinylimidazolium)nonane.2NTf2 DIL commercially available column with PSLB-IL100 = 4437.[146]

Table 6-2 presents the results for the McReynolds constants and the overall polarity of the new DILs. In addition, the McReynolds constants for the most polar known commercial column (SLB-IL111 with Pt = 4925) were determined and included for comparison. These values are reported within 0.5% standard deviation from literature values which is Pt = 4938 for SLB-IL111. There is no value for the i-eneC$_4$(mim)$_2$.2NfO DIL since it was not possible to coat a capillary column with this IL due to its solid nature. The general observation is that the i-eneC$_4$(mim)$_2$ cation is slightly more polar than its 2mC$_3$(mim)$_2$ counterpart by 300 to 400 polarity points (corresponding to 7% Pt for the most polar and 13% Pt for the least polar DILs). Between one fourth and one third of the polarity increase is due to the “X” term (π-π interactions) which is expected since there is a double bond in the i-eneC$_4$(mim)$_2$ cation.

The DILs showing the lowest polarity numbers were based on bis(fluorosulfonyl)imide, Nf$_2$, with polarities of 2461 and 2702 (PN 56 and 61) for the alkane and alkene substituted dications. Nf_2 is a symmetric anion and the only one, in this study, without a carbon atom. With polarities between 4200 and 4500 ($95 < PN < 102$), the fNTf and NfO anions gave more polar DILs. While NfO and fNTf containing DILs show very close polarity numbers, they interact differently with the probe molecules. The imide-based anion, fNTf, exhibited stronger π-π interactions (X term), whereas, the NfO anion engenders stronger polar (U term) and basic interactions (S term). The three bigger and more symmetric NTf_2, NPf_2, and CTf_3 anions produced DILs with high polarities between 5150 and 5800 ($116 < PN < 131$). The smallest triflate, TfO, anion produced the highest polar DILs ever reported with 5939 and 6312 (PN = 134 and 143, respectively). When the polarity numbers are compared with the SLB-IL111 numbers of the commercial column with a close to 5000 polarity, a pattern can be seen: for all DILs, the Y, Z and S polarity contributions make about one fifth each of the total value. The U terms are always the biggest, being a little bit below one fourth and the X term is always the smallest making between 13 and 16% of the total McReynolds polarity (Table 6-2). As observed experimentally, the DIL-based GC capillary columns are selective for polar compounds (U term), differentiating polar alcohols (Y term), less polar esters or ketones (Z term), or basic compounds (S term).

One exception is pointed out via the bold values in Table 6-2: the small triflate DILs behaved differently. The two dicationic TfO columns are the most polar of the entire set. However, the S value of $2mC_3(mim)_2$ TfO is 870, barely making 15% of the 5939 polarity and 525 points lower that its alkene counterpart that, with S = 1395, has the same level as the other DILs. The global polarity of the two TfO DILs is very high and similar because the Y and Z values of the $2mC_3(mim)_2$ DIL are respectively 112 and 104 points higher than its i-ene$C_4(mim)_2$ cation counterpart and, with X = 922, the X value of the i-ene$C_4(mim)_2$ DIL is only 29 points higher than that of the alkyl cation that has X =

893. A very significant difference in polarity contributions, with a lower basicity (S parameter) compensated by higher polar and dipolar characteristic (Y and Z parameters), is seen between the $2mC_3(mim)_2$ and i-ene$C_4(mim)_2$ cations as triflate salts. Such differences between the two cation polarities is unique to these two triflate DILs.

Table 6-2 Normalized McReynolds constants, total Pt number, and polarity numbers, P.N. for dicationic ionic liquid stationary phases.

DIL phase	**X´** benzene	**Y´** butanol	**Z´** 2-pentanone	**U´** nitro-propane	**S´** pyridine	**P_t**	**P.N.**
$2mC_3(mim)_2.2Nf_2$	297	516	523	634	491	2461	56
i-ene$C_4(mim)_2.2Nf_2$	399	574	561	655	513	2702	61
$2mC_3(mim)_2$.2fNTf	691	898	847	898	866	4200	95
i-ene$C_4(mim)_2$.2fNTf	802	915	892	969	935	4513	102
$2mC_3(mim)_2.2NTf_2$	805	1083	1088	1308	1196	5480	124
i-ene$C_4(mim)_2.2NTf_2$	863	1141	1186	1383	1233	5806	131
$2mC_3(mim)_2.2NPf_2$	679	1037	1077	1222	1129	5144	116
i-ene$C_4(mim)_2.2NPf_2$	751	1086	1138	1274	1261	5510	124
$2mC_3(mim)_2.2CTf_3$	677	971	1053	1255	1223	5179	117
i-ene$C_4(mim)_2.2CTf_3$	747	1061	1144	1308	1276	5536	125
$2mC_3(mim)_2$.2TfO	893	**1452**	**1322**	1402	**870**	5939	134
i-ene$C_4(mim)_2$.2TfO	922	1340	1218	1437	1395	6312	143
$2mC_3(mim)_2$.2NfO	568	914	834	1061	946	4323	98
SLB®-IL 111[a]	761	928	952	1193	1091	4925[b]	111

[a] The commercial SLB®-IL 111 GC column contains the 1,5-di(3,4-dimethylimidazolium)-pentane bis(trifluorosulfonyl)imide noted $C_5(m_2im)_2$, 2 NTf_2, dicationic ionic liquid.

[b] The literature reported polarity value for SLB-IL111 is 4938.

6.3.3 Analysis of polyaromatic hydrocarbons

PAHs are environmental pollutants that critically need to be monitored in a wide variety of matrices. EPA methods for determination of PAHs recommend the use of 5% phenylmethylpolysiloxane GC capillary columns.[118] Figure 6-1 shows the selectivity and separation comparison of a prepared mixture of 14 PAHs on the extremely polar $2mC_3(mim)_2.2CTf_3$ 30-m DIL column (top chromatogram), a commercial phosphonium-based polar SLB®-IL59 ionic liquid column (middle chromatogram), and a nonpolar 5% phenyl 95% polydimethylsiloxane column (SLB®-5ms, bottom chromatogram).

The 14 PAHs are all baseline separated on the ionic liquid columns when biphenylene and acenaphthylene (PAHs 3 and 5) as well as chrysene and triphenylene (PAHs 13 and 14 in Figure 6-1) co-eluted on the polysiloxane column. Further, the retention times on this column are only comparable to the $2mC_3(mim)_2.2CTf_3$ DIL column when it is operated at substantially higher temperatures. The separation of PAHs on the ionic liquid columns is mostly governed by polarizable interactions, as acenaphthylene (PAH 5) retained longer than acenaphthene (PAH 4) on these columns. An unprecedented selectivity in separation of anthracene and phenanthrene was achieved on the $2mC_3(mim)_2.2CTf_3$ column. The elution of anthracene before phenanthrene was never observed on commercial columns. Furthermore, the polar nature of $2mC_3(mim)_2.2CTf_3$ column significantly accelerated the separation process. All 14 compounds were separated within 17 min on the $2mC_3(mim)_2.2CTf_3$ column, whereas, the separation required 48 min to complete on the commercial SLB®-IL59. Clearly, the selectivity observed for the four-membered ring PAHs 9-14 is completely different on the $2mC_3(mim)_2.2CTf_3$ stationary phase with evenly distributed peaks and the polysiloxane column with close or co-elution of compounds 11-14 (Figure 6-1) confirming our previous results.[15]

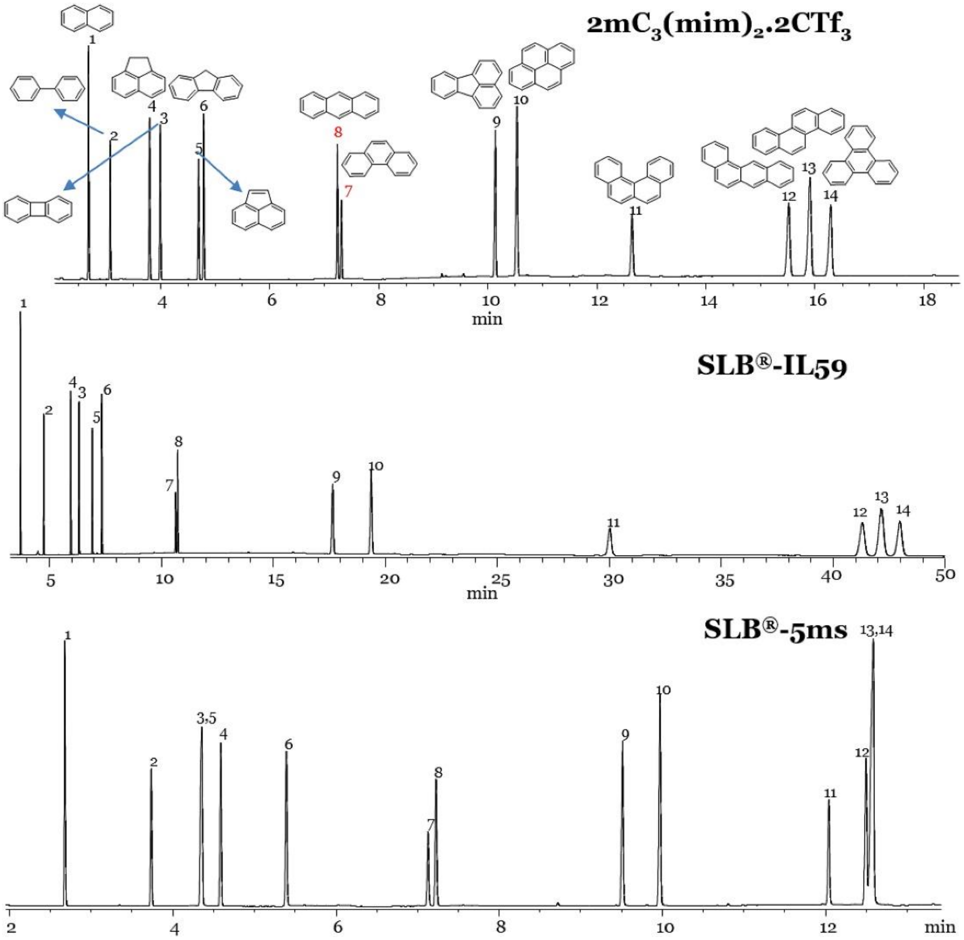

Figure 6-1 Analysis of PAHs on the 30 m × 250 µm × 0.2 µm 2mC3(mim)2.2CTf3 DIL column (top), SLB®-IL59 (middle), and 5% diphenyl 95% dimethylpolysiloxane (SLB®-5ms, bottom). Iinitial oven temperature of 140 °C with a rate of 11 °C/min ramp up to 300°C for the SLB®-5ms column or 240°C for the IL-based columns; He flow rate: 1.5 mL/min

6.3.4 Analyses of fatty acid methyl esters

6.3.4.1 Retention

It was established previously that the elution of FAMEs was faster on more polar IL-based columns.[43] This was verified with the polar newly prepared DIL polar columns for the FAMEs compounds as well as apolar alkanes used for KRI determination. Figure 6-2 shows the KRIs of three C18 FAMEs plotted versus the stationary phase polarity number. On the less polar Nf_2 columns (PNs 56 and 62), the C18 FAMEs have KRIs between 22.65 and 23.2; on the most polar TfO columns (PNs 134 and 142), the KRIs are between 29.0 and 30.6. It means that on the less polar DILs, the C18 FAMES elute similarly to C23 n-tricosane and, on the most polar DILs, they elute around C30 triacontane. The methyl ester group increases the FAME retention by 5 methylene units on the less polar DILs and by 12 methylene units on the most polar DILs. Figure 6-2 shows a monotonous increase in KRIs with the DIL polarity. The double bonds in the FAME alkyl chain increased the retention by a fraction of methylene unit. The 3 unsaturated bonds of the linolenate methyl ester (C18:3n3) produced KRIs of 23.14 on Nf2 and 30.62 on TfO compared to 22.65 and 29.43 for the oleate methyl ester (C18:1n9) with only one double bond.

6.3.4.2 Equivalent chain length and selectivity

The equivalent chain length (ECL) is commonly used to assess selectivity with unsaturated FAMEs.[48,58,59,194] It corresponds to the theoretical fractional saturated alkyl chain length that would give the same retention as that obtained for the unsaturated FAME. The ECL value is calculated using the two saturated FAMEs that bracket the peak of the unsaturated studied FAME mimicking the Kovats index calculation with linear alkanes. Table 6-3 lists the ECL values for oleic, linoleic and linolenic methyl esters

(C18:1n9 cis, C18:2n6, and C18:3n3, respectively) at 150 °C and 180 °C and Figure 6-2 shows the changes in ECL values plotted versus column polarity. ECLs increase with the increasing number of double bonds for any stationary phase and they also increase with the polarity of the stationary phase (Figure 6-2). For example, at 150 °C, the ECL numbers for the least polar (PN 56) DIL phase, $2mC_3(mim)_2$, $2Nf_2$, are 18.15, 18.40, and 18.86 for respectively the oleic, linoleic and linolenic FAMEs. These numbers are 19.12, 20.45, and 21.66, between one and three methylene units higher for the polar (PN 131) i-ene$C_4(mim)_2$, $2NTf_2$ DIL phase (Table 6-3).

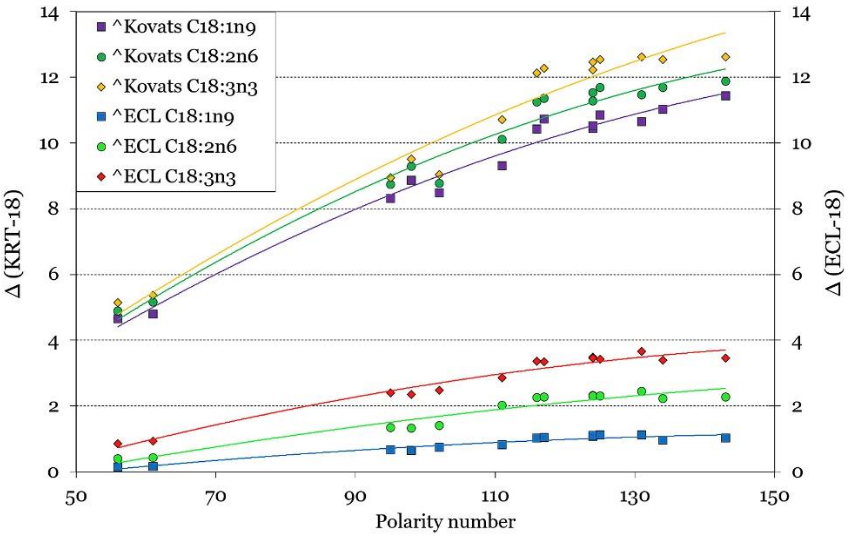

Figure 6-2 18 carbon chain length oleate (C18:1n9), linoleate (C18:2n6) and linolenate (C18:3n3) methyl esters Kovats retention index (KRI) and equivalent chain number (ECL) variation versus the polarity of the 13 DIL based GC columns. The KRI and ECL numbers use respectively n-octadecane (C18) and methyl stearate (C18:0) as references. They were obtained at 150°C isothermal temperature with 1 mL/min He flow rate

Figure 6-3 shows the selectivity ratio for the linoleic/oleic and linolenic/linoleic FAME separation on the 13 DIL columns sorted from left to right by increasing polarity. The two Nf$_2$ based columns with the lowest polarity have also the lowest selectivities for the two pairs of FAMEs with 1.014 for the linoleic/oleic separation and 1.026 for the linolenic/linoleic selectivities. The fNTf and NfO based ionic liquid columns have a selectivity of 1.036 for the linoleic/oleic pair and around 1.055 for the linolenic/linoleic pair. The eight remaining DIL columns have also selectivity around 1.055 for the linolenic/linoleic pair, but a better selectivity around 1.065 for the linoleic/oleic pair. For the C18 FAMEs, the observed selectivities obtained with the DIL columns are loosely related to polarity. C18 FAME selectivity is almost constant for DIL between PN 116 and PN 143 (Figure 6-3).

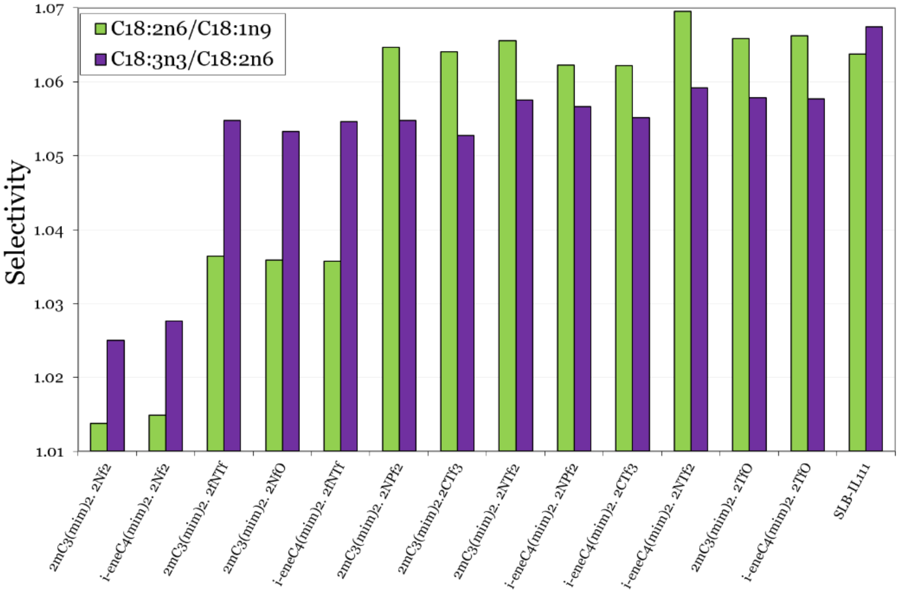

Figure 6-3 Selectivity ratio for the linoleic/oleic and linolenic/linoleic FAME separation by the DIL capillary columns sorted by increasing polarity (except the commercial column at far right). 30 m × 250 µm × 0.2 µm DIL column, 150°C isothermal separation, He 1.5 mL/min

Table 6-3 Equivalent chain length for C18 FAMEs on the DIL capillary columns at 150 °C and 180 °C. See experimental section for analysis methods

Dicationic IL		Oleate *cis*-C18:1n9		Linoleate C18:2n6		Linolenate C18:3n3	
	P.N.[a]	**150 °C**	**180 °C**	**150 °C**	**180 °C**	**150 °C**	**180 °C**
$\mathrm{2mC_3(mim)_2.\ 2Nf_2}$	*56*	18.15	18.22	18.4	18.49	18.86	19.01
$\mathrm{i\text{-}eneC_4(mim)_2.\ 2Nf_2}$	*61*	18.16	18.24	18.43	18.52	18.94	19.1
$\mathrm{2mC_3(mim)_2.\ 2fNTf}$	*95*	18.66	18.82	19.34	19.55	20.4	20.63
$\mathrm{i\text{-}eneC_4(mim)_2.\ 2fNTf}$	*102*	18.74	18.9	19.41	19.67	20.47	20.74
$\mathrm{2mC_3(mim)_2.\ 2NTf_2}$	*124*	19.07	19.34	20.32	20.64	21.49	21.78
$\mathrm{i\text{-}eneC_4(mim)_2.\ 2NTf_2}$	*131*	19.12	19.47	20.45	20.72	21.66	21.89
$\mathrm{2mC_3(mim)_2.\ 2NPf_2}$	*116*	19.02	19.28	20.25	20.55	21.36	21.6
$\mathrm{i\text{-}eneC_4(mim)_2.\ 2NPf_2}$	*124*	19.11	19.43	20.3	20.64	21.45	21.73
$\mathrm{2mC_3(mim)_2.2CTf_3}$	*117*	19.05	19.24	20.27	20.57	21.34	21.56
$\mathrm{i\text{-}eneC_4(mim)_2.\ 2CTf_3}$	*125*	19.12	19.4	20.31	20.62	21.43	21.7
$\mathrm{2mC_3(mim)_2.\ 2TfO}$	*134*	18.97	19.28	20.22	20.54	21.39	21.68
$\mathrm{i\text{-}eneC_4(mim)_2.\ 2TfO}$	*143*	19.02	19.33	20.28	20.6	21.45	21.74
$\mathrm{2mC_3(mim)_2.\ 2NfO}$	*98*	18.65	18.8	19.32	19.52	20.35	20.58
SLB-IL111®	*111*	18.82	19.05	20.02	20.36	21.37	21.66

[a]P.N.: polarity number

6.3.4.3 FAMEs in biodiesels

Fatty acids in animal fat, vegetable oil or waste cooking oil can be converted to FAMEs using an alkylation derivatization reagent.[198] The transesterification reaction involves the condensation of carboxyl group of fatty acid and hydroxyl group of methanol in the presence of acidic or basic catalyst.[85] Biodiesel will be obtained by blending these FAMEs with petroleum distillate to adjust viscosity, cetane index, freezing point and flash point.[82] Figure 6-4 presents the chromatograms of the B20 biodiesel blend on three different columns: a classical polyoxyethylene-based (PEG) polar column with polarity number 52 (Omegawax® 250, top), and two i-eneC_4(mim)$_2$ dicationic salts, the fNTf DIL with P.N. 102 (middle), and the TfO DIL with P.N. 143 (bottom). The retention and selectivity differences are clear: with the same temperature program, carrier gas flow, and column length and diameter, the retention times of n-pentacosane (C25) and palmitic acid methyl ester (C16:0) on the three columns are, 21.9 and 18.8 min on PEG, 13.1 and 10.8 min on fNTf DIL, and 10.0 and 11.7 min on TfO DIL (Figure 6-4). The decrease in retention times for apolar or semi-polar compounds with increasing polarity was previously noted and is herein confirmed.[15,55] The selectivity change is evident: C16:0 elutes 3.1 min before C25 on the PEG wax phase, it elutes only 2.3 min before C25 on fNTf DIL and it is retained 1.7 min longer than C25 on TfO DIL.

The increase in ECLs with the increased polarity (Table 6-2 and Figure 6-2) not only changes the alkane/FAME selectivity, but also affects the selectivity of saturated/unsaturated FAMEs.[55] The alkane peak eluting before the methyl palmitate (C16:0, the first major FAME in the biodiesel sample) peak is circled in Figure 6-4. It is the n-docosane (C22) peak on the PEG and fNTf DIL columns, but the n-heptacosane (C27) on the highly polar TfO column. For saturated/unsaturated FAME selectivity, the major peak in Figure 6-4 is linolenic FAME (C18:2n6) eluting 2.5 min before the arachidic (C20:0) peak on the PEG column (Figure 6-4, top), but C18:2n6 elutes just few seconds before C20:0 on the fNTf DIL column and it elutes after C20:0 on the most polar TfO DIL column (Figure 6-4, bottom). Clearly, besides producing faster analyses, the most polar DIL columns allow shifting the FAME peaks apart from the alkane peaks, facilitating biodiesel blend analyses.

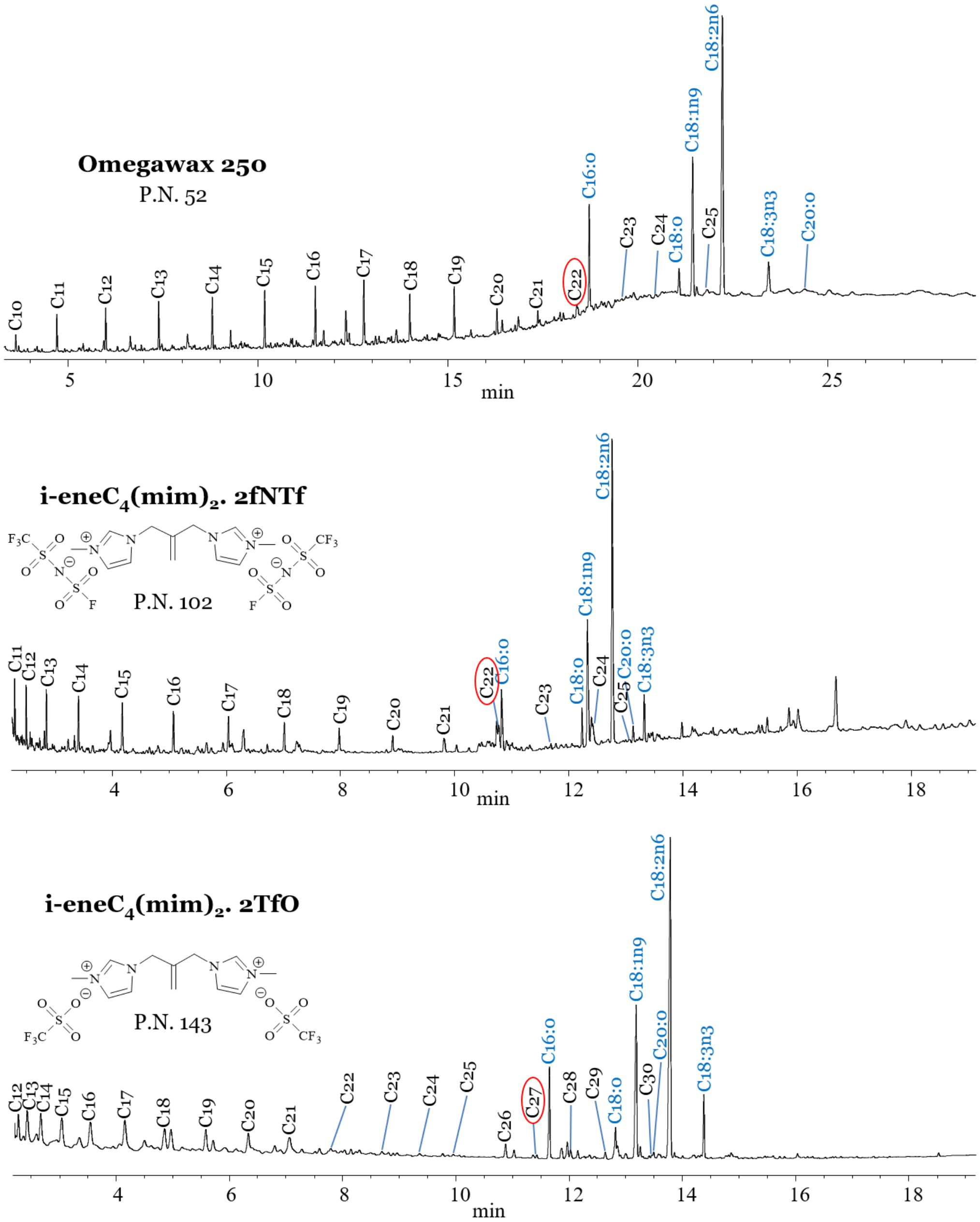

Figure 6-4 Analyses of B20 biodiesel blend on three different 30 m × 250 µm × 0.2 µm GC columns. Top: Omegawax® 250; middle: i-eneC$_4$(mim)$_2$.2 fNTf; bottom: i-eneC$_4$(mim)$_2$.2TfO. Initial temperature 50°C, ramp of 9°C/min till 220°C (20 min), He gas flow 1.5 mL/min. The circled alkane elutes just before methyl palmitate (C16:0)

6.3.4.4 Bacterial acid methyl esters

Gas chromatographic analyses of fatty acid profiles in bacteria cells is faster than petri dish for bacterial identification. This can be of great help in treating illnesses caused by food-borne microbial pathogens. Bacterial fatty acids have a great variety of alkyl chains including branched chains and cycles. Hydroxyl groups can also be found on bacterial fatty alkyl chains.[73,74] A 26-component bacterial FAME mixture was used as test mixture for our DIL columns. Figure 6-5 compares the separation of the BAME mixture on a PEG-based Supelcowax® 10 column (P.N. 52) and the 2mC$_3$(mim)$_2$-2NfO column (P.N. 98) obtained with the same temperature program and helium flow rate. The separation is completed 10 min faster on the DIL column. If the selectivity within chemical families, saturated, unsaturated and hydroxylated bacterial FAMEs is similar on the two columns, there are big differences between families. The hydroxylated bacterial FAMEs are clearly more retained than the saturated FAMEs on the DIL column. The peak of the hydroxylated lauric acid 2-OH-C12:0 bacterial methyl ester coelutes with the palmitic acid peak C16:0 on the PEG column. These two peaks are 4 min apart on the DIL column (arrows on Figure 6-5). Similarly, the methyl linoleate peak (C18:2) elutes 20 s before the methyl nonadecanoate (C19:0) on the PEG column. It elutes 20 s after C19:0 on the DIL column. Also, the coeluting *cis* and *trans* C18:1n9 (oleic and elaidic FAMEs) on the PEG column are baseline separated on the DIL column (arrow in Figure 6-5).

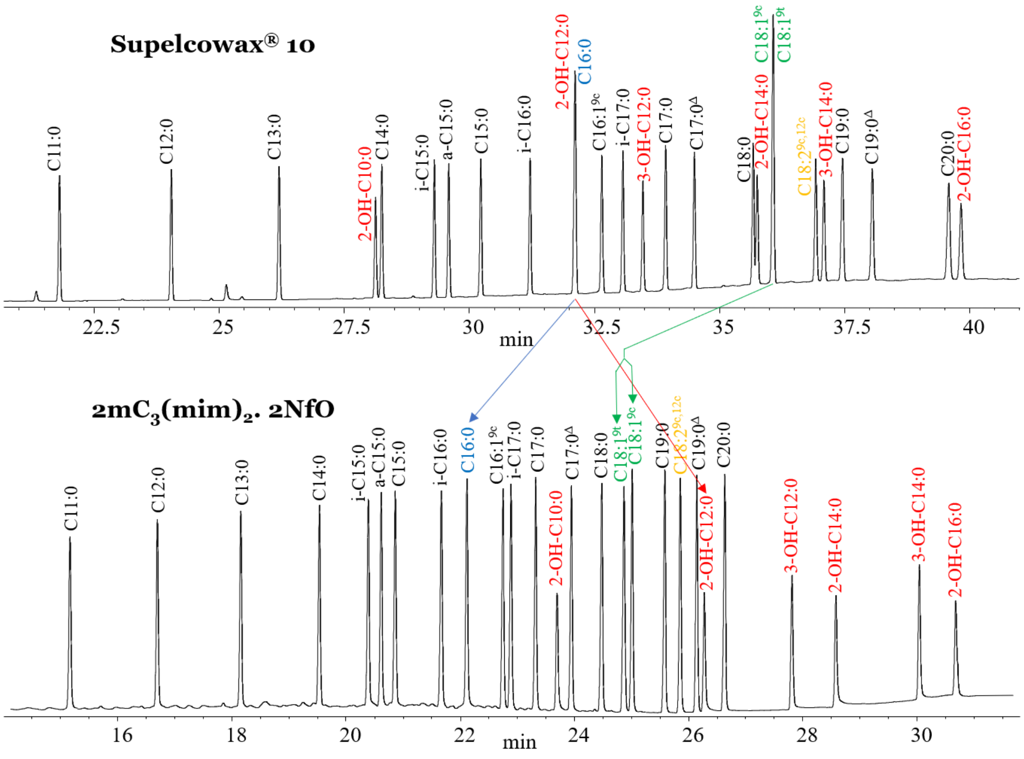

Figure 6-5 Analysis of bacterial acid methyl esters (BAMEs) on 30 m × 250 µm × 0.2 µm capillary columns. Top: PEG column (Supelcowax 10), bottom: $2mC_3(mim)_2$, 2NfO column. Temperature program: 1 min @ 50°C, ramp 5°C/min till 225°C (35 min); He flow 1 mL/min

6.4 Conclusions

It was demonstrated that the nature of anions present in dicationic ionic liquids have a significant impact on the physicochemical properties of the DILs. The two perfluoroalkyl sulfate anions produced the highest melting points and viscosities when incorporated with methylimidazolium dicationic moieties. With the fluoroalkylsulfonyl imide or carbide anions studied with the same dications, the lower melting points and lower DIL viscosities were obtained with anions containing fewer fluorine atoms. The highest thermal stability was observed with the symmetrical fluorosulfonylalkylated anions, all well above 300°C.

When used as stationary phase for gas chromatography, the thermal stability of these DILs was associated with a remarkably high polarity. This high polarity reduced the retention of apolar solutes while maintaining that of the more polar solutes. The selectivity observed in the separation of polycyclic aromatic hydrocarbons or fatty acid methyl esters is very different of that seen on classical PDMS and PEG based columns. It was shown that the FAMEs contained in biodiesel fuels were more retained than the apolar petroleum alkanes reducing interfering peaks and facilitating analyses. Similarly, in the analysis of bacterial FAMEs, hydroxylated FAMEs are significantly more retained than the others, here also facilitating bacterial identification.

DIL-coated capillary columns are already commercially available as bis(trifluoromethanesulfonyl)imide, having a great success in many applications thanks to their great orthogonality with other GC columns. The anion variations, described herein, could expand the field of applications.

Chapter 7 General Summary

Part one (Chapter 2-3)

A number of dicationic ionic liquids with high thermal stabilities were synthesized and used as GC stationary phase. Four different structural modifications were carried out to examine structure-property relationships. The effect of i) different cationic terminal groups, ii) linkage chain length, iii) alkyl substituent linked to the cationic group, and iv) different anionic species on the thermophysical properties of dicationic ILs were investigated. The aliphatic side chain induced more thermal stability than the aromatic substituent. Also, the NTf_2^- anion was found to provide greater stability at high temperatures. The DILs containing C9 spacer chain demonstrated ideal properties for gas chromatographic applications. Selected ILs with highest thermal stabilities and optimal properties were coated on the fused capillary columns and their selectivities were studied for high temperature GC applications. The phosphonium-based ILs were determined to be most stable, with maximum allowable operating temperature of 280 °C.

Part two (Chapters 4-5)

Branched-chain dicationic ILs with alkyl substituents located on the different positions of alkyl spacer chain were synthesized and their physicochemical properties were compared with their linear-chain counterparts. Thermal stabilities of branched-chain ILs are substantially influenced by the position of branching. Introduction of alkyl substituents on the α carbon led to a significant decrease in thermostability of DILs. Thanks to their low melting temperatures and relatively high viscosities, branched-chain DILs were used as GC stationary phase to separate fatty acid methyl esters. Excellent selectivity separation of fatty acids containing *cis* and *trans* positional isomers was achieved using these columns. The nature of the cationic head group was also found to impact the selectivity and polarity of IL-based stationary phases. Imidazolium-based ILs showed the highest polarity and best selectivity for separation of configurational isomers. The pyrrolidinium IL containing dimethyl substituent on the spacer chain was used for detailed analysis of C18:1 *cis* and *trans* fats in partially hydrogenated vegetable oil. The 30 m IL column operated at lower temperatures provided similar results obtained by 100 m bis-cyanopropyl polysiloxane column.

Part three (Chapter 6)

fourteen novel DILs composed of seven different sulfo-fluorinated anions and two branched-chain imidazolium-based dications were synthesized. Three major strategies were employed to modify these anions: i) enlarging or shortening the perfluoroalkyl chains in the anion; ii) introducing asymmetry in the imide anion; and iii) substituting the imide anion with the carbon based analogous anion, the triflide anion(CTf_3^-). The influence of the seven different anions on the thermophysical properties of the DILs was investigated. Ionic liquids containing symmetrical fluorosulfonylalkylated anions showed the highest thermal stabilities. DILs with perfluoroalkyl sulfate anions showed the highest melting points and viscosities. Capillary columns were prepared with the newly synthesized DILs and examined with different samples including polyaromatic hydrocarbons (PAHs) and FAMEs from various origins. The new IL-based columns showed McReynolds polarities ranging from 2461 to 6312. The polarity numbers for some of the new stationary phases went far beyond 111, the most polar commercialized stationary phase. The extremely polar ILs with triflate anions were utilized to separate the nonpolar petroleum alkanes from FAMEs contained in biodiesel fuels. The hydroxylated bacterial FAMEs were strongly retained on the nonaflate-based (NfO^-) IL column. Moreover, unique elution of anthracene before phenanthrene was obtained on the triflide-based (CTf_3^-) IL column.

Future work

The research which was performed during this study demonstrated the application of structurally-tuned ionic liquids as highly polar gas chromatography stationary phases. The exceptional selectivity of these stationary phases provides an opportunity for characterization of complex matrices such as fatty acid profiles in dairy and ruminant fats. Thanks to their extremely high polarity, many of these ILs can be utilized in multidimensional GC to provide superior orthogonality in the separation of complicated samples. Moreover, fast GC analysis of polarizable analytes (containing double bonds and/or triple C-C bonds) from nonpolar analytes can be achieved in shorter times without sacrificing resolution.

References

(1) Wasserscheid, P.; Welton, T. *Ionic liquids in synthesis*; John Wiley & Sons, **2008**.

(2) Tokuda, H.; Hayamizu, K.; Ishii, K.; Susan, M. A. B. H.; Watanabe, M. *J. Phys. Chem. B* **2004**, *108*, 16593-16600.

(3) Nan, H.; Anderson, J. L. *TrAC, Trends Anal. Chem.* **2018**, *105*, 367-379.

(4) Poole, C. F.; Lenca, N. *J. Chromatogr. A* **2014**, *1357*, 87-109.

(5) Anderson, J. L.; Armstrong, D. W. *Anal. Chem.* **2003**, *75*, 4851-4858.

(6) Patil, R. A.; Talebi, M.; Berthod, A.; Armstrong, D. W. *Anal. Bioanal. Chem.* **2018**, *410*, 4645–4655.

(7) Patil, R. A.; Talebi, M.; Xu, C.; Bhawal, S. S.; Armstrong, D. W. *Chem. Mater.* **2016**, *28*, 4315-4323.

(8) Maton, C.; De Vos, N.; Stevens, C. V. *Chem. Soc. Rev.* **2013**, *42*, 5963-5977.

(9) Talebi, M.; Patil, R. A.; Armstrong, D. W. *J. Mol. Liq.* **2018**, *256*, 247-255.

(10) Rooney, D.; Jacquemin, J.; Gardas, R. In *Ionic liquids*; Springer, **2009**, pp 185-212.

(11) Ho, T. D.; Zhang, C.; Hantao, L. W.; Anderson, J. L. *Anal. Chem.* **2013**, *86*, 262-285.

(12) Hallett, J. P.; Welton, T. *Chem. Rev.* **2011**, *111*, 3508-3576.

(13) Welton, T. *Chem. Rev.* **1999**, *99*, 2071-2084.

(14) Nacham, O. *Synthesis of new classes of ionic liquids and their utilization in biological and pharmaceutical analysis*. Iowa State University **2017**.

(15) Patil, R. A.; Talebi, M.; Sidisky, L. M.; Armstrong, D. W. *Chromatographia* **2017**, *80*, 1563-1574.

(16) Huang, K.; Han, X.; Zhang, X.; Armstrong, D. W. *Anal. Bioanal. Chem.* **2007**, *389*, 2265-2275.

(17) Anderson, J. L.; Ding, R.; Ellern, A.; Armstrong, D. W. *J. Am. Chem. Soc.* **2005**, *127*, 593-604.

(18) Jin, C.-M.; Ye, C.; Phillips, B. S.; Zabinski, J. S.; Liu, X.; Liu, W.; Jean'ne, M. S. *J. Mater. Chem.* **2006**, *16*, 1529-1535.

(19) Glukhov, L.; Krasovskiy, V.; Chernikova, E.; Kapustin, G.; Kustov, L.; Koroteev, A. *Russ. J. Phys. Chem. A* **2015**, *89*, 2204-2209.

(20) Shirota, H.; Mandai, T.; Fukazawa, H.; Kato, T. *J. Chem. Eng. Data* **2011**, *56*, 2453-2459.

(21) Payagala, T.; Huang, J.; Breitbach, Z. S.; Sharma, P. S.; Armstrong, D. W. *Chem. Mater.* **2007**, *19*, 5848-5850.

(22) Talebi, M.; Patil, R. A.; Sidisky, L. M.; Berthod, A.; Armstrong, D. W. *Anal. Chim. Acta* **2018**, *1042*, 155-164.

(23) Wu, B.; Reddy, R.; Rogers, R. *J. Sol. Energy Eng.* **2001**, 445-452.

(24) Bidikoudi, M.; Zubeir, L. F.; Falaras, P. *J. Matter. Chem. A* **2014**, *2*, 15326-15336.

(25) Decoppet, J.-D.; Moehl, T.; Babkair, S. S.; Alzubaydi, R. A.; Ansari, A. A.; Habib, S. S.; Zakeeruddin, S. M.; Schmidt, H.-W.; Grätzel, M. *J. Mater. Chem. A* **2014**, *2*, 15972-15977.

(26) Han, X.; Armstrong, D. W. *Org. Lett.* **2005**, *7*, 4205-4208.

(27) Xiao, J.-C.; Shreeve, J. n. M. *J. Org. Chem.* **2005**, *70*, 3072-3078.

(28) Armstrong, D. W.; He, L.; Liu, Y.-S. *Anal. Chem.* **1999**, *71*, 3873-3876.

(29) Frink, L. A.; Weatherly, C. A.; Armstrong, D. W. *J. Pharm. Biomed. Anal.* **2014**, *94*, 111-117.

(30) Frink, L. A.; Armstrong, D. W. *Anal. Chem.* **2016**, *88*, 8194-8201.

(31) Frink, L. A.; Armstrong, D. W. *J. Pharm. Sci.* **2016**, *105*, 2288-2292.

(32) Frink, L. A.; Armstrong, D. W. *Food Chem.* **2016**, *205*, 23-27.

(33) Frink, L. A.; Armstrong, D. W. *LC GC* **2016**, *34*, 6-13.

(34) Talebi, M.; Frink, L. A.; Patil, R. A.; Armstrong, D. W. *Food Anal. Methods* **2017**, *10*, 4062-4067.

(35) Jayawardhana, D. A.; Woods, R. M.; Zhang, Y.; Wang, C.; Armstrong, D. W. *LC GC Eur.* **2011**, *24*, 516.

(36) Weatherly, C. A.; Woods, R. M.; Armstrong, D. W. *J. Agric. Food Chem.* **2014**, *62*, 1832-1838.

(37) Poole, C. F.; Poole, S. K. *J. Sep. Sci.* **2011**, *34*, 888-900.

(38) Curto, N. L. *Application of an Ionic Liquid Column to the Analysis of Flavor and Fragrance Ingredients*. Seton Hall University **2016**.

(39) Anderson, J. L.; Ding, J.; Welton, T.; Armstrong, D. W. *J. Am. Chem. Soc.* **2002**, *124*, 14247-14254.

(40) Anderson, J. L.; Armstrong, D. W. *Anal. Chem.* **2005**, *77*, 6453-6462.

(41) Anderson, J. L.; Armstrong, D. W.; Wei, G.-T.; ACS Publications, **2006**.

(42) McReynolds, W. *J. Chromatogr. Sci.* **1970**, *8*, 685-691.

(43) Fanali, C.; Micalizzi, G.; Dugo, P.; Mondello, L. *Analyst* **2017**, *142*, 4601-4612.

(44) Christie, W. *Lipid Analysis: Isolation, Separation, Identification and Structural Analysis of Lipids*; Elsevier, **2003**.

(45) Delmonte, P.; Fardin-Kia, A. R.; Kramer, J. K.; Mossoba, M. M.; Sidisky, L.; Tyburczy, C.; Rader, J. I. *J. Chromatogr. A* **2012**, *1233*, 137-146.

(46) Delmonte, P.; Kia, A.-R. F.; Kramer, J. K.; Mossoba, M. M.; Sidisky, L.; Rader, J. I. *J. Chromatogr. A* **2011**, *1218*, 545-554.

(47) Zeng, A. X.; Chin, S.-T.; Nolvachai, Y.; Kulsing, C.; Sidisky, L. M.; Marriott, P. J. *Anal. Chim. Acta* **2013**, *803*, 166-173.

(48) Lin, C.-C.; Wasta, Z.; Mjøs, S. A. *J. Chromatogr. A* **2014**, *1350*, 83-91.

(49) Firestone, D. *Official methods and recommended practices of the AOCS*; AOCS, **2009**.

(50) Delmonte, P.; Kia, A.-R. F.; Hu, Q.; Rader, J. I. *J. AOCS Int.* **2009**, *92*, 1310-1326.

(51) Precht, D.; Molkentin, J. *Eur. J. Lipid Sci. Tech.* **2000**, *102*, 102-113.

(52) Precht, D.; Molkentin, J. *Int. Dairy J.* **1996**, *6*, 791-809.

(53) Sehat, N.; Rickert, R.; Mossoba, M. M.; Kramer, J. K.; Yurawecz, M. P.; Roach, J. A.; Adlof, R. O.; Morehouse, K. M.; Fritsche, J.; Eulitz, K. D. *Lipids* **1999**, *34*, 407-413.

(54) Yurawecz, M. P.; Roach, J. A.; Sehat, N.; Mossoba, M. M.; Kramer, J. K.; Fritsche, J.; Steinhart, H.; Ku, Y. *Lipids* **1998**, *33*, 803-809.

(55) Talebi, M.; Patil, R. A.; Sidisky, L. M.; Berthod, A.; Armstrong, D. W. *Anal. Bioanal. Chem.* **2017**, *410*, 4633–4643.

(56) Ragonese, C.; Tranchida, P. Q.; Dugo, P.; Dugo, G.; Sidisky, L. M.; Robillard, M. V.; Mondello, L. *Anal. Chem.* **2009**, *81*, 5561-5568.

(57) Dettmer, K. *Anal. Bioanal. Chem.* **2014**, *406*, 4931-4939.

(58) Mjøs, S. A.; Grahl-Nielsen, O. *J. Chromatogr. A* **2006**, *1110*, 171-180.

(59) Mjøs, S. A. *J. Chromatogr. A* **2003**, *1015*, 151-161.

(60) Tyburczy, C.; Delmonte, P.; Fardin-Kia, A. R.; Mossoba, M. M.; Kramer, J. K.; Rader, J. I. J. J. o. a.; chemistry, f. *J. Agric. Food Chem.* **2012**, *60*, 4567-4577.

(61) Inagaki, S.; Numata, M. *Chromatographia* **2015**, *78*, 291-295.

(62) Yoshinaga, K.; Asanuma, M.; Mizobe, H.; Kojima, K.; Nagai, T.; Beppu, F.; Gotoh, N. *Food Chem.* **2014**, *160*, 39-45.

(63) Fardin-Kia, A. R.; Delmonte, P.; Kramer, J. K.; Jahreis, G.; Kuhnt, K.; Santercole, V.; Rader, J. I. *Lipids* **2013**, *48*, 1279-1295.

(64) Delmonte, P.; Fardin-Kia, A. R.; Rader, J. I. *Anal. Chem.* **2013**, *85*, 1517-1524.

(65) Lock, A. L.; Bauman, D. E. *Lipids* **2004**, *39*, 1197-1206.

(66) Aldai, N.; Dugan, M. E.; Rolland, D.; Kramer, J. K. *Can. J. Anim. Sci.* **2009**, *89*, 315-329.

(67) Cruz-Hernandez, C.; Kramer, J.; Kennelly, J.; Glimm, D.; Sorensen, B.; Okine, E.; Goonewardene, L.; Weselake, R. *J. Dairy Sci.* **2007**, *90*, 3786-3801.

(68) Bauman, D. E.; Griinari, J. M. *Annu. Rev. Nutr.* **2003**, *23*, 203-227.

(69) Srigley, C. T.; Rader, J. I. *J. Agric. Food. Chem.* **2014**, *62*, 7268-7278.

(70) Ando, Y.; Sasaki, T. *J. Am. Oil Chem. Soc.* **2011**, *88*, 743-748.

(71) Gómez-Cortés, P.; Rodríguez-Pino, V.; Juárez, M.; de la Fuente, M. *Food Chem.* **2017**, *231*, 11-18.

(72) Fievez, V.; Colman, E.; Castro-Montoya, J.; Stefanov, I.; Vlaeminck, B. *Anim. Feed Sci. Technol.* **2012**, *172*, 51-65.

(73) Granafei, S.; Losito, I.; Salivo, S.; Tranchida, P. Q.; Mondello, L.; Palmisano, F.; Cataldi, T. R. *Anal. Chim. Acta* **2015**, *885*, 191-198.

(74) Chao, Y.; Guo, Z. B.; Du, Z. M.; Yang, H. Y.; Bi, Y. J.; Wang, G. Q.; Tan, Y. F. *Biomed. Environ. Sci.* **2012**, *25*, 711-717.

(75) Tucker, J. D.; Siebert, C. A.; Escalante, M.; Adams, P. G.; Olsen, J. D.; Otto, C.; Stokes, D. L.; Hunter, C. *Mol. Microbiol* **2010**, *76*, 833-847.

(76) Zeng, X.; Roh, J. H.; Callister, S. J.; Tavano, C. L.; Donohue, T. J.; Lipton, M. S.; Kaplan, S. *J. Bacteriol.* **2007**, *189*, 7464-7474.

(77) Katona, G.; Andreasson, U.; Landau, E. M.; Andreasson, L.-E.; Neutze, R. *J. Mol. Biol.* **2003**, *331*, 681-692.

(78) Verméglio, A.; Joliot, P. *Trends Microbiol.* **1999**, *7*, 435-440.

(79) Pinto, A. C.; Guarieiro, L. L.; Rezende, M. J.; Ribeiro, N. M.; Torres, E. A.; Lopes, W. A.; Pereira, P. A. d. P.; Andrade, J. B. d. *J. Braz. Chem. Soc.* **2005**, *16*, 1313-1330.

(80) Ragonese, C.; Tranchida, P. Q.; Sciarrone, D.; Mondello, L. *J. Chromatogr. A* **2009**, *1216*, 8992-8997.

(81) Webster, R.; Rawson, P.; Evans, D.; Marriott, P. *J. Sep. Sci.* **2016**, *39*, 2537-2543.

(82) Goding, J. C.; Ragon, D. Y.; O'Connor, J. B.; Boehm, S. J.; Hupp, A. M. *Anal. Bioanal. Chem.* **2013**, *405*, 6087-6094.

(83) Mogollón, N. G.; Ribeiro, F. A.; Poppi, R. J.; Quintana, A. L.; Chávez, J. A.; Agualongo, D. A.; Aleme, H. G.; Augusto, F. *J. Braz. Chem. Soc.* **2017**, *28*, 740-746.

(84) Mogollon, N. G. S.; de Lima Ribeiro, F. A.; Lopez, M. M.; Hantao, L. W.; Poppi, R. J.; Augusto, F. *Anal. Chim. Acta* **2013**, *796*, 130-136.

(85) Sato, R. T.; Stroppa, P. H. F.; Silva, A. D. d.; Oliveira, M. A. L. d. *Quim. Nova* **2016**, *39*, 352-355.

(86) Webster, R. e. L.; Evans, D. J.; Marriott, P. J. *Energy Fuels* **2015**, *29*, 2059-2066.

(87) McCormick, R. L.; Graboski, M. S.; Alleman, T. L.; Herring, A. M.; Tyson, K. S. *Environ. Sci. Technol.* **2001**, *35*, 1742-1747.

(88) Sushchik, N. N.; Kuchkina, A. Y.; Gladyshev, M. I. *Water Res.* **2013**, *47*, 3192-3200.

(89) Knothe, G.; Sharp, C. A.; Ryan, T. W. *Energy Fuels* **2006**, *20*, 403-408.

(90) EN14331, Liquid Petroleum Products—Separation and Characterization of Fatty Acid Methyl Esters (FAME) in Middle Distillate Fuels: rue de Stassart 36, B 1050 Bruxelles, **2004**.

(91) Visser, A. E.; Swatloski, R. P.; Reichert, W. M.; Mayton, R.; Sheff, S.; Wierzbicki, A.; Davis, J. H.; Rogers, R. D. *Int. J. Environ. Sci. Technol.* **2002**, *36*, 2523-2529.

(92) Anderson, J. L.; Pino, V.; Hagberg, E. C.; Sheares, V. V.; Armstrong, D. W. *Chem. Commun.* **2003**, 2444-2445.

(93) Boxall, D. L.; Osteryoung, R. A. *J. Electrochem. Soc.* **2004**, *151*, E41-E45.

(94) Breitbach, Z. S.; Armstrong, D. W. *Anal. Bioanal. Chem.* **2008**, *390*, 1605-1617.

(95) Cadena, C.; Anthony, J. L.; Shah, J. K.; Morrow, T. I.; Brennecke, J. F.; Maginn, E. J. *J. Am. Chem. Soc.* **2004**, *126*, 5300-5308.

(96) Carter, E. B.; Culver, S. L.; Fox, P. A.; Goode, R. D.; Ntai, I.; Tickell, M. D.; Traylor, R. K.; Hoffman, N. W.; Davis Jr, J. H. *Chem. Commun.* **2004**, 630-631.

(97) Earle, M. J.; Katdare, S. P.; Seddon, K. R. *Org. Lett.* **2004**, *6*, 707-710.

(98) Fletcher, K. A.; Pandey, S. *Langmuir* **2004**, *20*, 33-36.

(99) Gao, H.; Jiang, T.; Han, B.; Wang, Y.; Du, J.; Liu, Z.; Zhang, J. *Polymer* **2004**, *45*, 3017-3019.

(100) Kaar, J. L.; Jesionowski, A. M.; Berberich, J. A.; Moulton, R.; Russell, A. J. *J. Am. Chem. Soc.* **2003**, *125*, 4125-4131.

(101) Lee, J. K.; Kim, M.-J. *J. Org. Chem.* **2002**, *67*, 6845-6847.

(102) Luo, H.; Dai, S.; Bonnesen, P. V.; Buchanan, A.; Holbrey, J. D.; Bridges, N. J.; Rogers, R. D. *Anal. Chem.* **2004**, *76*, 3078-3083.

(103) Vijayaraghavan, R.; MacFarlane, D. *Chem. Commun.* **2004**, 700-701.

(104) Wasserscheid, P.; Hilgers, C.; Keim, W. *J. Mol. Catal. A Chem.* **2004**, *214*, 83-90.

(105) Wu, J.; Zhang, J.; Zhang, H.; He, J.; Ren, Q.; Guo, M. *Biomacromolecules* **2004**, *5*, 266-268.

(106) Zhao, H.; Malhotra, S. V. *Biotechnol. Lett.* **2002**, *24*, 1257-1259.

(107) Zhou, Y.; Antonietti, M. *J. Am. Chem. Soc.* **2003**, *125*, 14960-14961.

(108) Payagala, T.; Huang, J.; Breitbach, Z. S.; Sharma, P. S.; Armstrong, D. W. *Chem. Matter.* **2007**, *19*, 5848-5850.

(109) Sharma, P. S.; Payagala, T.; Wanigasekara, E.; Wijeratne, A. B.; Huang, J.; Armstrong, D. W. *Chem. Matter.* **2008**, *20*, 4182-4184.

(110) Ngo, H. L.; LeCompte, K.; Hargens, L.; McEwen, A. B. *Thermochim. Acta* **2000**, *357*, 97-102.

(111) Dearden, J. *Sci. Total Environ.* **1991**, *109*, 59-68.

(112) Izgorodina, E. I.; Forsyth, M.; MacFarlane, D. R. *Aust. J. Chem.* **2007**, *60*, 15-20.

(113) Bonhote, P.; Dias, A.-P.; Papageorgiou, N.; Kalyanasundaram, K.; Grätzel, M. *Inorg. Chem.* **1996**, *35*, 1168-1178.

(114) Montanino, M.; Carewska, M.; Alessandrini, F.; Passerini, S.; Appetecchi, G. B. *Electrochim. Acta* **2011**, *57*, 153-159.

(115) Rahman, M. M.; Liu, H. Y.; Prock, A.; Giering, W. P. *Organometallics* **1987**, *6*, 650-658.

(116) Harvey, R. G. In *PAHs and related compounds*; Springer: New York, NY, **1998**, pp 1-54.

(117) Manzano, C.; Hoh, E.; Simonich, S. L. M. *Environ. Sci. Technol.* **2012**, *46*, 7677-7684.

(118) Poster, D. L.; Schantz, M. M.; Sander, L. C.; Wise, S. A. *Anal. Bioanal. Chem.* **2006**, *386*, 859-881.

(119) Sun, P.; Armstrong, D. W. *Anal. Chim. Acta* **2010**, *661*, 1-16.

(120) Payagala, T.; Zhang, Y.; Wanigasekara, E.; Huang, K.; Breitbach, Z. S.; Sharma, P. S.; Sidisky, L. M.; Armstrong, D. W. *Anal. Chem.* **2008**, *81*, 160-173.

(121) Ding, J.; Desikan, V.; Han, X.; Xiao, T. L.; Ding, R.; Jenks, W. S.; Armstrong, D. W. *Org. Lett.* **2005**, *7*, 335-337.

(122) Cole, A. C.; Jensen, J. L.; Ntai, I.; Tran, K. L. T.; Weaver, K. J.; Forbes, D. C.; Davis, J. H. *J. Am. Chem. Soc.* **2002**, *124*, 5962-5963.

(123) Dyson, P. J.; Ellis, D. J.; Welton, T.; Parker, D. G. *Chem. Commun.* **1999**, 25-26.

(124) Bhawal, S. S.; Patil, R. A.; Armstrong, D. W. *RSC Adv.* **2015**, *5*, 95854-95856.

(125) Zeng, Z.; Phillips, B. S.; Xiao, J.-C.; Shreeve, J. n. M. *Chem. Mater.* **2008**, *20*, 2719-2726.

(126) Carda–Broch, S.; Berthod, A.; Armstrong, D. *Anal. Bioanal. Chem.* **2003**, *375*, 191-199.

(127) Dai, S.; Ju, Y.; Barnes, C. *J. Chem. Soc., Dalton Trans.* **1999**, 1201-1202.

(128) Chun, S.; Dzyuba, S. V.; Bartsch, R. A. *Anal. Chem.* **2001**, *73*, 3737-3741.

(129) Liu, R.; Liu, J.-f.; Yin, Y.-g.; Hu, X.-l.; Jiang, G.-b. *Anal. Bioanal. Chem.* **2009**, *393*, 871-883.

(130) Armstrong, D. W.; Zhang, L.-K.; He, L.; Gross, M. L. *Anal. Chem.* **2001**, *73*, 3679-3686.

(131) Carda-Broch, S.; Berthod, A.; Armstrong, D. W. Rapid Commun. Mass Spectrom. **2003**, *17*, 553-560.

(132) Tholey, A.; Heinzle, E. *Anal. Bioanal. Chem.* **2006**, *386*, 24-37.

(133) Chan, K.; Lanthier, P.; Liu, X.; Sandhu, J. K.; Stanimirovic, D.; Li, J. *Anal. Chim. Acta* **2009**, *639*, 57-61.

(134) Crank, J. A.; Armstrong, D. W. *J. Am. Soc. Mass Spectrom.* **2009**, *20*, 1790-1800.

(135) Lagrost, C.; Carrie, D.; Vaultier, M.; Hapiot, P. *J. Phys. Chem. A* **2003**, *107*, 745-752.

(136) Enders Dickinson, V.; Williams, M. E.; Hendrickson, S. M.; Masui, H.; Murray, R. W. *J. Am. Chem. Soc.* **1999**, *121*, 613-616.

(137) Doyle, K. P.; Lang, C. M.; Kim, K.; Kohl, P. A. *J. Electrochem. Soc.* **2006**, *153*, A1353-A1357.

(138) Nanayakkara, Y. S.; Perera, S.; Bindiganavale, S.; Wanigasekara, E.; Moon, H.; Armstrong, D. W. *Anal. Chem.* **2010**, *82*, 3146-3154.

(139) Wanigasekara, E.; Zhang, X.; Nanayakkara, Y.; Payagala, T.; Moon, H.; Armstrong, D. W. *Appl. Mater. Interfaces* **2009**, *1*, 2126-2133.

(140) Nanayakkara, Y. S.; Moon, H.; Payagala, T.; Wijeratne, A. B.; Crank, J. A.; Sharma, P. S.; Armstrong, D. W. *Anal. Chem.* **2008**, *80*, 7690-7698.

(141) Berthod, A.; He, L.; Armstrong, D. W. *Chromatographia* **2001**, *53*, 63-68.

(142) Cagliero, C.; Bicchi, C.; Cordero, C.; Liberto, E.; Sgorbini, B.; Rubiolo, P. *J. Chromatogr. A* **2012**, *1268*, 130-138.

(143) Krupčík, J.; Gorovenko, R.; Špánik, I.; Bočková, I.; Sandra, P.; Armstrong, D. W. *J. Chromatogr. A* **2013**, *1301*, 225-236.

(144) Ragonese, C.; Sciarrone, D.; Tranchida, P. Q.; Dugo, P.; Mondello, L. *J. Chromatogr. A* **2012**, *1255*, 130-144.

(145) Sanchez-Prado, L.; Lamas, J. P.; Garcia-Jares, C.; Llompart, M. *Chromatographia* **2012**, *75*, 1039-1047.

(146) Ragonese, C.; Sciarrone, D.; Tranchida, P. Q.; Dugo, P.; Dugo, G.; Mondello, L. *Anal. Chem.* **2011**, *83*, 7947-7954.

(147) Lambertus, G. R.; Crank, J. A.; McGuigan, M. E.; Kendler, S.; Armstrong, D. W.; Sacks, R. D. *J. Chromatogr. A* **2006**, *1135*, 230-240.

(148) Sciarrone, D.; Tranchida, P. Q.; Ragonese, C.; Schipilliti, L.; Mondello, L. *J. Sep. Sci.* **2010**, *33*, 594-599.

(149) Reid, V. R.; Crank, J. A.; Armstrong, D. W.; Synovec, R. E. *J. Sep. Sci.* **2008**, *31*, 3429-3436.

(150) Patil, R. A.; Talebi, M.; Xu, C.; Bhawal, S. S.; Armstrong, D. W. *Chem. Mater.* **2016**, *28*, 4315-4323.

(151) Grob, K.; Grob, G.; Grob Jr, K. *J. Chromatogr. A* **1981**, *219*, 13-20.

(152) Grob Jr, K.; Grob, G.; Grob, K. *J. Chromatogr. A* **1978**, *156*, 1-20.

(153) Tokuda, H.; Ishii, K.; Susan, M. A. B. H.; Tsuzuki, S.; Hayamizu, K.; Watanabe, M. *J. Phys. Chem. B* **2006**, *110*, 2833-2839.

(154) Tokuda, H.; Hayamizu, K.; Ishii, K.; Susan, M. A. B. H.; Watanabe, M. *J. Phys. Chem. B* **2005**, *109*, 6103-6110.

(155) Chang, J.-C.; Ho, W.-Y.; Sun, I.-W.; Tung, Y.-L.; Tsui, M.-C.; Wu, T.-Y.; Liang, S.-S. *Tetrahedron* **2010**, *66*, 6150-6155.

(156) Wang, R.; Jin, C.-M.; Twamley, B.; Shreeve, J. n. M. *Inorg. Chem.* **2006**, *45*, 6396-6403.

(157) Yoon, J.; Kim, S. K.; Singh, N. J.; Kim, K. S. *Chem. Soc. Rev.* **2006**, *35*, 355-360.

(158) Goossens, K.; Lava, K.; Bielawski, C. W.; Binnemans, K. *Chem. Rev.* **2016**, *116*, 4643-4807.

(159) D'Anna, F.; Noto, R. J. E. J. o. O. C. *Eur. J. Org. Chem.* **2014**, *2014*, 4201-4223.

(160) Tu, T.; Assenmacher, W.; Peterlik, H.; Schnakenburg, G.; Dötz, K. H. *Angew. Chem. Int. Edit.* **2008**, *47*, 7127-7131.

(161) Boydston, A. J.; Vu, P. D.; Dykhno, O. L.; Chang, V.; Wyatt, A. R.; Stockett, A. S.; Ritschdorff, E. T.; Shear, J. B.; Bielawski, C. W. *J. Am. Chem. Soc.* **2008**, *130*, 3143-3156.

(162) Guo, Z.; Song, N. R.; Moon, J. H.; Kim, M.; Jun, E. J.; Choi, J.; Lee, J. Y.; Bielawski, C. W.; Sessler, J. L.; Yoon, J. *J. Am. Chem. Soc.* **2012**, *134*, 17846-17849.

(163) Patil, S. K.; Patil, S. A.; Vadiyar, M. M.; Awale, D. V.; Sartape, A. S.; Walekar, L. S.; Kolekar, G. B.; Ghorpade, U. V.; Kim, J. H.; Kolekar, S. S. *J. Mol. Liq.* **2017**, *244*, 39-45.

(164) Tomé, L. C.; Aboudzadeh, M. A.; Rebelo, L. P. N.; Freire, C. S.; Mecerreyes, D.; Marrucho, I. M. *J. Mater. Chem. A* **2013**, *1*, 10403-10411.

(165) Han, X.; Armstrong, D. W. *Acc. Chem. Res.* **2007**, *40*, 1079-1086.

(166) Brown, P.; Butts, C. P.; Eastoe, J.; Hernández, E. P.; de Araujo Machado, F. L.; de Oliveira, R. J. *Chem. Commun.* **2013**, *49*, 2765-2767.

(167) Nacham, O.; Clark, K. D.; Yu, H.; Anderson, J. L. *Chem. Mater.* **2015**, *27*, 923-931.

(168) Fareghi-Alamdari, R.; Hatefipour, R.; Rakhshi, M.; Zekri, N. *RSC Adv.* **2016**, *6*, 78636-78647.

(169) Xue, L.; Gurung, E.; Tamas, G.; Koh, Y. P.; Shadeck, M.; Simon, S. L.; Maroncelli, M.; Quitevis, E. L. *J. Chem. Eng. Data* **2016**, *61*, 1078-1091.

(170) Erdmenger, T.; Vitz, J.; Wiesbrock, F.; Schubert, U. S. *J. Mater. Chem.* **2008**, *18*, 5267-5273.

(171) Rodrigues, A. S.; Almeida, H. F.; Freire, M. G.; Lopes-da-Silva, J. A.; Coutinho, J. A.; Santos, L. M. *Fluid Phase Equilib.* **2016**, *423*, 190-202.

(172) Kashyap, H. K.; Santos, C. S.; Murthy, N. S.; Hettige, J. J.; Kerr, K.; Ramati, S.; Gwon, J.; Gohdo, M.; Lall-Ramnarine, S. I.; Wishart, J. F. *J. Phys. Chem. B* **2013**, *117*, 15328-15337.

(173) Rodrigues, A. S.; Lima, C. F.; Coutinho, J. A.; Santos, L. M. *Phys. Chem. Chem. Phys.* **2017**, *19*, 5326-5332.

(174) Grob, K.; Grob, G. *J. Chromatogr. A* **1976**, *125*, 471-485.

(175) Zheng, W.; Mohammed, A.; Hines Jr, L. G.; Xiao, D.; Martinez, O. J.; Bartsch, R. A.; Simon, S. L.; Russina, O.; Triolo, A.; Quitevis, E. L. J. T. J. o. P. C. B. *J. Phys. Chem. B* **2011**, *115*, 6572-6584.

(176) Sun, M.; Liu, D. Q.; Kord, A. S. *Org. Process Res. Dev.* **2010**, *14*, 977-985.

(177) Sanchez, L. G.; Espel, J. R.; Onink, F.; Meindersma, G. W.; Haan, A. B. d. *J. Chem. Eng. Data* **2009**, *54*, 2803-2812.

(178) Aparicio, S.; Atilhan, M.; Karadas, F. *Ind. Eng. Chem. Res.* **2010**, *49*, 9580-9595.

(179) Cao, Y.; Mu, T. *Ind. Eng. Chem. Res.* **2014**, *53*, 8651-8664.

(180) Cacho, J. I.; Campillo, N.; Viñas, P.; Hernández-Córdoba, M. *RSC Adv.* **2016**, *6*, 20886-20891.

(181) Weber, W.; Andersson, J. T. *Anal. Bioanal. Chem.* **2014**, *406*, 5347-5358.

(182) Álvarez, J. G.; Gomis, D. B.; Abrodo, P. A.; Llorente, D. D.; Busto, E.; Lombardía, N. R.; Fernández, V. G.; Álvarez, M. D. G. *Anal. Bioanal. Chem.* **2011**, *400*, 1209-1216.

(183) Cagliero, C.; Bicchi, C.; Cordero, C.; Liberto, E.; Rubiolo, P.; Sgorbini, B. *J. Chromatogr. A* **2017**, *1495*, 64-75.

(184) Cagliero, C.; Bicchi, C.; Cordero, C.; Liberto, E.; Rubiolo, P.; Sgorbini, B. *Anal. Bioanal. Chem.* **2018**, 1-12.

(185) Weatherly, C. A.; Zhang, Y.; Smuts, J. P.; Fan, H.; Xu, C.; Schug, K. A.; Lang, J. C.; Armstrong, D. W. *J. Agric. Food Chem.* **2016**, *64*, 1422-1432.

(186) Fan, H.; Smuts, J.; Bai, L.; Walsh, P.; Armstrong, D. W.; Schug, K. *Food Chem.* **2016**, *194*, 265-271.

(187) Hammann, S.; Vetter, W. *J. Chromatogr. B* **2015**, *1007*, 67-71.

(188) Nosheen, A.; Mitrevski, B.; Bano, A.; Marriott, P. J. *J. Chromatogr. A* **2013**, *1312*, 118-123.

(189) Zeng, A. X.; Chin, S. T.; Marriott, P. J. *J. Sep. Sci.* **2013**, *36*, 878-885.

(190) Tyburczy, C.; Mossoba, M. M.; Rader, J. I. *Anal. Bioanal. Chem.* **2013**, *405*, 5759-5772.

(191) Destaillats, F.; Guitard, M.; Cruz-Hernandez, C. *J. Chromatogr. A* **2011**, *1218*, 9384-9389.

(192) Gu, Q.; David, F.; Lynen, F.; Vanormelingen, P.; Vyverman, W.; Rumpel, K.; Xu, G.; Sandra, P. *J. Chromatogr. A* **2011**, *1218*, 3056-3063.

(193) Rodríguez-Sánchez, S.; Galindo-Iranzo, P.; Soria, A. C.; Sanz, M. L.; Quintanilla-López, J. E.; Lebrón-Aguilar, R. *J. Chromatogr. A* **2014**, *1326*, 96-102.

(194) Berthod, A.; Ruiz-Ángel, M.; Carda-Broch, S. *J. Chromatogr. A* **2017**.

(195) Seki, S.; Kobayashi, T.; Kobayashi, Y.; Takei, K.; Miyashiro, H.; Hayamizu, K.; Tsuzuki, S.; Mitsugi, T.; Umebayashi, Y. *J. Mol. Liq.* **2010**, *152*, 9-13.

(196) Gouveia, A. S.; Bernardes, C. E.; Tomé, L. C.; Lozinskaya, E. I.; Vygodskii, Y. S.; Shaplov, A. S.; Lopes, J. N. C.; Marrucho, I. M. *Phys. Chem. Chem. Phys.* **2017**, *19*, 29617-29624.

(197) Walther, C. *Maschinenbau* **1931**, *10*, 670-675.

(198) Bose, S.; Armstrong, D. W.; Petrich, J. W. *J. Phys. Chem. B* **2010**, *114*, 8221-8227.

Biographical Information

Mohsen Talebi obtained his Bachelor of Science degree in chemistry, and his Masters in organic chemistry from Shiraz University in Iran. He then chose to further his education by joining Dr. Daniel Armstrong’s group in 2014 at the University of Texas at Arlington. His research focused on the development of structurally-tuned ionic liquids and their application as highly polar gas chromatography stationary phase.